Characterization of the role of the tumor suppressor FLCN using *Caenorhabditis elegans* and mammalian cells

Elite Possik

Department of Biochemistry
Goodman Cancer Research Center
McGill University
Montreal, Quebec, Canada

November 2015

A thesis submitted to McGill University in partial fulfillment of the requirements of the degree of Doctor of Philosophy

Table of Content

ACKNOWLEDGEMENTS

First, I would like to thank God for his help along my path.

Foremost, I am profoundly indebted to my supervisor Dr. Arnim Pause. My work would not have been possible if not for his valuable guidance each step of the way. I greatly appreciate his patience, stimulus, and advice. Surely, working in his Lab conferred me the ability to look at things from different angles and think outside the box. This experience gave me the opportunity to become not only a better scientist but also a better person.

A special thanks to my research advisory committee Dr. Julie St-Pierre and Dr. Christian Rocheleau for their valuable help and comments. I specifically thank Dr. Rocheleau for teaching me how to perform *C. elegans* injections.

I am very thankful to all my colleagues, past and present members of the Pause laboratory, for their friendship and support. Specifically, I would like to thank our laboratory manager Dr. Marie-Claude Gingras for her assistance and advice along the way. I specifically thank the undergraduate students Lorena Panaite, Jacky Leung, Arm Omr, Andrew Ajisebutu, and the Masters student Tarika Vijayaraghavan for their help in my projects.

I also acknowledge Dr. David Hall, Professor at the Albert Einstein College of Medicine, for his hospitality and supervision to the electron microscopy part of this project. I thank from his Lab, Mr. Ken Nguyen who taught me this technique. My visit to Dr. Hall's lab is an unforgettable experience.

I would like to thank colleagues from Dr. Richard Roy's laboratory and specifically Shaolin Li for his help in techniques and for reagents.

I am thankful to my family Joseph, Odile, Jalal, and Christelle for their support through my Ph.D.

And last but certainly not least, I thank my husband Antoine for his endless support and patience along this long journey. He has been always there to encourage and motivate me, in rainy and sunny days. Finally, to my daughter Sara, I love you! Your beautiful smile keeps me going.

ABSTRACT

Birt-Hogg-Dubé is a dominantly-inherited syndrome that increases predisposition to cancer mainly renal tumors and cysts. Folliculin (FLCN), a protein highly conserved across evolution, is the tumor suppressor responsible for this disease. Despite the intensive research effort spent since its discovery in 2001, the cellular role of FLCN remains unclear and how its loss leads to tumorigenesis is not yet defined. FLCN is a binding partner of the 5'AMP-activated protein kinase (AMPK), a central regulator of energy homeostasis. However, the genetic and functional links as well as the phenotypic outcomes on cells/organisms have not been established. In this thesis, we investigated the role of FLCN in the model organism *Caenorhabditis elegans (C. elegans)* and in mammalian cells. In the first part, we demonstrate that FLCN is an evolutionary conserved negative regulator of AMPK. Loss of FLCN in worms and mammals activates AMPK signaling and induces autophagy, improving cellular bioenergetics, and leading to an advantageous resistance to several metabolic stresses including oxidative stress, anoxia, heat, and nutrient deprivation. In the second part, we highlight the discovery of a novel function for FLCN/AMPK in the regulation of glycogen metabolism and resistance to hyperosmotic stress in *C. elegans*. We show that loss of *flcn-1*, leads to AMPK-dependent glycogen accumulation and resistance to hyperosmotic conditions. Upon exposure to salt stress, glycogen reserves are rapidly degraded, leading to the accumulation of the organic osmolyte glycerol, which is crucial for organismal survival to hyperosmotic environments. Importantly, we also show that that the regulation of glycogen metabolism by FLCN is evolutionary conserved and that glycogen accumulates in kidneys from mice lacking FLCN and in renal tumors from BHD patients. Results of this part demonstrate a dual role for glycogen reserves: an energy reservoir and a store that fuels osmolyte production. In the third part, we investigate the transcriptional regulation

downstream FLCN-1 in *C. elegans*. The results of this chapter indicate that the transcriptional profiles upon loss *flcn-1* at basal level significantly overlap with published stress response signatures including oxidative stress, hyperosmotic stress, and infection with pathogens. Furthermore, we found that loss of *flcn-1* in *C. elegans* leads to increased resistance to pathogens impinging on a possible role for FLCN-1 in the regulation of innate immunity. Finally, we found that many stress response genes upregulated in *flcn-1* animals are downregulated in *hlh-30* mutant animals, and that the hyperosmotic stress resistance in *flcn-1* nematodes is abolished upon loss of *hlh-30*, supporting a potential role of the TFEB worm homolog, HLH-30, in stress response downstream FLCN-1. Altogether, these studies have established FLCN as an evolutionary conserved negative regulator of AMPK, and have led to the discovery of two distinct pathways of stress resistance downstream FLCN/AMPK, a pathway of resistance to metabolic stresses and another that confers resistance to hyperosmotic stress, and both pathways might be supporting tumorigenesis.

RÉSUMÉ

Birt-Hogg-Dubé est un syndrome héréditaire qui augmente le risque de développer un cancer principalement des tumeurs et des kystes du rein. Folliculine (FLCN), hautement conservée à travers l'évolution, est la protéine suppresseur de tumeurs responsable de cette maladie. Malgré l'intense effort de recherche consacré depuis sa découverte, en 2001, la fonction de la protéine FLCN demeure obscure et comment son absence mène au cancer n'est pas encore défini. FLCN est un partenaire de la protéine-kinase (AMPK), un complexe impliqué dans la régulation du métabolisme cellulaire. Toutefois, les liens génétiques, fonctionnels, et phénotypiques n'ont pas été établis. Dans cette thèse, nous avons étudié le rôle de FLCN dans l'organisme modèle *Caenorhabditis elegans (C. elegans)* et dans des cellules de mammifères. Dans la première partie, nous démontrons que FLCN régule négativement l'AMPK, une fonction conservée à travers l'évolution. L'absence de la protéine FLCN active l'AMPK et induit l'autophagie, améliorant la bioénergétique cellulaire, et menant à une résistance avantageuse à plusieurs stress métaboliques incluant le stress oxydatif, l'anoxie, la chaleur et la carence en nutriments. Dans la deuxième partie, nous mettons en évidence la découverte d'une nouvelle fonction du complexe FLCN/AMPK dans la régulation du métabolisme du glycogène et dans l'adaptation au stress hyperosmotique chez *C. elegans*. Nous démontrons que l'absence de FLCN conduit à l'accumulation du glycogène et à la résistance aux conditions hyperosmotiques de manière dépendante de l'AMPK. Lors de l'exposition à un stress salin, les réserves de glycogène sont rapidement dégradées, conduisant à l'accumulation de l'osmolyte organique glycérol, un facteur essentiel pour l'adaptation de l'animal au stress hyperosmotique. Nous avons également prouvé que la régulation du métabolisme du glycogène par FLCN est conservée à travers l'évolution et que le glycogène s'accumule dans les reins de souris dépourvues de FLCN et dans la tumeur

rénale d'un patient atteint par le syndrome BHD. Les résultats de cette partie démontrent un double rôle pour les réserves de glycogène: un réservoir d'énergie et un conservateur important de métabolites intermédiaires pour la production d'osmolytes en cas de besoin. Dans la troisième partie, nous étudions les changements transcriptionnels subis suite à l'absence de *flcn-1* chez *C. elegans*. Les résultats de ce chapitre indiquent un chevauchement significatif avec des groupes de gènes induits par différents types de stress incluant le stress oxydatif, le stress hyperosmotique, et l'infection par des agents pathogènes. En outre, nous avons constaté que l'absence de *flcn-1* chez *C. elegans* augmente la résistance aux pathogènes suggérant un rôle possible pour FLCN-1 dans la régulation de l'immunité innée. Nous avons aussi constaté que de nombreux gènes surexprimés chez les mutants nématodes *flcn-1* sont régulés négativement chez les mutants *hlh-30* et que la résistance au stress hyperosmotique des nématodes mutants *flcn-1* est abolie par l'absence de l'*hlh-30*, soutenant un rôle possible de l'homologue de TFEB, HLH-30, dans la signalisation d'adaptation au stress en aval de la protéine FLCN-1. Ensemble, ces études ont démontré que FLCN régule négativement l'AMPK à travers l'évolution, et ont conduit à la découverte de deux voies distinctes de résistance au stress en aval de FLCN/AMPK, une voie de résistance aux stress métaboliques et une autre qui confère la résistance au stress hyperosmotique, et les deux voies pourraient soutenir la tumorigenèse.

LIST OF FIGURES

LIST OF TABLES

LIST OF ABBREVIATIONS

8-OHdG	8-hydroxy-2-deoxyguanosine
ACC	Acetyl-CoA carboxylases
ADP	Adenosine diphosphate
AGE-1	Ageing alteration-1
AICAR	5-aminoimidazole-4-carboxamide-1-β-D-ribonucleoside
AMP	Adenosine monophosphate
AMPK	5'AMP-activated protein kinase
APAF1	Apoptotic protease-activating factor-1
ATP	Adenosine triphosphate
C. elegans	*Caenorhabditis elegans*.
CAMKK	Ca^{2+}/calmodulin-activated protein kinase kinases
CED-3	Cell death abnormal 3
CED-4	Cell death abnormal 4
CED-9	Cell death abnormal 9
CQ	Chloroquine
CREB	cAMP-response element binding protein
CYP 450	Cytochrome P450
DAF-16	Abnormal dauer formation
DAF-2	Abnormal dauer formation 2
DAVID	Database for Annotation, Visualization and Intergrated Discovery
DENN	Differentially expressed in normal cells and neoplasia
dsRNA	Double stransded RNA
E. Coli	*Escherichia coli*
EGF	Epidermal growth factor
EM	Electron microscopy
ER stress	Endoplasmic reticulum stress
ERR	Estrogen-related receptor
FLCN	Folliculin
FNIP1	Folliculin-interacting protein 1
FNIP2	Folliculin-interacting protein 2
FNIPL	FNIP-like
FTC133	Follicular thyroid carcinoma cells 133
FUDR	5-fluoro-2'-deoxyuridine
GABARAP	GABA receptor-associated protein
GEFs	Guanine nucleotide exchange factors
GLUT1	Glucose transporter 1
GLUT4	Glucose transporter 4
GPDH	Glycerol-3-phosphate dehydrogenase
GSY-1	Glycogen synthase 1 *(C. elegans)*
GYS-1	Glycogen synthase 1
H_2O_2	Hydrogen peroxide

HIF1	Hypoxia inducible factor 1
HIF2	Hypoxia inducible factor 2
HLH-30	Helix loop helix 30
$HO^{\bullet}$),	Hydroxyl radical
INF-γ	Interferon gamma
kb	Kilobase pairs
kDa	Kilodaltons
KO	Knock out
MEFs	Mouse embryonic fibroblasts
MiTF	Microphtalmia transcription factor
MnSOD2	Manganese superoxide dismutase 2
mTOR	mammalian target of Rapamycin
N2	Wild-type
NaCl	Sodium chloride
NFAT5	Nuclear factor-activated T cell 5
NF-κb	Nuclear factor kappa B
NRF1	Nuclear respiratory factor 1
NRF2	Nuclear respiratory factor 2
$O_2^{\bullet-}$	Superoxide anion
osr-1	Osmotic stress resistance
PAS	Periodic acid schiff
PDGF	Platelet-derived growth factor
PGC1	Proliferator-activated receptor gamma 1 co-activator
PKP4	Plakophilin-4
PPARs	Peroxisome proliferator-activated receptors
PQ	Paraquat
PYGL-1	Glycogen phospharylase 1
RCC	Renal cell carcinoma
RNAi	RNA interference
ROS	Reactive oxygen species
Rpt4	ATPase 4
SOD1	Superoxide dismutase
TCA	Tricarboxylic acid
TEM	Transmission electron microscopy
TFE3	Transcription factor E3
TFEB	Transcription factor EB
TGF-β	Transforming growth factor beta
Thr172	Threonine 172
TNF-α	Tumor necrosis factor alpha
TSC2	Tuberous sclerosis complex 2
VEGF	Vascular endothelial growth factor
VHL	Von Hippel-Lindau
Wt	Wild-type

CONTRIBUTION OF AUTHORS

Chapter 2

In chapter 2, I provided figures/panels:

2.1: A, B, D, E, F, H, I

2.2: B, C, D, E, F

2.3: A, B, C

2.4: A, B, C, D, E, G, I

2.5: A, B, C, D, E

2.6: B, C

Zahra Jalali performed the following experiments:

2.1: C, D, G

2.2: A

2.3: D

2.4: D, F, H

2.6: A

Laetitia Chotard performed experiment 2.3E

Yan Nouet performed experiments: 2.7: A. C, F, I and 2.8

Ming Yan performed experiments: 2.7: B, D, E

Marie-Claude Gingras performed experiment 2.7G and 2.8

Chapter 3

In chapter 3, I performed all experiments except those for figure 3.7. Periodic acid schiff (PAS) staining on mice samples was accomplished at the McGill histology facility and I performed the imaging. Barry Coull provided PAS staining images on the human BHD tumors and normal kidney samples. Analysis of gene expression in human kidney tumors and correlation with FLCN expression was performed by Sanaz Manteghi For figure 3.5E, Andrew Ajisebutu contributed to the generation of the triple mutant *flcn-1(ok975); gpdh-1(kb24); gpdh-2(kb33)* strain and helped with the survival analysis on hyperosmotic stress. Mathieu Flamand generated the rescue strain that I used in figure 3.1F.

Chapter 4

For this chapter, I generated all figures and tables except panels 4.5D and 4.5E that were performed in the Irazoqui Lab. The microarray experiment was performed by Genome Quebec and results were analyzed by Greg Voisin. I validated the microarray results by qRT-PCR, and performed the gene ontology classification and gene overlap analysis.

PUBLICATIONS

Arising from work presented in this thesis:

Folliculin regulates ampk-dependent autophagy and metabolic stress survival.
Possik E*, Jalali Z*, Nouët Y, Yan M, Gingras MC, Schmeisser K, Panaite L, Dupuy F, Kharitidi D, Chotard L, Jones RG, Hall DH, Pause A.
PLoS Genet. 2014 Apr 24;10(4):e1004273.
*Co-first authors

FLCN and AMPK confer hyperosmotic stress resistance via remodeling of glycogen stores.
Possik E, Ajisebutu A, Manteghi S, Gingras MC, Vijayaraghavan T, Flamand M, Coull B, Schmeisser K, Duchaine T, Van Steensel M, Hall DH, Pause A.
PLoS Genet. *(In press)*.

Measuring oxidative stress resistance of *Caenorhabditis elegans* in 96-well microtiter plates.
Possik E, Pause A.
J Vis Exp. 2015 May 9;(99):e52746.

Transcriptional regulation of stress response genes via FLCN and AMPK.
Possik E, Vijayaraghavan T, Irazoqui J, Pause A. *(In preparation)*.

Other publications:

The tumor suppressor folliculin regulates AMPK-dependent metabolic transformation.
Yan M, Gingras MC, Dunlop EA, Nouët Y, Dupuy F, Jalali Z, Possik E, Coull BJ, Kharitidi D, Dydensborg AB, Faubert B, Kamps M, Sabourin S, Preston RS, Davies DM, Roughead T, Chotard L, van Steensel MA, Jones R, Tee AR, Pause A.
J Clin Invest. 2014 Jun;124(6):2640-50.

Randomized codon mutagenesis reveals that the HIV Rev arginine-rich motif is robust to substitutions and that double substitution of two critical residues alters specificity.
Possik E, Bou Sleiman MS, Ghattas IR, Smith CA.
J Mol Recognit. 2013 Jun;26(6):286-96.

DEDICATION

To my husband Antoine and daughter Sara
you are my light...

CHAPTER 1 - LITERATURE REVIEW

1.1 Renal cancer

Renal cell carcinoma (RCC) is the most common type of cancerous kidney lesions affecting more than 270,000 individuals worldwide every year [1]. Since it is asymptomatic at the early stages, RCC is often detected at late stages causing deaths in nearly 44% of affected individuals [1]. Based on year 2015 estimates, almost 6200 Canadian patients are diagnosed with RCC and 1800 are estimated to die from it [2].

Although RCC accounts for 90% of kidney cancer types, it is not a single disease, but it consists of different subtypes classified based on distinct histological, pathophysiological, and molecular properties [3]. Major subtypes include clear-cell RCC, hereditary type I papillary RCC, type II papillary RCC, chromophobe RCC, and oncocytomas [3-6]. Importantly, clear-cell RCC is the most common among subtypes accounting for almost 75% of the cases and is associated with mutations in the *VHL* tumor suppressor gene, which causes the von Hippel-Lindau (VHL) syndrome [6]. The VHL syndrome is an inherited cancer syndrome that predisposes to malignant and benign tumors in many organs including brain, kidney, spinal cord and pancreas [6]. Patients with the VHL syndrome inherit a germline mutation in the *VHL* gene and a second sporadic mutation occurs later over time leading to cancer [6]. The VHL protein is a component of an E3 ubiquitin ligase protein complex responsible of ubiquitination and targeting the hypoxia inducible factor (HIF) transcription factor for proteasomal degradation [7-10]. Consequently, mutations in the *VHL* gene lead to HIF stabilization, and a subsequent transcriptional upregulation of genes involved in adaptation upon low oxygen such as the vascular endothelial growth factor (VEGF), glucose transporters GLUT1 and GLUT4, and the platelet-derived growth factor (PDGF) [11]. HIF is essential to drive tumorigenesis since most cancerous microenvironments are hypoxic. Therefore, an enhanced angiogenesis by HIF activation

increases glucose uptake and promotes tumor survival [11]. Similarly to the renal tumor suppressor role of VHL, Folliculin (FLCN) acts as a renal tumor suppressor protein responsible for the Birt-Hogg-Dubé cancer syndrome [12].

1.2 Birt-Hogg Dubé Syndrome

1.2.1 What is BHD disease?

Birt-Hogg-Dubé is an autosmal dominant neoplastic syndrome that has been first described in 1977 by three Canadian doctors, Birt, Hogg, and Dubé. This disease is characterized by skin lesions named fibrofolliculomas, pulmonary cysts or pneumothoraces, and an increased presdisposition to renal cysts and tumors [13-26]. In contrast to the VHL syndrome which is characterized by the development of clear-cell RCC only, BHD-associated renal tumors are heterogeneous and comprise all subtypes, clear-cell RCC, papillary type I and type II RCC, kidney chromophobe, and oncocytoma [3,15,16,23]. Importantly, BHD syndrome shares many clinical features with other hamartoma syndromes, which are caused by mutations in important tumor suppressor genes and key metabolic regulators, leading to malignant and benign tumors in multiple organs. Hamartoma syndromes similar to BHD include Cowden Syndrome, Peutz-Jeghers syndrome and Tuberous sclerosis complex caused by the loss of function of PTEN, LKB1 and TSC1 or TSC2 tumor suppressors, respectively [27-30].

1.2.2 The BHD disease gene: FLCN

BHD is caused by germline mutations in the BHD gene, which encodes FLCN, a 64KDa protein, expressed in most tissues [12]. Two separate research groups have mapped the FLCN gene to chromosome 17p11.2 in 2001 by linkage analysis [31,32] and positional

cloning [26]. The BHD gene consists of 14 exons spanning 20kb of the human genomic DNA [26]. BHD patients carry germline mutations in the FLCN gene and acquire "second-hit" somatic mutations throughout their lives leading to loss of heterozygosity [25,33]. This is supported by the loss of the FLCN mRNA in renal tumors [34]. Importantly, most mutations occur on exon 11, both in cases of familial inherited BHD or sporadic cases of BHD syndrome, rendering it a hotspot [26]. Additionally, most mutations are predicted to truncate the protein by introduction of stop codon [35].

The BHD gene product, FLCN, comprises a hydrophobic N-terminal sequence, an N-glycosylation site, three myristoylation sites, and a glutamic acid-rich coiled coil domain [26]. Although FLCN does not share a significant homology to any known protein [34], it is highly evolutionary conserved, from yeast to mammals, suggesting that it plays a central biological role [26]. Recently, crystallization of the Carboxy-terminal region suggests that FLCN shares a distant structural homology with differentially expressed in normal cells and neoplasia (DENN) domain proteins [36]. Proteins comprising the DENN domain generally belong to the family of RAB guanine nucleotide exchange factors (GEFs) and play important role in vesicular trafficking [37]. FLCN is known to act as a classical renal tumor suppressor, first because second hit mutations were detected in renal tumors from BHD patients [25,33], and second because the FLCN transcript is not detected in these tumors [34].

1.2.3 FLCN-interacting proteins

1.2.3.1 AMPK

In 2006, FLCN was found to bind the 5'AMP-activated protein kinase (AMPK) [38], a central regulator of energy homeostasis. AMPK is a heterotrimeric protein complex highly

conserved across evolution, from yeast [39], nematodes [40,41], and flies [42] to mammals [43-46]. AMPK comprises a catalytic subunit α and two regulatory subunits β and γ [43,45,46]. It is generally activated upon energy crisis which could be triggered by starvation or exercise and other stresses in order to restore energy levels. In general, activation of AMPK induces catabolic processes which generate energy, and suppresses the energy-consuming anabolic processes [44,46]. Allosteric activation of AMPK by binding of AMP to the γ subunit has been reported and is suggested to increase its activity by tenfold [47]. AMPK could also be also activated more than a 100 fold via phosphorylation of a critical threonine residue in the catalytic domain by upstream kinases [48]. The AMPK regulation by upstream kinases and phosphatases is not fully elucidated. In mammals, LKB1 is the major upstream kinase that phosphorylates AMPK on Thr 172, and the AMP-binding to the γ subunit, modulates AMPK activation by LKB1, since it favors Thr172 phosphorylation and prevents its dephosphorylation [49-51]. LKB1 acts with the help of two accessory proteins conserved across evolution, STRAD and MO25 [49-51]. Ca^{2+}/calmodulin-activated protein kinase kinases and specifically CaMKKβ are other AMPK activators that act in response to increases in Ca^{2+} intracellular levels [52].

AMPK is normally activated by metabolic stresses that inhibit ATP production such as starvation, mitochondrial poisons, oxygen deprivation, and exercise [43,53]. AMPK orchestrates signaling cascades via activation of downstream targets involved in cellular energy homeostasis. For instance, AMPK regulates cell growth by inhibiting the mammalian target of rapamycin (mTOR) by phosphorylation of the tumor suppressor tuberous sclerosis complex 2 (TSC2) or the regulatory associated protein of mTOR (raptor) [30,54]. The inhibition of mTORC1 prevents this complex from activating downstream substrates involved in cell growth and proliferation. AMPK also regulates cell growth via phosphorylation of p53 and CDK inhibitor p27 [55,56].

Autophagy which is a self-degradation process that eliminates damaged cellular components and produces energy is also activated by AMPK [57]. Autophagy is introduced in more details in section 1.4. AMPK activates autophagy via inhibition of mTORC1 [58,59], which is a negative regulator of autophagy, or by directly activating the autophagy process through phosphorylation of the autophagy gene ULK1 [58,60]. The regulation of autophagy via ULK1-dependent activation by AMPK is evolutionarily conserved [58]. The worm homolog of ULK1, ATG-1, has been also shown to be required for the AMPK-dependent autophagy in *C. elegans* [58]. Other autophagy components have been also found to be targets of AMPK [61].

AMPK orchestrates many metabolic enzymes and transcription factors to regulate cellular metabolism. For instance, AMPK controls fatty acid synthesis via phosphorylation of Acetyl-CoA carboxylases ACC1 and ACC2, key enzymes in this process [62,63]. Upon acute energy crisis, AMPK suppresses glycogen synthesis via phosphorylation of glycogen synthase-1 (GYS-1) on site 2 (S7) [64,65]. AMPK also controls glucose uptake by inducing the expression of the glucose transporter GLUT-4 and by regulating its translocation to the cellular plasma membranes following exercise and insulin [66,67].

The AMPK-dependent regulation of transcription to adapt to stressful situations has received a lot of interest. In addition to its ability to phosphorylate a large number of transcription factors and transcriptional coactivators involved in stress response, AMPK has been shown to directly regulate transcription through phosphorylation of histone H2B on serine 36 and chromatin remodeling. AMPK has been also shown to regulate H2B O-GlgNAcylation via phosphorylation of O-linked β N-acetylglucosamine transferase, inhibiting its association with the chromatin. Many transcription factors and transcriptional coactivators function downstream AMPK signaling. For instance, AMPK regulates mitochondrial gene expression via phosphorylation of the transcriptional coactivator

proliferator-activated receptor gamma 1 co-activator (PGC-1), which is a master controller of ERRα, NRF1, NRF2, and PPARs [68,69-73]. AMPK also regulates the CREB family of transcription factors in mammals and in lower organisms [74,75]. Recent work has demonstrated that AMPK is able to phosphorylate HIF-1 [76]. In parallel to this finding, our laboratory recently demonstrated that HIF-1 target genes are regulated by AMPK [77]. The role of AMPK in stress response is evolutionarily conserved. In lower organisms, other than controlling stress resistance mechanisms, AMPK signaling also influences lifespan. In *C. elegans*, the α2 catalytic subunit of AMPK is required to extend lifespan and resist various stresses including oxidative stress, dietary restriction, heat, and starvation [41,78-80].

How FLCN regulates AMPK function and which downstream events are affected remain unclear since both AMPK activation and inhibition upon loss of FLCN have been reported. This is discussed in more details in section 1.2.4 of this chapter.

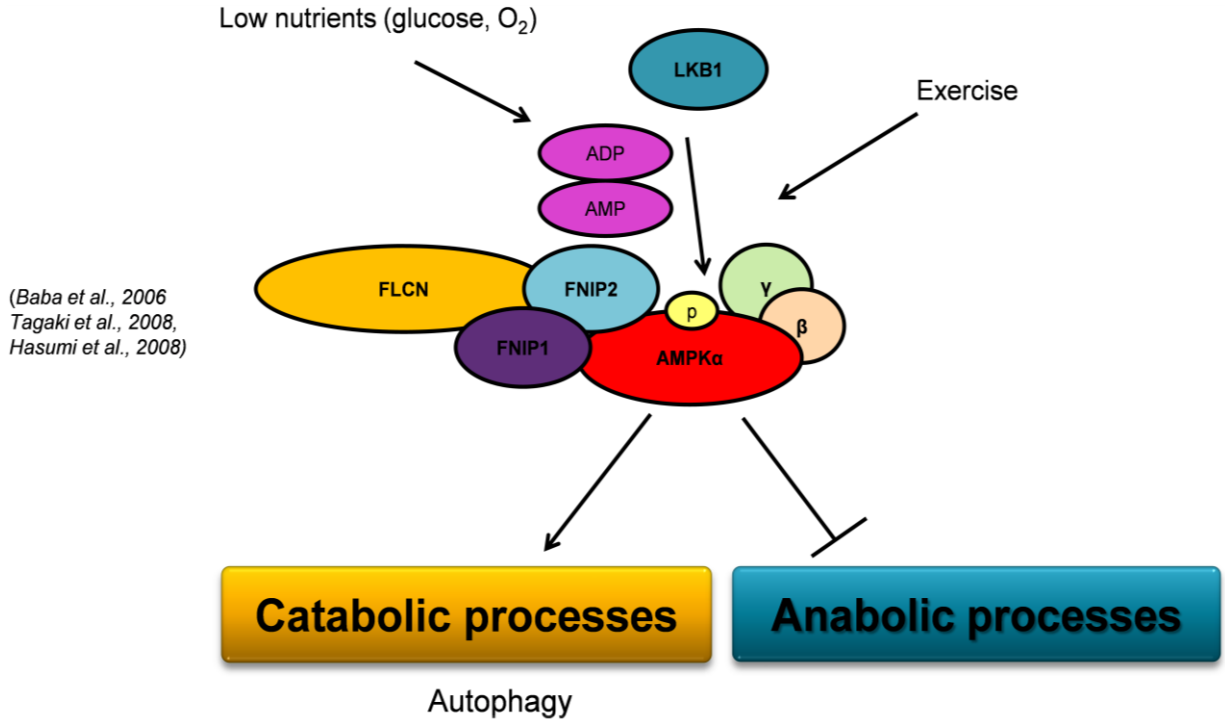

Figure 1.1: Schematic representation of AMPK signaling.

AMPK is a heterotrimeric complex comprising 3 subunits α, β, and γ. It is activated by upstream kinases upon low energy which could be caused by exercise, low oxygen, or nutrient deprivation, via phosphorylation of Thr 172 in the catalytic loop of the α subunit. In general, AMPK activation leads to the inhibition of anabolic processes and the activation of catabolic processes including autophagy.

1.2.3.2 Folliculin-interacting proteins: FNIP1 and FNIP2

FNIP1 and FNIP2 have been identified as binding partners of the FLCN/AMPK complex [38,81]. FNIP1 is an evolutionary conserved 130KDa protein that interacts with FLCN through the C-terminus region and phosphorylates it [38]. FLCN and FNIP1 were shown to colocalize in the cytoplasm and are associated with AMPK and mTOR signaling [38]. FNIP1 has been recently shown to be essential for the proper maintenance of metabolic homeostasis and B-cell development and maturation in mice [82,83]. Recently, two research groups have demonstrated that FLCN and FNIP1 localize to the lysosome and are responsive

to the cellular abundance in amino acids [84,85]. Upon high amino acid levels, FLCN and FNIP1 are recruited to the lysosomes and bind Rag GTPases leading to the activation of mTORC1 and subsequent sequestration of Transcription factor EB (TFEB) in the cytoplasm, a transcription factor responsible for lysosomal biogenesis [85]. In contrast, when amino acid levels are low, FLCN and FNIP1 detach from the lysosome, leading to the inactivation of mTORC1 and the nuclear translocation of TFEB [85]. FNIP2 is homologous to FNIP1 and shares 49% identity and 74% similarity [81,86]. FNIP2 is also known as a FNIP-like or FNIPL protein and has been demonstrated to be important to induce apoptosis upon O6-methylguanine DNA mispairing [87]. Similarly to the amino acid-dependent regulatory role of FLCN/FNIP1 on the lysosomes, FNIP2 also localizes to the lysosome, and the FLCN/FNIP2 complex binds lysosomal Rag GTPases, activating mTORC1 when amino acid levels are sufficient [84]. FNIP2 mutation leads to the hypomyelination of the brain and a myelination defect of the spinal cord in the Weimaraner dog [88]. FNIP1 and FNIP2 bind the C-terminus of FLCN [38,86,89]. Most FLCN mutations in BHD patients are predicted to introduce a stop codon and truncate the protein, which leads presumably to its inability to bind FNIP1 and FNIP2, suggesting that FNIP1 and FNIP2 significantly contribute to the biological role of FLCN.

1.2.3.3 Other FLCN-interacting proteins

Other FLCN binding partners have been also identified. FLCN has been recently shown to interact with Rag proteins on the surface of lysosomes to modulate mTORC1 activity upon amino acid stimulation, independently of the scaffolding FNIP1 and FNIP2 proteins [84,85,90]. ULK1 and GABARAP are other FLCN-interacting proteins known for their involvement in the autophagy process [91]. Moreover, the regulatory particle triple-A ATPase 4 (Rpt4) and Plakophilin-4 (PKP4), which are involved in ribosomal RNA synthesis

and cytokinesis and Rho signaling respectively, have been also shown to interact with FLCN [92-94]. However, how these interactions are linked to the cellular role of FLCN and how they could drive BHD-related tumorigenesis remains unclear.

1.2.4 The FLCN cellular functions

1.2.4.1 Signaling pathways regulated by FLCN

Since the discovery of the FLCN gene, diverse FLCN-related cellular functions have been reported. However, it remains unclear whether these biological processes are directly regulated by FLCN or they are simply a result of indirect effects related to FLCN. FLCN has been shown by several groups to regulate AMPK and mTORC1 signaling, an expected finding since FLCN binds AMPK [38,89,95,96]. However, it was uncertain how FLCN regulates AMPK and mTORC1 functions since both activation and inhibition of these signaling pathways have been reported [38,87,96-99]. Therefore, the cellular response to FLCN loss appeared to be context-dependent and confusing in regards to AMPK-mTORC1 signaling.

In addition to AMPK-mTORC1 signaling [38,89,95,96], FLCN loss has been shown to lead to deregulation in tumor-driving signaling pathways that alter metabolism, cellular proliferation, and cell death. Such pathways include apoptosis [98,100], cell-cell adhesion [94,99], autophagy [101,102], cilia regulation [103], TGF-β signaling [98,104], B-cell development [83], and stem cell differentiation [105], rendering the understanding of the FLCN-mediated tumor suppression mechanism very difficult.

1.2.4.2 Transcription factors and transcription coactivators regulated by FLCN

Genome wide gene expression analyses and protein arrays upon FLCN deficiency have been performed in multiple systems and cell lines to determine pathways regulated by FLCN [93,106,107]. Using UOK257 cells, a *FLCN*-deficient kidney cell line derived from a BHD tumor, and in comparison to UOK257 cells rescued for *FLCN* expression, loss of *FLCN* has been linked to tumorigenesis via regulation of key genes involved in TGF-β, angiogenesis, and cadherin signaling [106]. Another study exploited renal and non renal FLCN-deficient cell lines to determine differential gene expression and found an alteration in the expression of genes involved in Wnt and cadherin signaling pathways [107]. Moreover, by performing gene expression profiling of six renal tumors isolated from BHD patients, another research group have demonstrated that mitochondrial and oxidative phosphorylation-related genes are highly upregulated in BHD tumors and correlate with a deregulation in the PGC1α signaling [108]. As mentioned earlier, PGC1α is a key transcriptional co-activator involved in the regulation of cellular mitochondrial biogenesis and function [109,110].

This last result is in accordance with several reports, including a new manuscript published by our laboratory [77], that link aberrant FLCN and FNIP1 signaling to the induction of mitochondrial biogenesis via PGC-1 [77,111,112]. Specifically, Hasumi et al., demonstrated that the selective knock out of *Flcn* in mouse muscles increases mitochondrial biogenesis and oxidative metabolism [111]. Accordingly, *Fnip1* null mice have been recently shown to display an increased mitochondrial biogenesis and function in a PGC1α-dependent manner [112]. Our research team has also demonstrated a requirement for PGC1α in the metabolic reprogramming of cancer cells lacking *FLCN* and *AMPK* [77].

Other transcriptional co-activators and transcription factors have been also linked to FLCN including transcription factors E3 and EB (TFE3 and TFEB) [85,104] and the

hypoxia-inducible factors HIF-1α and HIF-2α [77,97]. TFE3 and TFEB belong to the micropthalmia family of transcription factors and have been associated with human renal cancer [113]. In fact, TFEB and TFE3 genes fusions are frequently observed in renal cell carcinomas [113]. However, the mechanistic details of how these fusions might drive carcinogenesis have not been clearly resolved yet [113]. FLCN loss has been shown to promote the nuclear translocation of TFE3 and the expression of GPNMB [104], an important hallmark for kidney cancer. Accordingly, FLCN has been also shown to regulate lysosomal function via mTORC1-dependent phosphorylation and sequestration of TFEB, another transcription factor from the Microphtalmia-associated transcription factor family (MiTF) [85].

Among other transcription factors regulated by FLCN, HIF-1α is central to promote angiogenesis and cancer cell survival [11]. Loss of FLCN in cells has been also shown by us and by others to increase the activity of the HIF-1α [77,97]. Specifically, we have shown in a recent publication in parallel to this work that the HIF-1α target genes are significantly induced in cells lacking FLCN and that HIF-1α is essential to promote the formation of colonies on soft agar in the absence of FLCN [77].

Whether these transcription factors coordinate together to drive carcinogenesis in BHD patients remains elusive. Future work aiming to address this point would be of great interest and will contribute to the understanding of BHD disease.

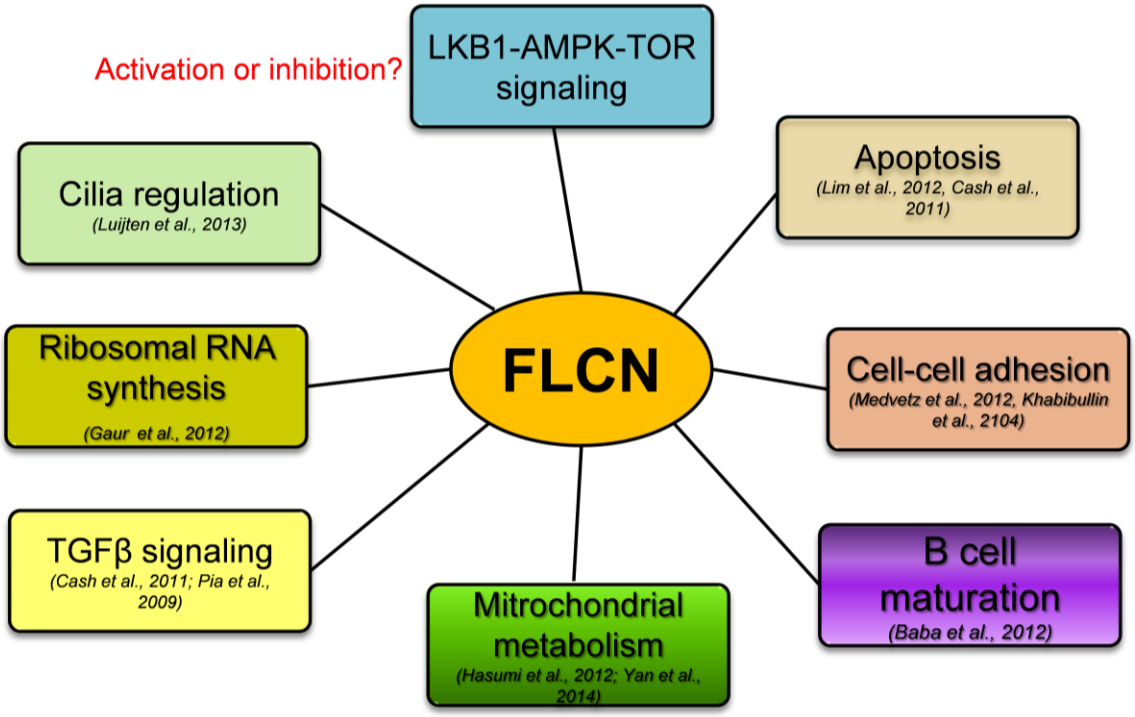

Figure 1.2: Diverse cellular functions attributed to FLCN.

1.3.3 Model organisms to study FLCN

1.3.3.1 Mammalian BHD models

FLCN has been extensively studied using mammalian models including mouse, rat and dog models as well as lower eukaryotic including *Schizosaccharomyces pombe*, *Drosophila melanogaster*, and *Caenorhabditis elegans*. Briefly, in all mammalian models, loss of FLCN resulted in prominent and fast apparition of kidney tumors and cysts indicating that FLCN acts as a renal tumor suppressor [96,114-117]. Importantly, homozygous loss of FLCN led to embryonic lethality in the Nihon rat and mice models while heterozygous loss of FLCN led to the prominent development of renal tumors and cysts in these models [96,114,115]. Importantly, kidney-specific homozygous loss of FLCN in mice resulted in the development of enlarged kidney cysts and tumors as early as three weeks postpartum causing

renal failure and death [116,117]. In addition to mice and rat models, a naturally occurring mutation in the canine chromosome 5 on a region overlapping with FLCN in the German Shepherds dog has been originally described in 1985 [118] and shown to result in kidney neoplasm and skin nodules similarly to BHD syndrome in humans [119]. Constitutive homozygous mutation of FLCN in dogs has been also shown to be lethal [119]. Notably, in all mammalian models, mice, rats, and dogs, the loss of heterozygozity in renal cysts and tumors has been reported, demonstrating that FLCN is a conserved classical renal tumor suppressor that functions according to the Knudson two-hit theory [120,121].

1.3.3.2 Invertebrate BHD models

Lower eukaryotic models have been also developed to genetically study upstream and downstream signaling pathways related to FLCN including models in *Drosophila melanogaster* [122] , *Caenorhabditis elegans* [123] and *Schizosaccaromyces pombe* [124]. Briefly, loss of FLCN in both yeast and *Drosophila* was linked to TOR signaling and nutrient-related metabolic regulation [122,124]. In *C. elegans*, loss of *flcn-1* has been linked to the extension of lifespan via *hif-1* [123]. The FLCN-1-dependant regulation of lifespan is in conflict with our results in chapter 2, because of the use of 5-fluoro-2'-deoxyuridine (FUDR), a drug that inhibits the eggs from hatching but "artefactually" influences the lifespan of certain *C. elegans* mutants [125-127]. Findings in the *C. elegans* model and the discussion of the results of this work as compared to *Gharbi et al., 2013*, are developed in more details in chapter 2 [123].

1.3 The nematode *C. elegans*

1.4.1 An overview

Although mammalian model organisms such as mice and rats are highly advantageous to study disease-related biological processes in humans due the close anatomical and physiological similarities between systems, they have disadvantages including space, cost, and time-consuming transgenic technologies. The nematode *C. elegans* has emerged as an excellent model organism to study conserved signaling pathways. In fact, many biological processes are highly evolutionary conserved such that findings in *C. elegans* are applicable to humans. *C. elegans* is a soil free living nematode that relies primarily on bacteria as a food source and could be easily grown and maintained in laboratories at low cost. The size of adult animals is approximately 1 mm in length and 0.2 mm in diameter. The reproductive life cycle is relatively fast. At 22ºC, the embryos develop and eggs hatch after 14 hours from laying time. When conditions are favorable and the food source is available, the first larvae L1 develop and pass through three other larval stages (L2, L3 and L4) reaching the young adulthood stage and adulthood within approximately 46 hours [128]. When conditions are unfavorable such as high temperature, crowding, or when the food source is unavailable, *C. elegans* larvae enter arrest stages including the L1 arrest and the dauer arrest phases. In the dauer stage, the larvae could endure stressful environmental conditions for several months, and reenter the L4 stage when conditions are favorable [128]. *C. elegans* adult animals live approximately 20 to 25 days rendering this animal a remarkable model for aging and stress response studies [128].

Other than it could be easily maintained and that it has a rapid life cycle, another great advantage is that the *C. elegans* genome is fully sequenced and that approximately 60% of the *C. elegans* genes are similar to genes in the human genome [129,130]. Moreover, gene

downregulation using double-stranded RNA could be simply performed by feeding *E. coli* bacteria engineered to produce the dsRNA [131]. Based on this, RNAi feeding libraries have been developed covering most of the *C. elegans* genes, which allows the performance of large genetic screens [132-134]. Moreover, mutant strains are available for genetic studies and many phenotypes are easy to observe and score. Importantly, several tools have been invented and developed including microscopy, transgenesis techniques, biochemical methods, and others to speed up worm research, rendering *C. elegans* an attractive tool to study pathways linked to diseases in humans [130,135].

1.4.2 C. elegans as a model to study cancer signaling pathways

The major signaling pathways that regulate central cellular functions in higher vertebrates including Insulin, Wnt, Ras, Notch, TGF-β signaling are highly conserved across evolution. Importantly, deregulation in pathways that regulate proliferation, cell death, and metabolism is associated with tumor formation and dissemination. Although *C. elegans* nematodes do not develop tumors *per se*, the molecular pathways that lead to cancer in humans are conserved across evolution and lead to other phenotypic outcomes in the worm, which have been successfully used by researchers, to genetically determine molecular interactions and to screen for anticancer drugs [136-138]. In this section, we will specifically develop apoptosis and autophagy since they are linked to cancer initiation and progression and they are directly related to the work presented herein.

1.4.2.1 Apoptosis in C. elegans

Apoptosis or programmed cell death is a fundamental component in the development of *C. elegans* nematodes [139]. Pioneering studies in *C. elegans* led to the discovery of evolutionarily conserved key players implicated in this important biological process. There

are two types of programmed cell death in *C. elegans*: "developmental cell death" which occurs in the somatic tissues throughout worm development, and "germ cell death" which takes place in the gonads of adult hermaphrodites [139-142]. During the embryonic and postembryonic stages of *C. elegans* development, only 131 cells out of 1,090 cells and always the same ones undergo apoptosis to form the adult hermaphrodite [139-142]. The morphological changes in apoptotic *C. elegans* cells are similar to those of mammalian cells and include the DNA fragmentation, chromatin condensation, and the changes in mitochondrial and plasma membrane potentials [139]. Genetic screens for mutants with abnormal cell death in *C. elegans* led to the discovery of four major evolutionarily conserved genes involved in this process: *"cell death abnormal" ced-9, ced-4*, *ced-3*, and *"egg-laying defective" egl-1* [143-145]. Apoptosis is a signal transduction cascade that leads to the activation of the worm homolog of caspase 3, CED-3, which triggers cell death [146-149]. Similarly to the mammalian apoptotic signal transduction pathway, the pro-apoptotic BH3-domain-only protein EGL-1, negatively regulates CED-9, the worm homolog of the anti-apoptotic protein BCL-2, which in turn acts as a negative regulator of CED-4, an adapter protein similar to the mammalian apoptotic protease-activating factor-1 (APAF1), which induces CED-3 (Figure 1.3) [143,150,151 ,152,153]. The binding between CED-4 and CED-3 and the formation of the apoptosome is central to apoptosis induction [153].

Recently, other than being implicated in the regulation of programmed cell death, the apoptosis genes have been shown to regulate *C. elegans* stress response and longevity. In fact, *ced-3* mutant animals have been recently shown to resist several types of stresses including ER stress, heat stress, osmotic stress [154]. Another recent publication has also linked the intrinsic apoptotic pathway to longevity and stress response in *C. elegans* [155]. However, it remains unclear how apoptotic genes are linked to stress resistance in *C. elegans*.

Deregulation of apoptosis in humans has been linked to several diseases including cancer. It is now well-known that some oncogenic mutations that inhibit apoptosis can drive tumor initiation, progression, and metastasis [156]. The accumulation of DNA damage or the defect in DNA repair cause genomic instability leading to the accumulation of mutations, which could transform a normal cell into a malignant cell that divides and proliferates to form tumors [156]. However, cells have developed strategies to prevent cellular transformation, mostly through checkpoints that assess the level of cellular damage and lead to either damage repair or cell cycle arrest and apoptosis [156]. Therefore, the suppression of apoptosis bypasses cellular checkpoints and promotes the survival of malignant populations, which proliferate to generate tumors. A well-known example is the involvement of the tumor suppressor p53 in this process and how its mutation promotes carcinogenesis [157]. Specifically, the "guardian of the genome" p53, is stabilized by stress and cellular damage signals and leads to cell cycle arrest or apoptosis [157]. In many cancers, p53 is mutated and its mutation in mice increases the risk of developing tumors, which has been correlated with the loss of apoptotic ability in many cases. In accordance, many cancers express high levels of the anti-apoptotic protein Bcl-2 supporting that altered cellular apoptosis levels could lead to cancer [158].

Several reports have linked loss of FLCN to resistance to apoptosis. In 2011, Cash et al. reported that loss of FLCN in cells leads to the intrinsic resistance to apoptosis through deregulation of the TGF-β signaling pathway and the reduction in the level of the pro-apoptotic protein Bcl-2 [98]. Accordingly, both FLCN and FNIP1 have been shown to negatively regulate Bcl-2, inhibiting apoptosis in B cells [83]. Moreover, the FNIP2 protein has been also shown to suppress apoptosis [87]. The inhibition of apoptosis by loss of FLCN and its interacting partners supports the initiation and progression of tumorigenesis in BHD patients.

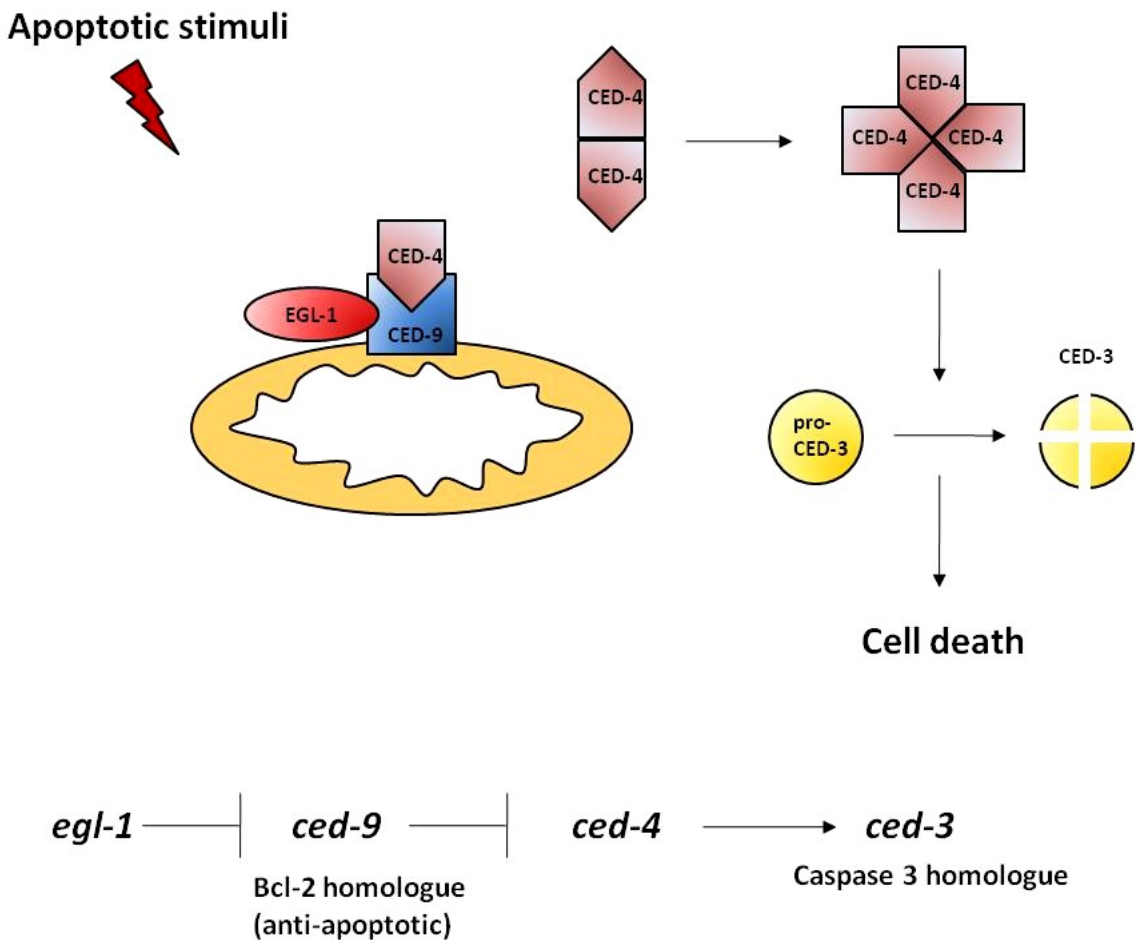

Figure 1.3: Schematic representation of apoptosis in *C. elegans*.

Upon an apoptotic stimulus, EGL-1 binds CED-9 enabling the release of CED-4, which forms the apoptosome, a complex required to activate the worm homolog of caspase 3, CED-3, and induce apoptosis.

1.4.2.2 Autophagy in C. elegans

Autophagy is an evolutionarily conserved "self-degradation" process through which cytosolic compartments and organelles are delivered to the lysosome for degradation (Figure 1.4) [159]. Autophagy exists in three forms: microautophagy where cytosolic components are directly engulfed in lysosomes, mitophagy which involves degradation of mitochondria, and macroautophagy (noted herein as autophagy) where cytosolic material are enclosed in a double-membrane autophagosomal structure that is delivered to lysosomes for degradation by acidic hydrolases [159].

Autophagy is activated by different stresses including nutrient deprivation, oxidative stress, hypoxia, temperature shifts, and others, to eliminate damaged macromolecules and to produce energy [159,160]. Studies in yeast and later in *Drosophila*, mice, and *C. elegans*, greatly contributed to the discovery and characterization of autophagy genes and demonstrated an important role for autophagy in cell growth, development, survival, death, and aging. In *C. elegans*, autophagy is essential for the formation of the dauer stage [161]. Inhibition of autophagy genes causes defects in dauer formation [161]. Autophagy genes were shown to be required for the adaptation of multiple organisms to unfavorable environmental conditions. In *C. elegans*, autophagy genes were shown to be required for resistance to pathogen infection [162], hypoxic injuries [163] and starvation [161,164]. Autophagy activation has been also reported to protect against oxidative stress and is suggested to retard age-related diseases and extend lifespan [137,165,166]. Importantly, the level of autophagic activity decreases with age leading to intracellular damage, cell death, and age-related diseases. As the first genetic link between autophagy and lifespan, inhibition of beclin, *bec-1* in *daf-2* long-lived *C. elegans* mutants has been shown to severely reduce their lifespan [161]. Later, numerous longevity pathways including dietary restriction [164],

calcineurin [167], spermidine [168], resveratrol [169], w-6 polyunsaturated fatty acids [170] have been shown to require autophagy in order to extend *C. elegans* lifespan [171].

The aging and stress resistance function of autophagy is conserved from nematodes to mammals. In *Drosophila melanogaster*, loss of ATG7 reduced lifespan, increased hypersensitivity to nutrient deprivation and oxidative stress, and led to the accumulation of ubiquitin-positive aggregates in degenerating neurons [172]. Moreover, the overexpression of ATG5 in mice was demonstrated to induce autophagy, increase oxidative stress resistance, and extend lifespan [173].

Deficiency in the autophagic pathway causes many human diseases including cancer. Although autophagy has been shown to protect against tumorigenesis since it plays a central role in the clearance of damaged cellular macromolecules and organelles, increasing evidence suggest that autophagy could also acquire tumor-promoting functions [174-177]. By supplying cancer cells with energy, autophagy may promote their survival, since they are often exposed to nutrient deprivation and hypoxia due to lack of blood vessels.

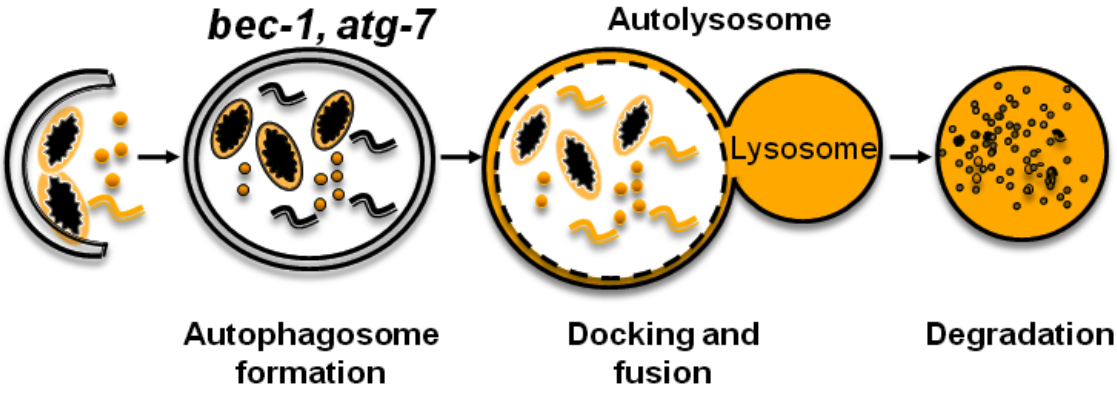

Figure 1.4: Schematic representation of autophagy in *C. elegans*.

Macroautophagy starts with vesicle elongation and nucleation leading to the formation of an autophagosome comprising cytosolic material and organelles to be degraded. The autophagosome fuses with the lysosome forming the autolysosome. The material is then degraded and recycled.

1.4.3 C. elegans stress resistance and cancer

The balance between autophagy and apoptosis is a key factor in the cellular decision between life and death. These two pathways are connected and deregulation in this balance is a main factor in carcinogenesis. Upon cellular exposure to stress, when the damage cannot be repaired, cells normally undergo programmed cell death to eliminate them. When cells escape these control mechanisms and are unable to die, resistant clones emerge which could lead to cancer. Therefore, mechanisms of resistance to stress are often utilized by cancer cells to survive and proliferate. Importantly, the pathways that lead to stress resistance in *C. elegans* are highly evolutionarily conserved and similar mechanisms could be adopted by cancer cells to survive harsh nutrient-deficient and hypoxic microenvironments. In this

section, we highlight stress resistance pathways in *C. elegans* which are linked to tumorigenesis in humans. Specifically, we focus on two types of stresses, oxidative stress and hyperosmotic stress in *C. elegans*, since they are recurrently used in the work presented in this thesis.

1.4.3.1 Oxidative stress

In eukaryotes, oxidative phosphorylation, which takes place in the electron transport chain of the mitochondria, is the main driver of energy production in the form of ATP. Reactive oxygen species (ROS) are a natural byproduct of this process. The main ROS include the superoxide anion ($O_2^{\cdot -}$), the hydroxyl radical ($HO^{\cdot}$), and hydrogen peroxide (H_2O_2) [178]. Despite their important role as signaling molecules, excessive ROS can lead to DNA damage, protein carbonylation, and lipid oxidation. An imbalance between ROS production and detoxification causes oxidative stress, which leads to energy depletion, cellular damage, and triggers cell death [178,179]. Oxidative stress contributes to aging and to the development of many life-threatening diseases including cancer, diabetes, cardiovascular, and neurodegenerative diseases [180-186].

Cells have evolved enzymatic and non-enzymatic defense strategies to maintain proper ROS levels and to protect their constituents against oxidative damage [178,179]. Superoxide dismutase (SOD) enzymes act first to convert superoxide to H_2O_2, which is converted later to water by catalase or peroxidase enzymes [180]. There are three SOD isoforms in humans and five in *C. elegans* [187]. In mammals, SOD1 is localized in the cytoplasm, the nucleus, and in lysosomal compartments. SOD2 and SOD3 enzymes are localized in the mitochondria or excreted to the extracellular matrix, respectively [187]. In *C. elegans*, SOD-2 and SOD-3 are mitochondrial isoforms, SOD-1 and SOD-5 are cytoplasmic, and SOD-4 is predicted to be extracellular [187,188]. In mice, SOD2 deficiency leads to

lethality shortly after birth and the absence of any SOD enzyme renders the animals more sensitive to oxidative stressors such as paraquat [189-191]. In *Drosophila*, deficiency in SOD1 or SOD2 enzymes dramatically shortens lifespan and increases hypersensitivity to oxidative stress [192,193]. In *C. elegans*, SOD enzymes are also required for oxidative stress resistance, yet they were shown to be dispensable for lifespan extension [194,195]. The increased ROS production was shown to increase the activity of SOD and catalase enzymes in *C. elegans* [80,196]. Non enzymatic defense strategies include mostly molecules that react faster with ROS as compared to cellular macromolecules, protecting essential cellular components. Despite the protective role of ROS detoxifying enzymes, some ROS molecules escape the antioxidant defense mechanisms and lead to oxidative damage. Detection, repair, and degradation of the damaged cellular components are essential defense strategies during oxidative stress [178,179].

The implication of oxidative stress in cancer is widely accepted due to the ROS-damaging effects to cellular macromolecules. ROS molecules may participate to cancer initiation by inducing DNA damage, introducing new genetic mutations, and causing genomic instability [178,179,186,197-201]. In mice, oxidative stress induced DNA damage and the formation of modified bases 8-OHdG, a main type of base modification used as a measurement of DNA oxidative damage [202]. Lipids are also attacked by ROS to form lipid peroxyl radicals and lipid hydroperoxides, which have the ability to diffuse across cellular membranes, changing their structure and function [197,198,201]. Protein oxidation modifies protein structure, activity, which interferes with signaling pathways and disrupts cellular homeostasis [197,198,201]. Additionally, by acting as signaling molecules, ROS can alter cellular gene expression and modulate signaling pathways in order to increase cellular proliferation and decrease apoptosis [197,198,201]. Cytokines and growth factors including interferon γ (INF-γ), platelet-derived growth factor (PDGF), transforming growth factor β

(TGF-β), tumor necrosis α (TNFα) and others often induce ROS production speeding up cancer proliferation and survival [199]. AP-1 and nuclear factor kappa B (NF-κb), which play important roles in cellular growth, proliferation, and survival, are examples of ROS-induced transcription factors [198,203]. Furthermore, ROS regulate key signaling pathways involved in cellular proliferation, apoptosis, survival to hypoxic microenvironment, metastasis, including MAPK/ERK1/2, PI3K/Akt, IKK, NF-kB and others [199]. Moreover, oxidative stress has been also tightly linked to inflammation, a main factor that drives tumorigenesis.

Importantly, genetic pathways that alter oxidative stress resistance in *C. elegans* are often linked to cancer in humans. For instance, AMPK, TOR, Insulin, SKN-1/NRF2, CEP-1/p53 and other signaling pathways modulate oxidative stress resistance in *C. elegans* and contribute to cancer in humans [41,78,80,204,205,206]. Similarly, mutations in antioxidant defense enzymes and mitochondrial genes modulate oxidative stress resistance in *C. elegans* and are linked to tumorigenesis in humans [195]. For instance, MnSOD2 has been shown to be frequently deleted in several types of human tumors suggesting that it plays a protective role against cancer initiation [207]. In contrast, the levels of MnSOD2, a novel cancer biomarker, are heightened in cancer cells, presumably due to the increase in ROS levels, which in this case, act as second messengers to promote tumorigenesis [208,209]. Furthermore, catalase overexpression in mammary cancer cells decreased cancer aggressiveness and improved responsiveness to chemotherapy [210].

Unlike cell culture experiments where *in vivo* factors are only partially reproduced, it is of great significance to study oxidative stress in model organisms [136,211]. Several methods aiming to study mechanisms of oxidative stress resistance in *C. elegans* have been developed [78-80]. Specifically, the measurement of *C. elegans* oxidative stress in 96 well plates, a method that we frequently used in this work and that has been recently published (Figure 1.5) [212], is an attractive method to dissect carcinogenesis-related oxidative stress

signaling in humans. Finding pathways, that if altered, provide an optimal ROS balance is thus essential and the screening for drugs that modulate the resistance to oxidative stress could be an incremental cancer cure. Performing these screenings in *C. elegans* is an advantageous fast, inexpensive, and reliable method that has great potential and value for the understanding and treatment of human diseases linked to oxidative stress.

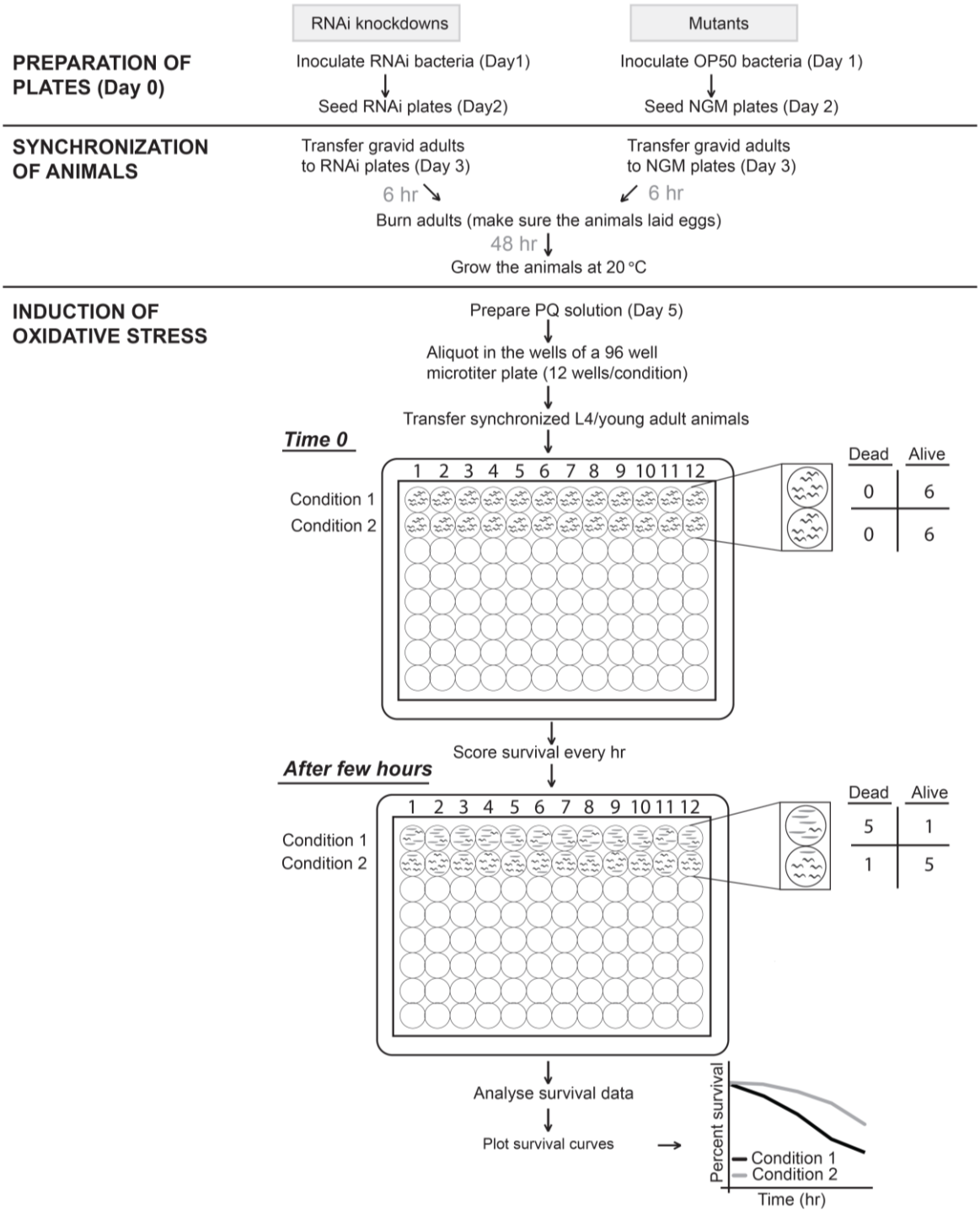

Figure 1.5: Schematic figure of the method of oxidative stress resistance determination in 96 well plates in *C. elegans*.

Synchronized L4/young adult animals grown on NGM plates and fed with OP50 bacteria are transferred to the wells of a 96 well microtiter plate containing 100mM PQ and survival is measured hourly until a large number of worms are dead. In the case of RNAi knockdowns, the same procedure is followed except that the synchronized animals are grown on plates supplemented with IPTG, and are fed with the HT115 bacteria harboring the plasmid that will knockdown the target gene upon expression.

1.4.3.2 Hyperosmotic stress

Hyperosmotic stress is another stress related to oxidative stress and associated with inflammation and tumorigenesis. When the extracellular osmolarity is higher than the intracellular osmolarity, cells experience hyperosmotic stress, which promotes water flux out of the cell, causing cellular shrinkage, protein and DNA damage, cell cycle arrest and cell death. Most organisms are exposed chronically or accidentally to high salinity environments and the ability to adapt to the availability of water is essential for life. In humans, many organs are exposed to water stress, due to water evaporation such as the skin, or through water osmosis into more concentrated aqueous environments due to physiological processes such as in kidneys, colon, and bladder [213]. Cells/tissues/organisms have evolved adaptive strategies to cope with threatening hyperosmotic environments. These strategies include cytoskeletal rearrangements to offset the mechanical pressure, the upregulation of antioxidant enzymes to neutralize the sudden increase in reactive oxygen species, the induction of transporters to regulate water transport, and the upregulation of heat shock proteins to ensure protein homeostasis [213-215]. In addition to the above-mentioned strategies, the synthesis of compatible organic solutes also called osmolytes is a strategy widely used by all organisms which keeps cellular osmotic pressure equal to that of the external environment [216].

Model organisms including yeast and the nematode *C. elegans* have largely advanced the understanding of signaling pathways involved in the sensing and adaptation mechanisms to hyperosmotic stress. In yeast, the high osmolarity glycerol (HOG)/p38 MAP kinase pathway leads to the transcriptional upregulation of glycerol-3-phosphate dehydrogenase, a rate limiting enzyme in glycerol synthesis [217,218]. In *C. elegans*, hyperosmotic stress also triggers glycerol production mainly via transcriptional induction of glycerol-3-phosphate dehydrogenase *(gpdh-1)* [219]. The GATA transcription factors, ELT-2 and ELT-3, were

shown to be required for *gpdh-1* induction upon stress in osmotic stress resistance mutants [220]. A genome-wide RNAi screen identified several regulators of *gpdh-1* including components involved in protein homeostasis, extracellular matrix, metabolism, and transcription [221]. Importantly, several *C. elegans* mutants display heightened glycerol levels due to constitutive activation of *gpdh-1* [221]. For instance, osmotic stress resistance *osr-1*, osmotic avoidance mutants such as *osm-7*, *osm-8*, and *osm-11*, and mutants of the cuticle collagen including *dpy-7*, *dpy-8*, *dpy-9*, and *dpy-10*, exhibit a transcriptional upregulation of *gpdh-1* and a subsequent heightened glycerol content [220,221]. These mutants are also resistant to osmotic stress demonstrating an important role of glycerol content in resistance to hypertonic environments [222-224]. Although the Hog/p38 pathway is the major regulator of glycerol production in yeast, and despite its important role in the resistance to hyperosmotic stress in both yeast and *C. elegans*, it does not seem to regulate *gpdh-1* transcription in *C. elegans* [224]. Supporting this result, the mutants which display a constitutive activation of *gpdh-1*, do not all require the MAPK/Hog1/p38 pathway for survival to hyperosmotic stress [222-224]. This is not surprising since osmoregulation in multicellular organisms is more complicated and involves osmosensing and osmolyte production in multiple tissues in the animal as compared to unicellular eukaryote. Similarly to its involvement in the response to hyperosmotic stress in lower eukaryotes, the p38/MAPK signaling pathway is also induced by hyperosmotic stress in mammalian cells [225].

Importantly, recent evidence suggest that hypertonic stress significantly contributes to the development of many human diseases including cancer, since both renal and non-renal cells are frequently exposed to hypertonic stresses. For instance, VEGF, which is a master regulator of angiogenesis, has been shown to be induced in human colon cancer cells upon hyperosmotic stress [226]. Moreover, the EGF signaling and the induction of metalloproteases ADAM 9, 10, and 17 have been also associated with hyperosmotic stress in

colon cancer cells [227]. Additionally, several recent reports have linked hyperosmotic stress to the upregulation of S100A4, a protein directly involved in tumor progression and metastasis [228,229]. The expression of S100A4 is mediated by the nuclear factor-activated T cell 5 (NFAT5), a transcriptional regulator of hypertonic stress-regulated genes [228,229]. Upon hyperosmotic environments, damaged cells undergo senescence and/or apoptosis to prevent the formation of resistant clones [214]. Cancer cells might arise by escaping senescence and activating mechanisms that favor resistance to apoptosis even upon damage. Supporting this idea, the recurrent treatment of lymphocyte cells with hyperosmotic medium has been recently shown to lead to the development of an anti-apoptotic cell population [230].

Although, the link between hyperosmotic stress resistance in *C. elegans* and carcinogenesis in humans is not clear, it is possible that the pathways that lead to hyperosmotic stress resistance in *C. elegans* also trigger cancer cell survival in humans. Experiments aiming to address this link will be of great value and are important to elucidate the role of hyperosmotic stress in the promotion of tumorigenesis.

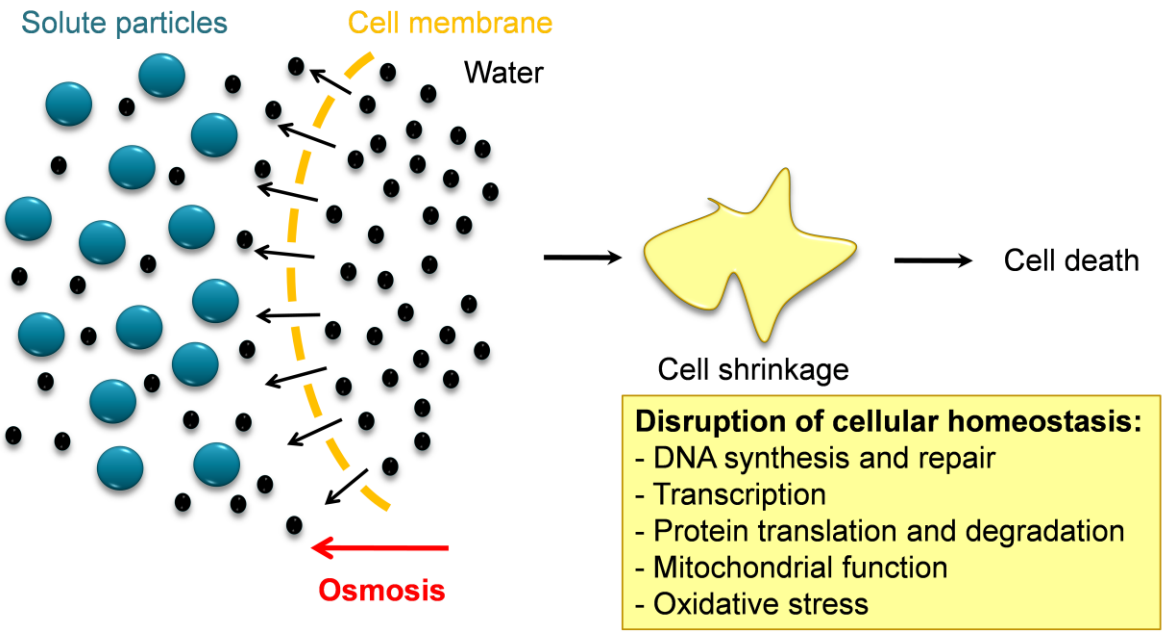

Figure 1.6: Consequences of hyperosmotic stress on cellular functions.

Hyperosmotic stress leads to water loss, cellular shrinkage, and disruption of cellular homeostasis processes, causing cell death.

1.5 An overview of *C. elegans* intermediary metabolism: insights into cancer

The intermediary metabolic pathways, which are chemical reactions related to energy biosynthesis and mobilization, are conserved across eukaryotes and orthologs of most enzymes involved in these metabolic pathways exist in *C. elegans* [231]. These nematodes normally generate ATP by glycolysis, a series of enzymatic reactions that generally breakdown glucose molecules to generate pyruvate, a very important metabolic intermediate. These reactions generate small amounts of ATP. Under aerobic conditions, pyruvate is converted into Acetyl-CoA, which enters the tricarboxylic acid (TCA) cycle in the mitochondria where it undergoes a series of oxidation reaction to generate more ATP via ATP-synthase [231].

The worm intestine is one of the major organs implicated in the biosynthesis and storage of energy reserves including yolk particle, lipids, and glycogen [232]. Immuno-electron micrographs of the *C. elegans* intestine have demonstrated the accumulation of yolk granules, which are dark electron dense vesicles, rich in lipids and proteins (Figure 1.7) [233]. The yolk particles accumulate with age and are synthesized in the intestine and transported later to the pseudoceolom (body cavity) of *C. elegans* animals. These granules have been shown to play central roles during reproduction and animal development [233] and are important for survival to starvation during L1 diapause [234,235].

Fatty acid, amino acid, and carbohydrate metabolisms have been also linked to stress resistance and lifespan in *C. elegans* [236-242]. The breakdown of fat is a major source of energy, and long-lived and stress-resistant mutant nematodes such as *daf-2* and *age-1* have been shown to acquire an altered fatty acid metabolism and an increase in fat content [236]. Moreover, the metabolic profiles of amino acids and carbohydrates in *C. elegans* also reveal the existence of a signature for longevity and stress resistance [241,242]. The food supplementation of all amino acids except Phenylalanine and Aspartate has been shown to prolong *C. elegans* lifespan [240]. Additionally, Tauffenberger and Parker have recently shown that the supplementation with glucose promotes resistance to stress, a phenotype that has been linked to insulin signaling, AMPK, and sirtuins signaling in *C. elegans* [237].

In *C. elegans*, glycogen and trehalose are two major reservoirs of glucose molecules. Trehalose is an alpha-1-linked non-reducing disaccharide of glucose present in microorganisms, plants, fungi, insects, nematodes and some other invertebrates [243-246]. It is synthesized by trehalose-6-phosphate synthases and is degraded by trehalase enzymes [231]. Trehalose has been shown to be required for the extension of lifespan [247] and for the protection against hyperosmotic shock and dehydration in *C. elegan*s [244,245]; two stresses

that result in severe damage of macromolecules. While trehalose is formed from two glucose molecules, glycogen is a glucose polymer complex carbohydrate that also serves as a major source of energy in all organisms [231]. Glycogen synthase and glycogen phospharylase are two important evolutionarily conserved enzymes that catalyze glycogen synthesis and breakdown, respectively [231]. In *C. elegans*, glycogen is normally found in the hypodermis, intestine, and muscles tissues (Figure 1.7). While glycogen has been also shown to mediate a parental-associated effect of stress resistance in *C. elegans* embryos [248], two recent reports have also linked glycogen to hyposmotic-anoxic stress resistance in *C. elegans* [238,239]. However, the mechanism of resistance through glycogen metabolism is not clearly elucidated.

Similarly to the role of carbon source molecules in the stress resistance of lower eukaryotes, cancer cells rely on metabolic reprogramming to generate ATP and survive. In fact, the metabolic properties of cancer cells drift significantly in comparison to those of normal cells [249]. In the 1920s, Otto Warburg has first suggested that an alteration of cellular metabolism could be a major cause of cancer and that cancer cells rely on glycolysis rather than mitochondrial oxidative phosphorylation to produce energy even under aerobic normal conditions [250]. With the advancement of metabolite measurement techniques over the past years, large evidences clearly highlight a key role of metabolism in fueling cancer growth and proliferation [249]. In addition to the reliance on glycolysis, the deregulation of glycogen metabolism and the accumulation of glycogen have been observed in many cancer cell lines and have been associated with cancer aggressiveness and metastasis [251-255].

The relationship between aberrant FLCN signaling and metabolism has been explored in mammalian systems [77,108,111]. We have recently shown that cancer cells lacking FLCN undergo a metabolic reprogramming that favors glycolysis and increases ATP

production [77]. This is in accordance with other published reports showing an increased mitochondrial metabolism and gene expression upon loss of FLCN [111]. In this thesis, using *C. elegans* as a model system, we link stress resistance mechanisms including autophagy and apoptosis to changes in cellular metabolism associated with aberrant FLCN and AMPK signaling.

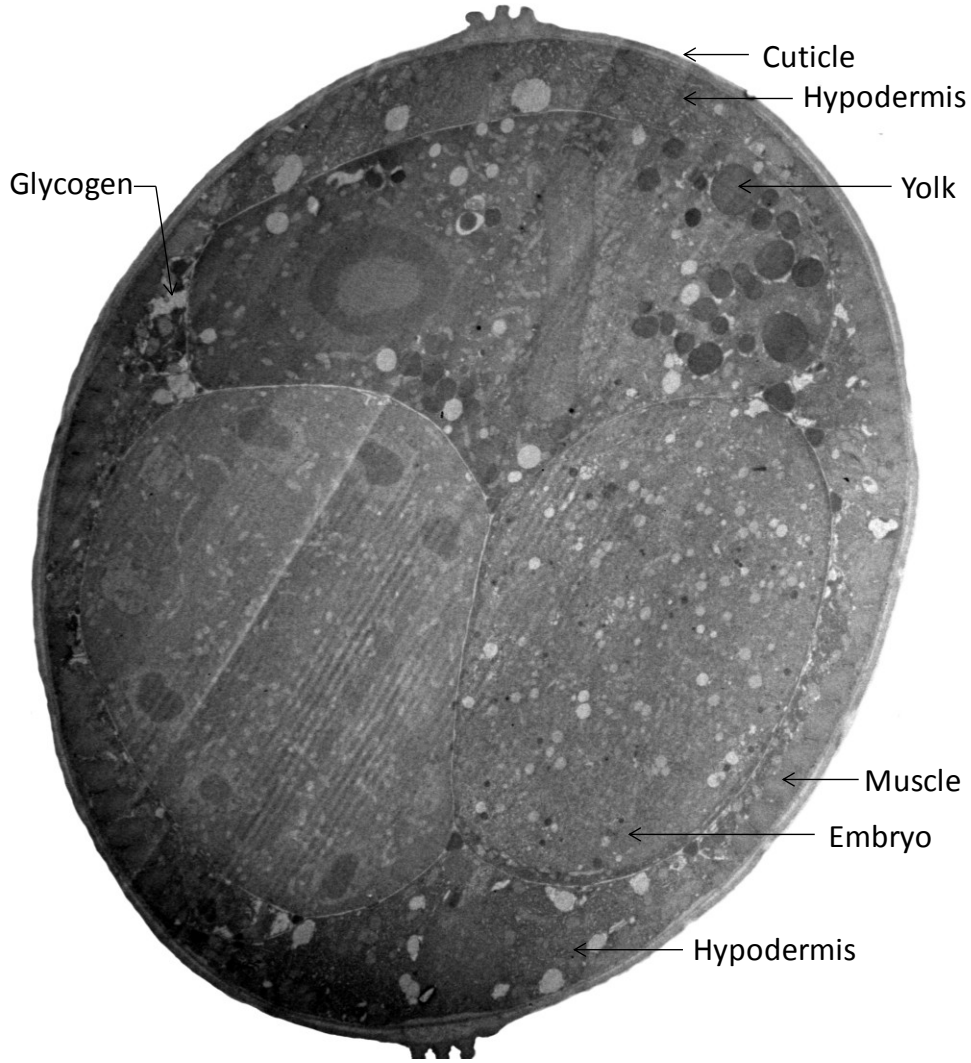

Figure 1.7: Electron micrograph showing a cross section of a wild-type *C. elegans* nematode.

This image has been taken during the electron microscopy work presented later in this thesis. The cuticle surrounds the body of the animal. The hypodermis, muscle, intestine, and the germline/embryo tissues are annotated. The white background of this image has been added by Photoshop. Images with higher magnification of the glycogen stores are presented in chapter 3.

1.6 Research rationale and objectives

Although FLCN is highly conserved across evolution, how loss of FLCN in BHD patients leads to the formation of renal cysts and tumors remains elusive. Diverse cellular functions have been attributed to FLCN, yet it is unclear whether they are direct or indirect effects, which rendered the understanding of the FLCN-mediated tumor suppression mechanism very difficult. FLCN has been shown to bind the 5'AMP-activated protein kinase (AMPK) [38], a central regulator of cellular metabolism [43]. However, the importance and functional consequences of the FLCN-AMPK interaction are unknown and both inhibition and stimulation of AMPK have been reported upon loss of function of FLCN function [97,100].

Model organisms and notably the nematode *C. elegans* have emerged as excellent models to study metabolic regulation and have greatly advanced our understanding of stress response pathways in humans. Since studies in mammalian cells have led to unclear roles for FLCN, the goal of my studies is to genetically determine its function and its interaction with upstream and downstream signaling pathways including AMPK.

Using *C. elegans* and mammalian cells, chapter 2 demonstrates that FLCN is an evolutionary conserved negative regulator of AMPK function. We specifically show that loss of FLCN increases resistance to energy stresses in an AMPK-dependent manner, via increased autophagy and heightened cellular energy. Chapter 3 demonstrates that FLCN-1 regulates hyperosmotic stress resistance via AMPK-dependent remodeling of glycogen stores in *C. elegans*. Chapter 4 shows that loss of *FLCN-1* in *C. elegans* induces a stress response transcriptome prior to stress. Finally, chapter 5 discusses major findings presented in this thesis and suggests future work and perspectives.

CHAPTER 2

FLCN REGULATES AMPK-DEPENDENT AUTOPHAGY AND METABOLIC STRESS SURVIVAL

PLoS Genet. 2014 Apr 24;10(4):e1004273.

Authors/Affiliation

Elite Possik[1,2,5], Zahra Jalali[1,2,5], Yann Nouët[1,2], Ming Yan[1,2], Marie-Claude Gingras[1,2], Kathrin Schmeisser[1,2], Lorena Panaite[1,2], Fanny Dupuy[1,3], Dmitri Kharitidi[1,2], Laëtitia Chotard[1,2], Russell G. Jones[1,3], David H. Hall[4]and Arnim Pause[1,2]

[1]Goodman Cancer Research Center, McGill University, Montréal, Québec, H3A 1A3, Canada

[2]Department of Biochemistry, McGill University, Montréal, Québec, H3G 1Y6, Canada

[3]Department of Physiology, McGill University, Montréal, Québec, H3G 1Y6, Canada

[4]Department of Neuroscience, Albert Einstein College of Medicine, NY10461, New York, USA

[5]These authors contributed equally to this work

2.1 PREFACE TO CHAPTER 2

The *FLCN* gene is responsible for the hereditary human tumor disease called Birt-Hogg-Dubé syndrome (BHD). Patients that inherit an inactivating mutation in the *FLCN* gene develop lung collapse as well as tumors in the kidney, colon, and skin. It is not clear yet what the exact function of this protein is in the cell or an organism. In this chapter, we used a simple model organism (the round worm *C. elegans*) to study the function of FLCN. We found that it is involved in the regulation of energy metabolism in the cell. FLCN normally binds and blocks the action of another protein (AMPK), which is involved in the maintenance of energy levels. When energy levels fall, AMPK is activated and drives a recycling pathway called autophagy, where cellular components are recycled producing energy. In the absence of FLCN in worms and mammalian cells, like in tumors of BHD patients, AMPK and autophagy are chronically activated leading to an increased energy level, which makes the cells/organism very resistant to many stresses that would normally kill them, which in the end could lead to progression of tumorigenesis.

2.2 Abstract

Deregulation of AMPK signaling has been implicated in many human diseases, which emphasizes the importance of characterizing AMPK regulators. The tumor suppressor *FLCN*, responsible for the Birt-Hogg Dubé renal neoplasia syndrome (BHD), is an AMPK-binding partner but the genetic and functional links between FLCN and AMPK have not been established. Strikingly, the majority of naturally occurring *FLCN* mutations predisposing to BHD are predicted to produce truncated proteins unable to bind AMPK, pointing to the critical role of this interaction in the tumor suppression mechanism. Here, we demonstrate that FLCN is an evolutionarily conserved negative regulator of AMPK. Using *Caenorhabditis elegans (C. elegans)* and mammalian cells, we show that loss of FLCN results in constitutive activation of AMPK which induces autophagy, inhibits apoptosis, improves cellular bioenergetics, and confers resistance to energy-depleting stresses including oxidative stress, heat, anoxia, and serum deprivation. We further show that AMPK activation conferred by FLCN loss is independent of the cellular energy state suggesting that FLCN controls the AMPK energy sensing ability. Together, our data suggest that FLCN is an evolutionarily conserved regulator of AMPK signaling that may act as a tumor suppressor by negatively regulating AMPK function.

2.3 Introduction

Birt-Hogg-Dubé syndrome (BHD) is an autosomal dominant neoplasia disorder that was originally described by Hornstein and Knickenberg in 1975 and by Birt, Hogg, and Dubé in 1977 as a disorder associated with colon polyps and fibrofolliculomas of the skin [13,14]. Toro et al. recognized in 1999 that BHD patients were also predisposed to develop kidney cancer mostly of the onococytic, chromophobe, or mixed subtype [15]. However, later studies showed a predisposition for all subtypes of kidney cancer including clear cell and papillary subtypes [16]. In addition, BHD confers an increased risk of pulmonary cysts, spontaneous pneumothorax, and cysts of the kidney, pancreas, and liver [15,17-26].

The gene responsible for BHD, *FLCN*, was mapped to chromosome 17p11.2 by linkage analysis [31,32] and identified in 2002 by positional cloning [26]. *FLCN* encodes a novel cytoplasmic 64kDa protein FLCN, which is expressed in most epithelial tissues [34]. BHD patients carry a loss of function germline mutation in one *FLCN* allele and acquire a second hit somatic mutation or loss of heterozygosity in the remaining wild-type copy in their renal tumors [3,33]. In addition, strains of rats, mice, and dogs with a germline mutation in the *Flcn* gene developed spontaneous kidney tumors with a loss of function in the second allele pointing to a tumor suppressor function of FLCN [120,121,256,257]. However, homozygous deletion of *Flcn* resulted in embryonic lethality in these species [89,96]. Finally, ablation or restoration of *FLCN* in human cancer cells revealed tumor suppressor function in xenograft and soft agar assays [96,106].

Though the FLCN protein presents no significant homology to any known protein, it is highly conserved from unicellular organisms (yeast) through mammalian species (rodents, dog, humans). Moreover, two 130 kDa folliculin-interacting proteins, FNIP1 and FNIP2 have been identified [38,81,86] and implicated in some of the *FLCN* phenotypes in B-cell and stem cell differentiation, and the regulation of apoptosis upon DNA damage [82,83,100,105].

Several studies identified both FLCN and FNIP1/2 as AMPK (5'AMP-activated protein kinase) binding proteins [38,87,258,259]. However, no clear role for FLCN/FNIP1/2 in AMPK function has been described, since both inhibition and stimulation of AMPK have been reported upon loss of function of these genes [97,100]. Strikingly, the majority of naturally occurring *FLCN* mutations predisposing to BHD were predicted to generate truncated proteins unable to bind AMPK pointing to an essential role of this interaction in the tumor suppressor function. Since we and others have observed that FLCN regulates cellular metabolism [97,108,111], we hypothesized that FLCN may regulate cellular energy metabolism through its interaction with AMPK.

AMPK is an evolutionarily conserved master regulator of energy metabolism [43,57,260]. When energy levels drop, AMP or ADP bind to the γ regulatory subunit of AMPK and induce an allosteric conformational change [44,46]. This change leads to the activation of AMPK through phosphorylation of a critical threonine residue (Thr172) in the catalytic subunit and inhibition of its dephosphorylation. When animals and cells encounter stressful environmental conditions leading to lower energy levels, activated AMPK phosphorylates downstream metabolic targets to generate ATP and maintain bioenergetics [43,57,260]. For instance, AMPK activates autophagy, a lysosome-dependent degradation process that recycles cytosolic components to generate new cellular components and produce energy [261]. Recently, AMPK was shown to activate autophagy via binding and phosphorylation of the autophagy initiation kinase ULK1, Beclin 1, and Vps34 [60,61,262].

Since studies in mammalian cells have led to unclear roles for FLCN in AMPK function, we decided to study the genetic relationship between FLCN and AMPK in the model organism *C. elegans*. FLCN and AMPK are conserved in *C. elegans* and loss-of-function mutants are viable. AMPK activation promotes lifespan extension in *C. elegans* [41,74,78,80] and increases resistance to oxidative and other stresses [78-80,263-266].

Here we show that FLCN controls a distinct evolutionarily conserved energy stress pathway by acting as a negative regulator of AMPK function. Loss of FLCN function led to constitutive AMPK activation, which increased autophagy, resulting in inhibition of apoptosis, higher bioenergetics, and thereby enhancing survival to several metabolic stresses. Specifically, we find that the chronic activation of autophagy upon loss of FLCN modifies cellular metabolism, providing an energetic advantage that is sufficient to survive metabolic stresses such as oxidative stress, heat, and anoxia. We confirmed these *C. elegans* results in FLCN-deficient mouse embryonic fibroblasts (MEFs) and human cancer cells demonstrating strong conservation of this pathway throughout evolution. Our results demonstrate that FLCN inhibits AMPK and autophagy functions, which may lead to inhibition of tumorigenesis.

2.4 Results

2.4.1 Loss of flcn-1 confers resistance to oxidative stress in C. elegans

The *FLCN* gene product is highly conserved from *C. elegans* to humans with 28% identity and 50% similarity (Figure 2.1A). To determine the function of FLCN and whether it genetically interacts with AMPK in *C. elegans*, we used a strain carrying the *flcn-1(ok975)* mutation. The *ok975* mutation is an 817 bp insertion-deletion, predicted to truncate the protein at residue 141 resulting in a null or loss-of-function allele (Figure 2.1B). In accordance, the *C. elegans* FLCN-1 polyclonal antibody that we developed recognized a gene product at the predicted size in N2 wild-type but not in *flcn-1(ok975)* animals (Figure 2.1C). Importantly, we did not detect obvious developmental or morphological defects in *flcn-1(ok975)* animals compared to wild-type.

The *C. elegans* AMPK ortholog (*aak-2*; α2 catalytic subunit*)* modulates longevity and tolerance to stresses including oxidative stress, heat, anoxia, and dietary restriction [41,74,78-

80,265]. Since we did not observe a difference in lifespan between wild-type and *flcn-1(ok975)* animals (Figure 2.1D and Table 2.1), we investigated the function of FLCN-1 in stress response by treatment of animals with mild and acute oxidative stress. The *flcn-1(ok975)* mutation conferred an increased resistance to 4mM and 100mM paraquat (PQ), a superoxide inducer [267], which could be rescued in two different transgenic lines expressing FLCN-1 (Figures 2.1E and 2.1F and Tables 2.2 and 2.3). In addition, treatment with *flcn-1* RNAi increased the resistance of wild-type animals to low and high concentrations of PQ but did not further increase the resistance of the *flcn-1(ok975)* mutant animals, supporting that the *ok975* mutation is a loss-of-function allele (Figures 2.1G and 2.1H). A similar resistance phenotype was observed upon H_2O_2 treatment and was rescued with the two transgenic lines expressing *flcn-1* (Figures 2.1I). To exclude the possibility that the changes in stress resistance are not due to effects on lifespan of the animals, assays performed on 4mM PQ were accompanied with lifespan controls (Table 2.2). In conclusion, these results demonstrate that loss of FLCN increases resistance to oxidative stress in *C. elegans*.

2.4.2 Loss of flcn-1 confers an aak-2-dependent resistance to oxidative stress

Since FLCN binds to AMPK in mammalian cells, we aimed to determine whether *flcn-1* and *aak-2* interact genetically in *C. elegans*. Similarly to published results [41,78-80], *aak-2(ok524)* mutant animals were more sensitive to PQ stress compared to wild-type (Figures 2.2A and 2.2B and Tables 2.2 and 2.3). Strikingly, *flcn-1(ok975); aak-2(ok524)* double mutant animals displayed reduced survival upon treatment with 4mM PQ (Figure 2.2A and Table 2.2) and 100mM PQ (Figure 2.2B and Table 2.3), similarly to *aak-2(ok524)* single mutants, indicating that *aak-2(ok524)* is required for the *flcn-1(ok975)* phenotype. The *C. elegans* AMPKα1 homolog (AAK-1) was previously shown to be dispensable for

oxidative stress resistance [79]. Accordingly, the *aak-1(tm1944)* mutation did not abolish the increased survival of *flcn-1(ok975)* mutants to PQ (Figure 2.2C and Table 2.3). To further test whether the increased survival of *flcn-1(ok975)* mutants was also dependent on PAR-4, the *C. elegans* ortholog of LKB1 and major upstream kinase of AMPK [43,79], we measured survival to PQ upon *par-4* loss. Interestingly, *par-4(it57),* a strong loss of function allele, only partially suppressed the *flcn-1(ok975)* survival phenotype, leading to a significant increase in the resistance of *flcn-1(ok975); par-4(it57)* animals to PQ compared to *par-4(it57)* animals alone, suggesting that additional inputs might activate AAK-2 to mediate survival (Figure 2.2D and Table 2.3).

Based on these results, we anticipated that loss of *flcn-1* might lead to a constitutive activation of AAK-2 since the observed *flcn-1* loss of function phenotype is similar to the reported AAK-2 overexpression in terms of oxidative stress resistance [74,78]. Although we did not observe an increased abundance of phospho-AAK-2 at residue Thr234 (corresponding to Thr172 in human AMPKα) in *flcn-1(ok975)* animals compared to wild-type, our data demonstrate a significant increase in phospho-AAK-2 levels in *flcn-1(ok975); par-4(it57)* double mutants compared to *par-4(it57)* animals (Figure 2.2E and 2.2F). This is consistent with the observation that *par-4* is not fully required for the stress resistance phenotype (Figure 2.2D and Table 2.3). The increased phosphorylation of AAK-2 only in *par-4(it57)* mutants can be explained by the fact that PAR-4 is the major kinase that phosphorylates AAK-2 in certain tissues of the animal or cellular sub-compartments, which would mask the FLCN-dependent phosphorylation signal on AAK-2 induced by other upstream kinases [79]. Taken together, these results imply that *flcn-1* negatively regulates *aak-2* in *C. elegans*, and that loss of *flcn-1* confers an *aak-2*-dependent resistance to oxidative stress.

2.4.3 Resistance to oxidative stress in the absence of flcn-1 is not dependent on classical ROS detoxification pathways

The insulin/IGF-1-like (DAF-2)/FOXO3a (DAF-16) and target of rapamycin (TOR) signaling pathways are known to control lifespan and stress response in *C. elegans* and other organisms and have been linked to AMPK signaling [41,78,137,138,268]. While *daf-2(e1370)* mutants exhibited an increased survival to PQ compared to wild-type animals, the *flcn-1* mutation further increased the resistance of *daf-2(e1370)* animals (Figure 2.3A and Table 2.3). Consistently, *daf-16(mu86)* slightly reduced but did not suppress the resistance of the *flcn-1(ok975)* animals to PQ (Figure 2.3B and Table 2.3). Moreover, we found that the PQ resistance of the *flcn-1(ok975)* animals treated with TOR*(let-363)* RNAi was significantly higher than wild-type animals fed with the same RNAi (Table 2.3).

Transcriptional upregulation of ROS detoxification enzymes prior to stress could explain the increased survival of *flcn-1(ok975)* [180]. We did not observe a significant increase in the gene expression of superoxide dismutases (*sod-1, sod-2, sod-3, sod-4,* and *sod-5*) or catalases *(ctl-1, ctl-2,* and *ctl-3),* in *flcn-1(ok975)* mutants when compared to wild-type (Figure 2.3C). Furthermore, we quantified the oxidative damage to protein and DNA. Levels of protein carbonylation and DNA damage were equal in both wild-type and *flcn-1(ok975)* animals under basal conditions and were similarly induced after PQ treatment (Figures 2.3D and 2.3E). Taken together, these findings suggest that the increased survival of *flcn-1(ok975)* mutant to PQ may not be dependent on classical oxidative stress resistance mechanisms.

2.4.4 Increased autophagy upon loss of flcn-1 confers resistance to oxidative stress

Autophagy has been shown to mediate resistance to oxidative stress across evolution without a clear mechanistic explanation [269]. To investigate whether the increased oxidative stress resistance of *flcn-1(ok975)* mutants was due to autophagy, we measured autophagy levels using several methods. Using electron microscopy, we noticed the frequent appearance of autophagic vacuoles (Figure 2.4B) in *flcn-1(ok975)* mutants at the basal level compared to wild-type animals which increased under PQ treatment (Figures 2.4A and 2.4C). To confirm this result, we used a reporter strain that carries the integrated transgene expressing GFP::LGG-1 (LC3 ortholog). LC3 localizes to pre-autophagosomal and autophagosomal membranes, and GFP-positive puncta are thought to represent autophagosomal structures in this strain [161,164,270]. Importantly, we observed a significant increase in the number of GFP-LGG-1 positive puncta in *flcn-1(ok975)* mutants compared to wild-type animals under basal conditions (Figure 2.4D). Consistently, treatment of GFP::LGG-1 animals with *flcn-1* RNAi increased the number of GFP-LGG-1 puncta (Figure 2.4D). Previous studies in yeast, *C. elegans*, and mammalian cells have demonstrated that LGG-1-II (or LC3-II) is degraded inside the autolysosomes, and that the GFP fragment is resistant to degradation and accumulates when autophagy is induced [271-274]. Therefore, we performed western blot analysis on wild-type and *flcn-1* protein extracts to assess the level and cleavage of GFP-LGG-1. Importantly, western blot analysis showed that both cleaved LGG-1-II and released GFP were increased in *flcn-1(ok975)* mutants, indicating higher autophagic activity (Figure 2.4E).

AMPK has recently been shown to directly induce autophagy in mammals via phosphorylation of autophagy proteins including ULK-1, VPS-34 and BEC-1 [60,61,262]. Moreover, loss of *aak-2* reduced autophagy in *daf-2* mutant animals, while *aak-2* overexpression induced autophagy [262]. Based on these results, we questioned whether the

increased autophagy in *flcn-1(ok975)* animals depends on *aak-2*. Importantly, RNAi treatment against *aak-2* significantly reduced the number of puncta in *flcn-1(ok975)* mutants, demonstrating an *aak-2*-dependent mechanism (Figure 2.4D).

Inhibition of autophagy genes in *C. elegans* reduced survival to certain stresses such as anoxia, starvation and pathogens [162,163,270]. We aimed to determine whether the increased survival of *flcn-1(ok975)* animals to oxidative stress was dependent on autophagy. Strikingly, inhibition of the essential authophagy genes *atg-7* and *bec-1* using RNAi markedly abolished the resistance of *flcn-1(ok975)* to PQ (Figures 2.4F-2.4I and Tables 2.2 and 2.3). Taken together, these results demonstrate that loss of *flcn-1* induces autophagy, which is required for *flcn-1*-mediated stress resistance.

2.4.5 Autophagy increases energy levels upon loss of flcn-1

Autophagy is a process that generates catabolic substrates for mitochondrial ATP production and allows cellular macromolecules to be recycled. Since we did not observe a difference in oxidative damage between wild-type and *flcn-1(ok975)* mutant, and since PQ is known to severely decrease ATP levels by inhibiting oxidative phosphorylation [275-277], we wondered if *flcn-1* is mediating an increased resistance to energy stress by employing autophagy as a source of energy. To test this hypothesis, we measured ATP levels prior and after 13 hours of 10mM PQ treatment. Strikingly, we found that *flcn-1* mutant animals have higher levels of ATP before PQ treatment compared to wild-type (Figure 2.5A). As expected, PQ treatment decreased the ATP levels in both wild-type and *flcn-1*, yet ATP levels in *flcn-1(ok975)* nematodes remained higher than wild-type. Importantly, *flcn-1(ok975)* mutants treated with PQ exhibited equal amounts of ATP when compared to the non-treated wild-type animals (Figure 2.5A). To test if the increased energy in *flcn-1(ok975)* mutants is dependent

on autophagy, we treated the wild-type and *flcn-1* nematodes with *atg-7* RNAi and measured ATP levels. Strikingly, downregulation of autophagy completely suppressed the increased ATP levels in *flcn-1(ok975)* mutants in presence or absence of PQ (Figure 2.5A).

To further confirm that loss of *flcn-1* confers resistance to low energy levels, we measured the resistance of wild-type and *flcn-1(ok975)* nematodes to heat stress and anoxia, both of which are known to result in a strong depletion of energy [278]. Accordingly, when exposed to 35°C, the mean survival of *flcn-1(ok975)* animals was significantly higher compared to wild-type (Figure 2.5B and Table 2.4). In addition, the recovery rates after a 26 hours anoxic injury were faster in *flcn-1(ok975)* compared to wild-type (Figure 2.5C and Table 2.5). In conclusion, our data describe a novel mechanism for AAK-2-dependent resistance to oxidative stress, which depends on maintenance of energy homeostasis via autophagy.

2.4.6 Loss of flcn-1 protects against cell death and increases survival to stress

The interplay between autophagy and apoptosis determines the decision between life and death which is very important for the genetic integrity of the cell [279]. The activation of autophagy has been shown to protect against cell death in *C. elegans* and mammals [163,279-281]. To see whether *flcn-1* controls apoptosis in animals, we determined the number of apoptotic cell corpses in the gonad arms of wild-type and *flcn-1* animals upon PQ treatment. As expected, we found that PQ treatment significantly increased the number of apoptotic corpses in wild-type animals (Figure 2.6A). However, the increase in *flcn-1* was much lower suggesting that loss of *flcn-1* protects against cell death. To determine whether the decreased cell death in *flcn-1* nematodes depends on the activation of autophagy, we pretreated the wild-type and *flcn-1(ok975)* nematodes with *atg-7* RNAi and then measured the number of apoptotic corpses upon PQ treatment. Importantly, the inhibition of the autophagy gene *atg-7*

increased the number of apoptotic corpses, up to the same level, in both wild-type and *flcn-1* suggesting that the FLCN-1-dependent activation of autophagy protects against cell death (Figure 2.6A).

Importantly, the apoptotic pathway is conserved from animals to mammals. When cells are destined to die, the BH3 only protein EGL-1 binds and inhibits the BCL-2 homolog CED-9, which activates the caspase CED-3 and leads to death (Figure 1.4) [282]. Therefore, we treated wild-type and *flcn-1(ok975)* animals with *egl-1* and *ced-3* RNAi and assessed their survival to 100mM PQ. Importantly, downregulation of *egl-1* or *ced-3* using RNAi increased the resistance of wild-type animals which was not observed in *flcn-1(ok975)* animals suggesting that the inhibition of the apoptotic pathway leads to the increased resistance (Figures 2.6B-2.6D and Table 2.3). Consistently, treatment of wild-type and *flcn-1(ok975)* animals with *ced-9* RNAi abolished the survival of *flcn-1* animals (Figure 2.6E and Table 2.3). Importantly treatment of *aak*-2*(ok524)* animals with *ced-3* RNAi did not increase their resistance to PQ suggesting that this phenotype depends on AAK-2 (Table 2.3). The increased stress response by inhibition of apoptosis has been recently reported [154]. Although it is not clear whether the apoptosis inhibition in the gonad arms delays organismal death in *C. elegans* or whether apoptotic genes acquire non apoptotic functions, our data suggest an AMPK-dependent involvement of the apoptotic pathway in the increased survival of *flcn-1* animals to PQ stress (Table 2.3).

2.4.7 The FLCN-dependent regulation of AMPK, autophagy, apoptosis, and metabolic stress survival is evolutionarily conserved

To test whether the FLCN functions that we identified in *C. elegans* are evolutionarily conserved, we used wild-type ($Flcn^{+/+}$) and knockout ($Flcn^{-/-}$) MEFs. First, we examined the

cellular resistance to serum starvation (-FBS), which reduces energy levels and induces oxidative stress in a physiological manner (Figure 2.7A) [267]. *Flcn*$^{-/-}$ MEFs were unaffected by serum starvation, as demonstrated by a significant maintenance of cell survival after 4 days of serum starvation, which eliminated almost 80% of wild-type cells. Rescue of wild-type FLCN expression (resc.) reverted this protective phenotype (Figure 2.7A).

Moreover, in accordance with the *C. elegans* results, phospho-AMPK levels were increased upon loss of *Flcn* in MEFs, which could be rescued by expression of wild-type *Flcn,* suggesting that FLCN acts a negative upstream regulator of AMPK (Figures 2.7B). Additionally, down regulation of *Flcn* by shRNA in MEFs lacking AMPKα (*Ampk*$^{-/-}$) did not increase resistance to serum starvation suggesting that the increased resistance to starvation-induced stress depends on AMPK (Figures 2.7C).

Next, we asked whether the AMPK activation in *Flcn*$^{-/-}$ MEFs could be further activated. Importantly, phosphorylation levels of AMPK and its target ACC were maximal in *Flcn*$^{-/-}$ cells and did not further increase upon serum starvation (Figure 2.7I). Similarly, treatment with AICAR (5-amino-1-β-D-ribofuranosyl-imidazole-4-carboxamide), an AMP analogue, increased AMPK activation in wild-type as marked by elevated pACC levels but not in *Flcn*$^{-/-}$MEFs (Figure 2.7I). These results demonstrate that loss of FLCN leads to maximal AMPK activation, which appears uncoupled from its energy sensing function.

Moreover, we wondered whether loss of FLCN also increases autophagy in MEFs similarly to the results obtained in *C. elegans*. Importantly, *Flcn*$^{-/-}$ MEFs displayed an increased number of autophagosomes at the basal level and under serum starvation conditions when compared to wild-type cells as determined by the GFP-LC3 reporter (Figures 2.7D and 2.7E). In addition, chloroquine (CQ) treatment, which inhibits the acidification of autolysosomes, further increased the number of autophagosomes in *Flcn*$^{-/-}$ MEFs suggesting that the autophagy process is not impaired (Figures 2.7E). In agreement with the heightened

autophagy, we observed an increase in the activating AMPK-dependent phosphorylation site at the autophagy initiating kinase ULK1 (Figure 2.7I). To determine whether the increased resistance to serum starvation was due to increased autophagy as we observed in *C. elegans*, we inhibited autophagy using CQ or *Bec-1* shRNA. Inhibition of autophagy strongly suppressed the survival advantage upon serum starvation in *Flcn*$^{-/-}$ MEFs (Figures 2.7F).

Next, we determined whether the chronic activation of autophagy is leading to an energy surplus, which is required for the stress resistance phenotype conferred by loss of FLCN. Similarly to what we found in *C. elegans*, *Flcn*$^{-/-}$ MEFs displayed increased ATP levels under basal conditions (Figure 2.7G). Serum starvation decreased ATP levels in wild-type MEFs, while *Flcn*$^{-/-}$ MEFs maintained ATP levels at wild-type levels (Figure 2.7G). Importantly, inhibition of autophagy with CQ abolished the increase in ATP in *Flcn*$^{-/-}$ MEFs (Figure 2.7G). The ATP, ADP, and AMP levels as well as phospho-creatine, a short term energy reserve, were all increased at the basal level in *Flcn*$^{-/-}$ cells as compared to wild-type, suggesting a general increase in cellular metabolism and energy storage (Figure 2.7H). Importantly, serum starvation decreased energy levels in *Flcn*$^{-/-}$ cells down to wild-type basal levels (Figures 2.7G and 2.7H).

To determine whether loss of FLCN in human cancer cells also conferred an advantage in energy homeostasis, we used the follicular thyroid carcinoma cells FTC-133 lacking FLCN expression, which we rescued for FLCN using stable transfection. First, we confirmed the findings that we obtained with wild-type and *Flcn*$^{-/-}$ MEFs. As expected, loss of FLCN conferred an increased phosphorylation of AMPK as well as a higher LC3 cleavage demonstrating that AMPK activation and autophagy in FLCN-deficient FTC cells is elevated compared to rescued cells (Figure 2.8A). Next, we aimed to determine whether the increased autophagy promoted by loss of FLCN heightens ATP levels at normal conditions in FTC cells. Similarly to what we observed in MEFs, loss of FLCN requires autophagy to increase

ATP levels (Figure 2.8B). To determine whether autophagy contributes to anchorage-independent growth conferred by loss of FLCN, we performed soft agar assays in the presence or absence of autophagy inhibition using *atg7* shRNAs. As expected, loss FLCN significantly increased the number of colonies growing in soft agar in an autophagy-dependent manner (Figures 2.8C and 2.8D). Taken together, these data demonstrate that loss of FLCN leads to an autophagy-dependent increase in ATP levels enabling FLCN-deficient animals/cells to resist metabolic stresses, which could constitute a tumor suppression mechanism.

2.5 Discussion

Maintenance of cellular bioenergetics and management of oxidative stress are essential for life. Here we highlight the discovery of an evolutionarily conserved signal transduction pathway mediated by the tumor suppressor FLCN and AMPK that is essential for resistance to metabolic stress. Loss of FLCN in *C. elegans* and mammalian cells leads to constitutive activation of AAK/AMPK, which in turn increases autophagy. Chronic activation of autophagy leads to increased ATP production and confers resistance to energy depleting stresses by inhibition of apoptosis. Together, our data identify FLCN as a key regulator of stress resistance and metabolism through negative regulation of AMPK (Figure 2.8E).

Several questions arise from these results. First, how is AAK-2 being activated in *flcn-1(ok975)* animals upon loss of PAR-4? Several upstream AMPK kinases other than LKB1 have been identified in mammalian cells, have been shown to affect AMPK activity [43]. Although these kinases have not been linked to AAK-2 in *C. elegans*, our data showed a significant basal phosphorylation of AAK-2 in *par-4(it57)* mutant animals. This is in

agreement with a recently published study showing that starvation and mitochondrial poisons increased phospho-AAK-2 levels in *par-4(it57)* mutant animals, and that the starvation-induced *aak-2* phenotypes were partially dependent on PAR-4 [283]. The fact that the AMPK signaling pathway is evolutionarily conserved suggests that AMPK upstream kinases other than PAR-4 are likely to exist in *C. elegans*. For instance, Pak1/Camkk-beta was first identified in yeast as Snf-1/AMPK-activating kinase and was proven later to act upstream of AMPK in mammalian systems [284-286]. Very recently, CAMKII overexpression was shown to increase lifespan in *C. elegans,* although the link to AAK-2 was not investigated [287]. Together, our data demonstrate that FLCN-1-dependent regulation of AAK-2 mediates an important novel pathway for stress resistance. Interestingly, this pathway is distinct from previously described AAK-2-mediated oxidative stress resistance mechanisms that involve ROS detoxification [78,80,196].

Another unexpected finding is that loss of *flcn-1* did not modulate *C. elegans* longevity under normal growth conditions. The observed increased AAK-2 activation upon loss of *flcn-1* is masked by PAR-4-dependent phosphorylation of AAK-2. General overexpression of AMPK extends lifespan and increase stress resistance [41,74,78,80,262,263,265,288]. Our data suggest that the signaling cascade downstream of FLCN-1/AAK-2 is different from the AAK-2 responses that modulate longevity. It is possible that the PAR-4-dependent activation of AAK-2 extends lifespan and increases stress resistance, while the AAK-2 activation by other upstream kinases only increases resistance to stress. Another possibility would be that a tissue-specific or sub-cellular AAK-2 activation might lead to different outcomes.

Importantly, our data indicate that loss of *flcn-1* extends lifespan only upon treatment with high concentrations (100uM) of the DNA synthesis inhibitor 5-fluoro-2'-deoxyuridine (FUDR) (Table 2.1), a phenotype that has been recently reported by Gharbi et al. [123]. This

drug is frequently used in *C. elegans* aging studies to prevent eggs from hatching and has been recently reported to "artefactually" affect lifespan in mitochondrial *C. elegans* mutants and modulate metabolism in the *daf-2* mutant strain [125-127]. It is not clear why *flcn-1(ok975)* animals exhibit an extension of lifespan only upon treatment with FUDR and what would be the potential mechanism of FUDR action. FUDR may act as a metabolic stressor especially that high FUDR concentrations above 100uM seem to be required to observe the effect on lifespan in *flcn-1(ok975)* animals. Interestingly, lower concentrations of FUDR (5-10uM) that are also sufficient to inhibit germ line proliferation had no effect on lifespan.

Here we show that the enhanced resistance to oxidative stress in the absence of FLCN-1 does not result from a decrease in oxidative damage or an increased transcriptional upregulation of ROS-detoxifying enzymes [78,80,196]. Instead, we show that loss of FLCN-1 activates AAK-2 thereby inducing autophagy. Accordingly, downregulation of *unc-51*, the ortholog of the autophagy kinase ULK1, was shown to suppress the increased number of positive GFP::LGG-1 foci upon overexpression of the kinase domain of AAK-2 in *C. elegans* [262]. More evidence was gathered in mammalian systems to support the direct activation of autophagy by AMPK [60,61,262]. In addition, we show that autophagy is required for the increased ATP in *flcn-1(ok975)* animals and *Flcn*$^{-/-}$ MEFs suggesting that the chronic activation of autophagy in the absence of FLCN recycles building blocks to produce ATP promoting stress resistance.

When energy levels drop in the cell, AMP or ADP bind to the γ regulatory subunit of AMPK and induce an allosteric conformational change [44,46], which leads to AMPK activation through phosphorylation of Thr172 in the catalytic subunit via inhibition of dephosphorylation activities. It is striking that loss of FLCN induces AMPK and autophagy in *flcn-1(ok975)* mutant animals and *Flcn*$^{-/-}$ MEFs, which exhibit high energy levels. These observations suggest that FLCN might be involved in the control of the energy sensing ability

of AMPK. The increased activation of AMPK despite high energy levels has been recently reported upon inhibition of two other inhibitors of AMPK activity [289,290].

The roles of AMPK and autophagy in cancer are puzzling [174,291-293]. Both AMPK activation and autophagy have been shown to acquire anti- and pro-tumor functions [174,291-293]. Our results imply that the AMPK-dependent activation of autophagy might be essential for FLCN-deficient tumor cells to acquire an energetic advantage and drive tumorigenesis. In analogy with our results, autophagy was recently shown to be required for tumor growth in many cancer models. A similar role for VHL, another renal tumor suppressor, in the regulation of autophagic events in renal cell carcinomas has been recently described [294]. In fact, the inhibition of autophagy by MiR-204 suppressed the tumor growth in VHL-deficient cells [294]. Moreover, the LC3B/ATG5-dependent autophagy was shown to be required for the development of VHL-deficient renal cell carcinomas in nude mice [294]. We suggest that the AMPK-dependent autophagy activation upon loss of FLCN promotes the survival of transformed cells, which normally undergo severe metabolic stresses as caused by hypoxia and lack of blood vessels [295]. In agreement with our results, four groups have recently reported that AMPK activation drives tumorigenesis via metabolic stress adaptation of different tumors [293,296,297]. In fact, AMPK is the best-characterized target of the tumor suppressor LKB1 and it was shown recently that loss of LKB-1/AMPK had a positive effect on tumor initiation but a negative effect on tumor progression/dissemination [292,298,299].

The fact that FLCN negatively regulates AMPK strongly implicates that it exerts physiological functions other than being a tumor suppressor. In the past ten years, FLCN was reported to be involved in the regulation of apoptosis, rRNA synthesis, TGF-β signaling, B-cell and stem cell differentiation, ciliogenesis, mitochondrial biogenesis, TOR signaling, epithelial polarization, and cytokinesis without the elucidation of the molecular mechanism

(Figure 1.2) [83,87,89,92-94,96,98,105,106,111]. While this report was under review, two reports have shown that loss of FLCN leads to mTOR inhibition and that it is involved in nutrient sensing via acting as a GTPase activating enzyme for the RAG GTPases [84,85]. It is possible that FLCN acts in two complexes. It binds to RAGs under starvation conditions leading to mTOR inhibition, while in normal conditions FLCN would bind AMPK, inhibiting its activity. However, it is not clear how the reported inhibition of mTOR activity upon loss of FLCN could lead to tumorigenesis, since mTOR was shown to be hyper-activated in tumors of BHD patients and mice devoid of FLCN [89].

In conclusion, we used the model organism *C. elegans* to decipher a genetic pathway, which is regulated by FLCN. We show that FLCN negatively regulates the activity of AMPK, which leads to increased autophagy, energy and survival to metabolic stress. Moreover, we confirmed conservation of this pathway in mammalian cells and suggest that chronic AMPK activation upon loss of FLCN potentiates tumorigenesis via increased autophagy leading to metabolic stress resistance and inhibition of apoptosis, which are two hallmarks of cancer cells [300].

2.6 Material and Methods

Antibodies, reagents and plasmids

The FLCN-1 nematode polyclonal antibody was generated in rabbits with a purified GST-FLCN-1 recombinant protein by the McGill animal resource center services. The ULK1-pSer555 (5869), AMPK-α (2532), AMPK-pThr172 (2531), ACC (3676) and ACC-pSer79 (3661) were purchased from Cell Signaling and the β-actin (AC74) antibody from Sigma-Aldrich. The following reagents were purchased from Sigma-Aldrich: AICAR, methyl viologen dichloride hydrate (Paraquat; PQ), chloroquine (CQ), Acridine Orange.

C. elegans strains, maintenance, RNAi and lifespan assays

C. elegans strains were obtained from the *Caenorhabditis* Genetics Center (see Table 2.6). The *flcn-1(ok975)* strain was outcrossed eight times to wild-type. Nematodes were maintained and synchronized using standard culture methods [128]. The RNAi feeding experiments were performed as described in [132], and bacteria transformed with empty vector were used as control. For all RNAi experiments, phenotypes were scored with the F1 generation except for *aak-2* knockdown (F2). Lifespan assays were performed according to standard protocols [301].

Transgenic strain construction

Expression constructs were generated using the pPD95.77 vector. pRF4 rol-6*(su1006)* was used as a co-injector marker. Transgenic lines were generated by microinjection into the gonad of adult hermaphrodite using standard techniques. The 2.8kb endogenous promoter of *flcn-1* was generated by PCR from wild-type genomic DNA (Forward primer 5'AAAACTGCAGCGTCTTCTCGTTTCACAGTAGTCA-3' and reverse primer: 5'GCTCTAGATTGAATTCTGTAAAAACATGAATTTGA-3') and cloned into pPD 95.77 at PstI and XbaI sites. *flcn-1* cDNA was obtained from an RT–PCR reaction performed on wild-type animals RNA extracts using the following: forward primer 5'GCTCTAGAATGCAAGCAGTAATAGCACTTTGT-3' and Reverse primer 5'CGGGATCCACGAGCAGTAGAGGTTTGAGACTG-3'. The *flcn-1* cDNA was subsequently cloned into pPD 95.77 (GFP expression plasmid-with *flcn-1* endogenous promoter region) at XbaI and BamHI sites.

Cell culture

Primary MEFs were isolated from C57BL/6 E12.5 *Flcn*$^{flox/flox}$ mice. *Ampk*$^{+/+}$ and *Ampk*$^{-/-}$MEFs were described in [93]. Cell lines were maintained in Dulbecco's modified Eagle's medium (DMEM) supplemented with 10% fetal bovine serum (FBS), 100 U/ml penicillin and 100μg/ml streptomycin (Invitrogen).

Stress resistance assays

Resistance to acute oxidative stress (100mM PQ and H_2O_2) was determined as described in [212]. Chronic oxidative stress was assessed on thirty post-fertile animals using 4mM PQ and survival was measured daily. For heat stress, one-day adult animals were transferred to NGM plates and exposed to 35ºC. Survival was measured at indicated time points until all animals died. Concerning anoxia stress, one-day old adult animals were transferred to NGM plates and left in a Bio-Bag Environmental Chamber Type A (Becton Dickinson Microbiology Systems) for 26 hours at 20ºC. Recovery rates were scored at indicated time points. For MEFs, cells were seeded (2×10^4 cells) in 12-well plates and FBS-free media was added 24 hours after plating. Cell numbers were counted daily and survival rates were determined as the percent cell number compared to day 0.

Autophagy analysis by fluorescent microscope

For *C. elegans*, autophagy levels were assessed in hypodermal seam cells of L3 animals using the GFP::LGG-1 transgenic reporter strain DA2123 (See Table 2.6). For MEFs, wild-type and *Flcn*$^{-/-}$ cells were infected with the *pMigR-1-LC*3-GFP, seeded on coverslip (50000 cells in 6 well-plate), serum starved for 12 hours and fixed with 4% paraformaldehyde. Autophagic-GFP positive puncta were quantified in at least 200 cells.

Pictures from nematodes and MEFs were acquired with a Zeiss fluorescence confocal microscope.

Determination of ATP content

For *C. elegans*, synchronized young adults were collected and washed in M9 buffer. Pellets were treated with three freeze/thaw cycles and boiled for 15 min. ATP content in *C. elegans* was measured using an ATP determination kit (Invitrogen) and in MEFs using Cell Titer-Glo Luminescent Cell Viability Assay (Promega). For *C. elegans*, levels were normalized to protein levels and in MEFs normalized to cell number.

DNA and protein oxidative damage assays

Genomic DNAs from worm pellets were purified using Phenol/Chloroform extraction and treated with RNase A for 1 hour at 37ºC. OxiSelect oxidative DNA damage ELISA assay was performed with 8µg of DNA following manufacturer's instructions (Cell Biolabs). Protein oxidative damage was assessed using Oxyblot Protein Oxidation Detection Kit (Millipore).

RNA extraction and real-time PCR

Synchronized young adult nematodes were harvested and total RNA was extracted with Trizol, purified using the RNeasy kit (Qiagen). Quantitative real-time PCR (qRT-PCR) was performed using Express SYBR Green qPCR supermix (Invitrogen) and LightCycler480 system (Roche). Catalase and SOD transcripts were normalized to housekeeping genes *cdc42*, *pmp-3*, and *Y45F10D.4* using Genorm [302]. For primer sequences see Table 2.7.

Protein extraction and western blotting

Cells and synchronized young adult nematodes were washed with ice-cold PBS and M9 respectively and lysed in the AMPK lysis buffer [303] supplemented with the complete protease and phosphatase inhibitors (Roche), 1mM DTT, and benzamidine 1µg/ml. Worm pellets were sonicated and cleared by centrifugation. Percent pAAK-2/pAMPK levels were quantified using ImageJ software and normalized for the AMPK levels.

Transmission electron microscopy

Transmission electron microscopy procedures were performed according to Hall et al., 1995 [122]. Briefly, synchronized L4 wild-type and *flcn-1* animals were separated in two groups and treated with M9 buffer or 50mM paraquat in M9 solution for 2 hours. After incubation, animals were washed three times with M9 buffer and plated on NGM plates allowing 30 minutes recovery. Animals were fixed at room temperature in 1% formaldehyde, 2.5% glutaraldehyde in 0.12 M sodium cacodylate buffer, at pH 7.4. Under a dissecting microscope, animals were cut open in a drop of the fix solution, allowing the fixative to penetrate. After 2 hours, animals were washed three times with 0.15M sodium-cacodylate buffer, at pH7.4. Animals were then post-fixed on ice for one hour in 1% Osmium tetroxide, 0.5% potassium ferrocyanide in 0.12M sodium-cacodylate buffer, at pH 7.4. Following post-fixation, animals were rinsed three times with 0.15M sodium cacodylate (pH7.4) and three more times with 0.15 sodium acetate buffer (pH5.2), and then stained for 7 hours at 4^0C, with 1% uranyl acetate in 1M sodium acetate buffer (pH5.2). Animals were then washed multiple times with 0.15M sodium acetate buffer and double distilled water, grouped, and embedded in 2% agarose in double distilled water. Agarose blocks were dehydrated with a series of increasing ethanol concentrations (30%, 50%, 70%, 95%, and 100% ethanol) and then placed for 45 min in 100% propylene oxide. Blocks were gradually infiltrated with resin using 1:3,

1:1, and 3:1 resin/propylene oxide mixtures. Blocks were further incubated in 100% resin for several hours, then positioned in a flat embedding mold and incubated in the oven at 60^0C for more than 2 days. Thin sections were cut on an RMC Powertome XL (Boeckler Instruments) using a diamond knife (DDK) and collected on Pioloform-coated copper slot grids. Grids were post-stained with 4% uranyl acetate and lead citrate and viewed using a Philips CM10 electron microscope (FEI) equipped with a Morada digital camera (Olympus) and iTEM software (Olympus SIS).

Soft agar assay

FTC cells were trypsinized, counted and resuspended in complete DMEM/F12 media. Two layered soft agar assay were undertaken in six well plates. The bottom layer contains 0.6% agar in complete DMEM/F12 media. The second layer encompasses 0.3% agar mixed with 0.5 million cells. Plates were cultured at 37◦C in 5% CO2.

Apoptosis assay

For worms, apoptotic germ cell corpses were visualized using Acridine Orange (AO) as described in [123]. Worms were incubated for 2 hours in M9 with or without 50mM PQ in OP50, supplemented with 2µl/ml AO (stock of 10mg/ml). Worms were then washed and transferred into light-protected recovery NGM plates for 45 min before visualization.

LC-MS/MS analysis

Targeted metabolite analysis was performed on an Agilent 6430 triple quadrupole mass spectrometer equipped with a 1290 Infinity UPLC system (Agilent Technologies, Santa Clara, CA, USA). Sample temperature was maintained at 4°C while solvents and column temperatures were maintained at 10°C. Metabolites were separated using a 4.0µm, 2.1×100.0mm Cogent Diamond Hydride column (MicroSolv Technology Corporation,

Eatontown, NJ, USA) operating at a flow rate of 0.4 ml/min and 5 µl sample injections. Separation solvent "A" consisted of 15 mM ammonium formate in H_2O, pH 5.8 and solvent "B" consisted of 15 mM ammonium formate in 85% acetonitrile in 15% H_2O, pH 5.8. Chromatography started with a 2 min hold at 97% B, followed by a 5 min gradient to 70% B, then washed for 3 min with 98% A, and re-equilibrated to starting conditions for 6 min. Separated metabolites were introduced to the mass spectrometer via electrospray ionization (ESI) operating in either positive or negative ionization mode and were analyzed by previously optimized multiple reaction monitoring (MRM). Quantification was accomplished by comparing MRM peak areas to those from standard calibration curves using Mass Hunter Quantitive Analysis Software (Agilent, Santa Clara, CA, USA). MRM transitions in negative ionization mode for quantifying and qualifying ions were MRM transitions in positive ionization mode were 212.0 → 90.1 and 212.0 → 114.1 for phosphocreatine and 132.0 → 44.2 and 132.0 → 90.1 for creatine. Gas temperature and flow were set at 350°C and 10 L/min. Nebulizer pressure was set at 50 psi and capillary voltage was +4000V.

Statistical Analyses

Data are expressed as means ± SEM. Statistical analyses for all data were performed by student's t-test, ANOVA, using Excel (Microsoft, Albuquerque, NM, USA), SPSS (IBM, Armonk, NY, USA) and prism software (GraphPad). For lifespan curve comparisons we used the Log-rank Mantel Cox test using GraphPad from Prism Statistical significance is indicated in figures (* $P<0.05$, ** $P<0.01$, *** $P<0.001$) or included in the supplementary tables.

2.7 Acknowlegments

We thank Richard Roy, Christian Rocheleau and Shaolin Li for support and reagents. We thank Michael Hengartner for *ced-3*, *ced-9*, and *egl-1* RNAi feeding clones, Joseph Avruch for *let-363* RNAi feeding clone, Nahum Sonenberg for the shRNA against *Bec-1*

construct, Laura Schmidt for the *Flcn*$^{flox/flox}$ mice and other reagents, and Daina Avizonis and Gaelle Bridon from the McGill Metabolomics core facility for technical assistance and advice. We thank Mr. Ken Nguyen for his help in processing animals for electron microscopy. We also thank the previous lab members Abbas Ghazi and Nathalie Ng Kuet Leong for initiation of the project and Jacky Leung, and Amr Omer for technical support. We acknowledge the *Caenorhabditis* Genetic Center for *C. elegans* strains.

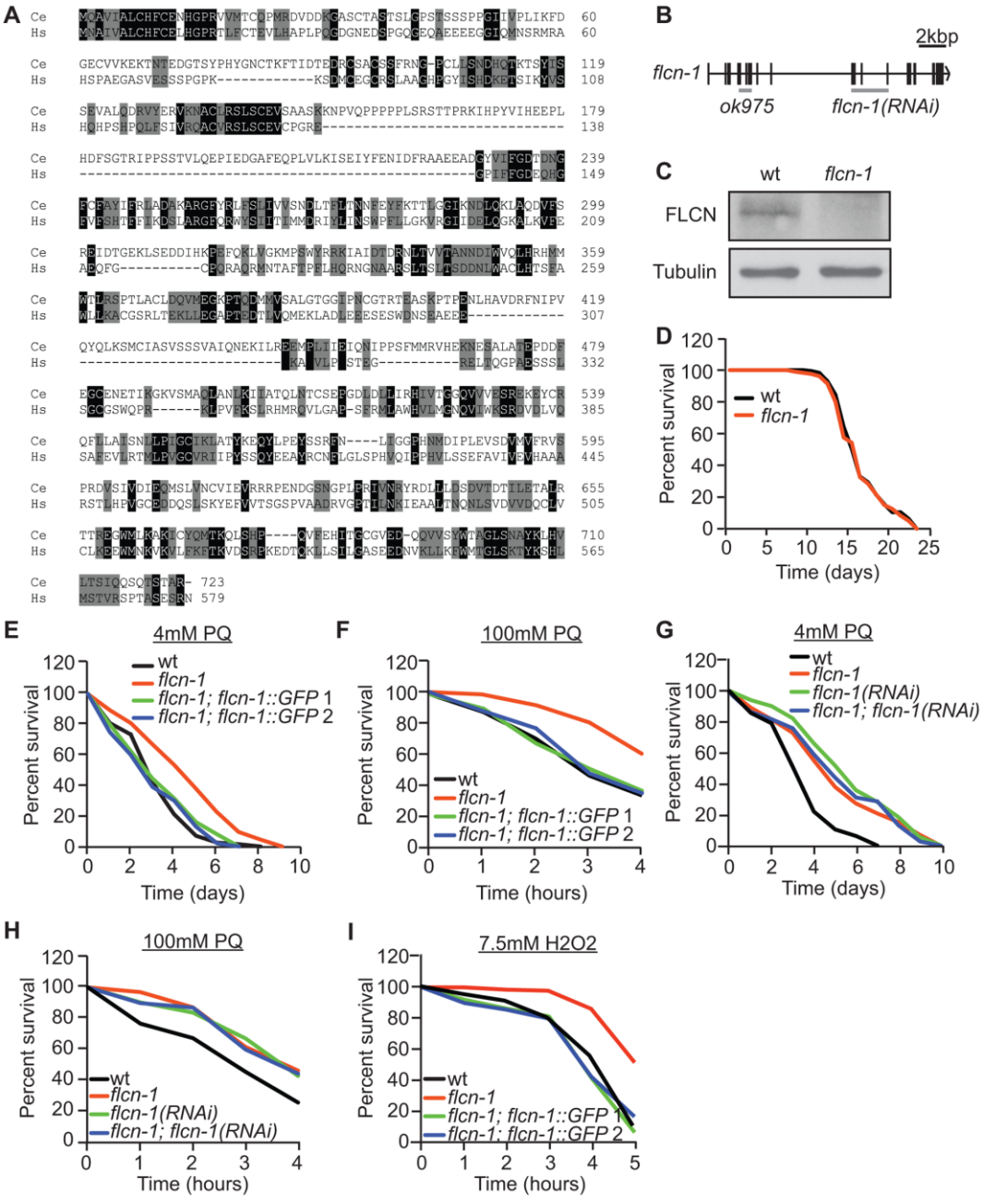

Figure 2.1: Loss of *flcn-1* confers resistance to oxidative stress in *C. elegans*.

(A) Amino acid alignment of the human and *C. elegans* Folliculin sequences (accession numbers: human AF517523, *C. elegans* HE963850). Identical (black) and similar (grey) amino acids are highlighted. (B) Genomic structure of *flcn-1*. The *ok975* mutation and the genomic region targeted by RNAi are indicated. (C) Western blot analysis of FLCN-1 protein levels in wild-type and *flcn-1(ok975)* worm protein lysates. (D) Lifespan of wild-type and *flcn-1(ok975)* nematodes at 20°C (also see Table 2.1). (E-H) Percent survival of indicated worm strains treated with 4mM or 100mM PQ (also see Tables 2.2, 2.3). (I) Percent survival of wild-type and *flcn-1(ok975)* animals after 3h treatment with increasing H_2O_2 concentrations.

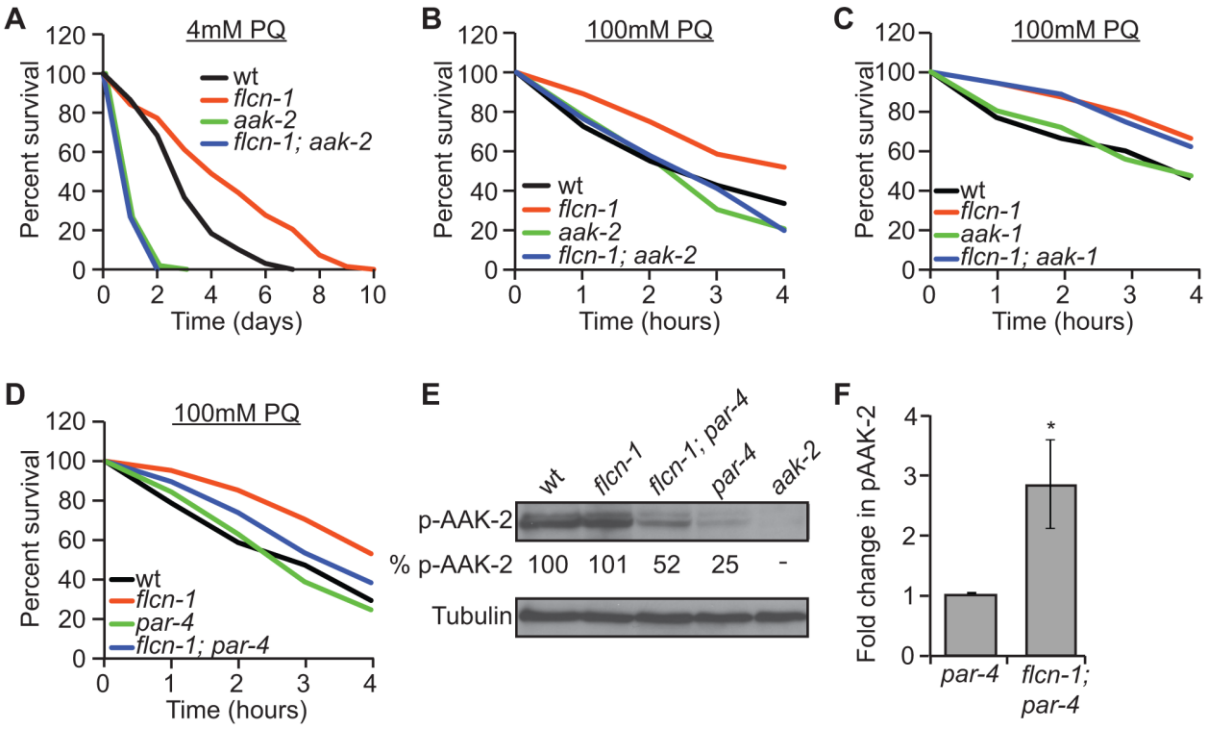

Figure 2.2: Loss of *flcn-1* confers an *aak-2*-dependent resistance to oxidative stress.

(A, B, C, D) Percent survival of indicated worm strains treated with 4mM or 100mM PQ. See also Tables 2.2 and 2.3. (E) Western blot analysis of pAAK-2 (Thr234) protein levels in indicated worm strains. Data represent the means ± SEM, n≥3.

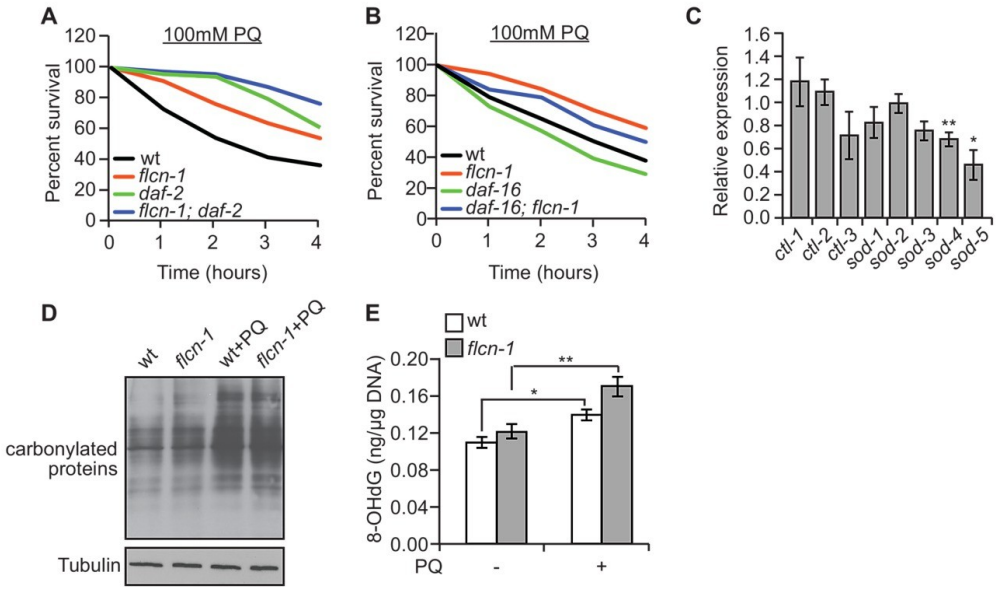

Figure 2.3: The increased survival of *flcn-1* animals to paraquat might not be dependent on classical oxidative stress resistance mechanisms.

(A and B) Percent survival of indicated worm strains treated with 100mM PQ. See also Table 2.3 (C) Relative mRNA levels of the indicated *C. elegans* catalase and SOD genes in wild-type and *flcn-1(ok975)* animals. (D and E) Quantification of the oxidative protein (D) and DNA (E) damage measured in animals treated with or without PQ. Data represent the mean ± SEM, n≥3.

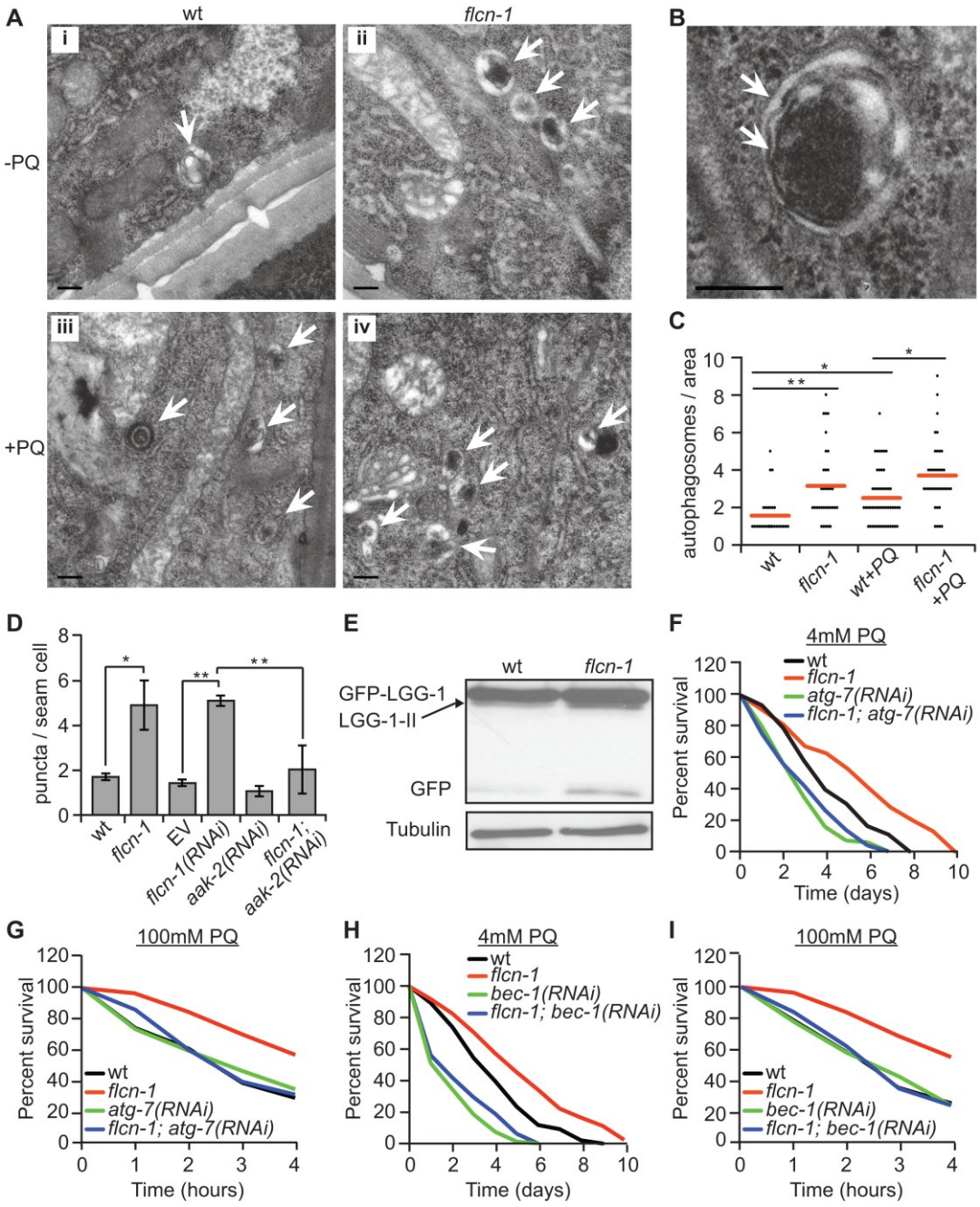

Figure 2.4: Loss of *flcn-1* activates autophagy resulting in oxidative stress resistance in *C. elegans.*

(A and B) Representative electron micrographs from longitudinal sections of the hypodermis in indicated nematodes strains. Arrows represent autophagic vacuoles (A) and autophagosomal membranes (B). Scale bars: 0.2 µm (A and B). (C) Quantification of the autophagic events observed in defined surface area of 4.25 um^2 of electron micrographs taken from at least 5 animals. (D) Number of LGG-1::GFP positive autophagosome puncta in the seam cells of the indicated worm strains. (E) Western blot analysis of the LGG-1::GFP cleavage profile (LGG-1-I, GFP) in worm protein extracts. (F, G, H, I) Percent survival of indicated strains upon 4mM (F and H) or 100mM (G and I) PQ. Data represent the means ± SEM, n≥3. Also see Tables 2.2 and 2.3.

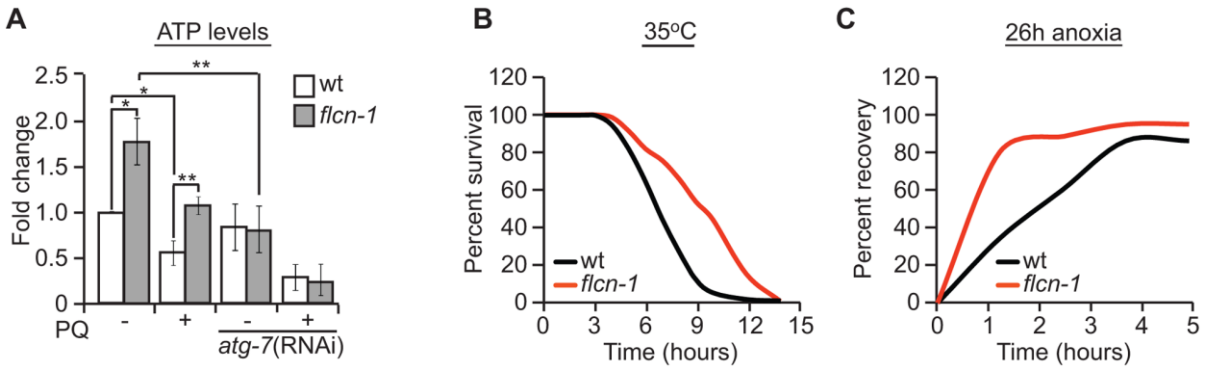

Figure 2.5: Loss of FLCN stimulates cellular energy production and resistance to energy stress.

(A) Relative ATP levels measured in the indicated worm strains treated with or without PQ. (B) Percent survival of wild-type and *flcn-1(ok975)* nematodes upon heat stress (35^0C). (C) Recovery rate of wild-type and *flcn-1*(ok975) strains after 26h anoxic injury. See tables 2.4 and 2.5. Data represent the mean ± SD, n≥3.

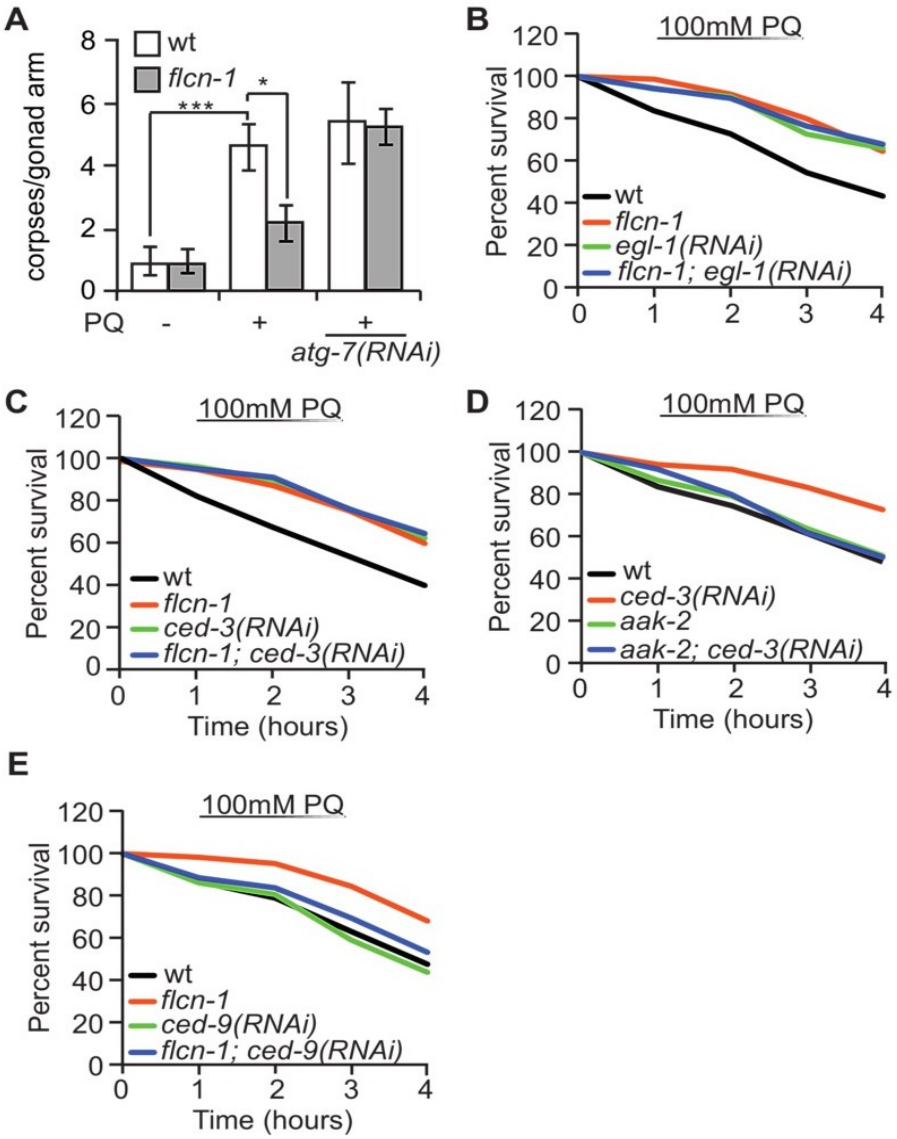

Figure 2.6: Autophagy activation conferred by loss of Folliculin protects against apoptosis.

(A) Quantification of the number of acridine orange positive apoptotic cell corpses in the gonad arms of the indicated strains. (B–E) Percent survival of the indicated worm strains treated with the indicated RNAi feeding clones and exposed to 100mM PQ. See also table 2.3. Data represent the means ± SEM N≥3.

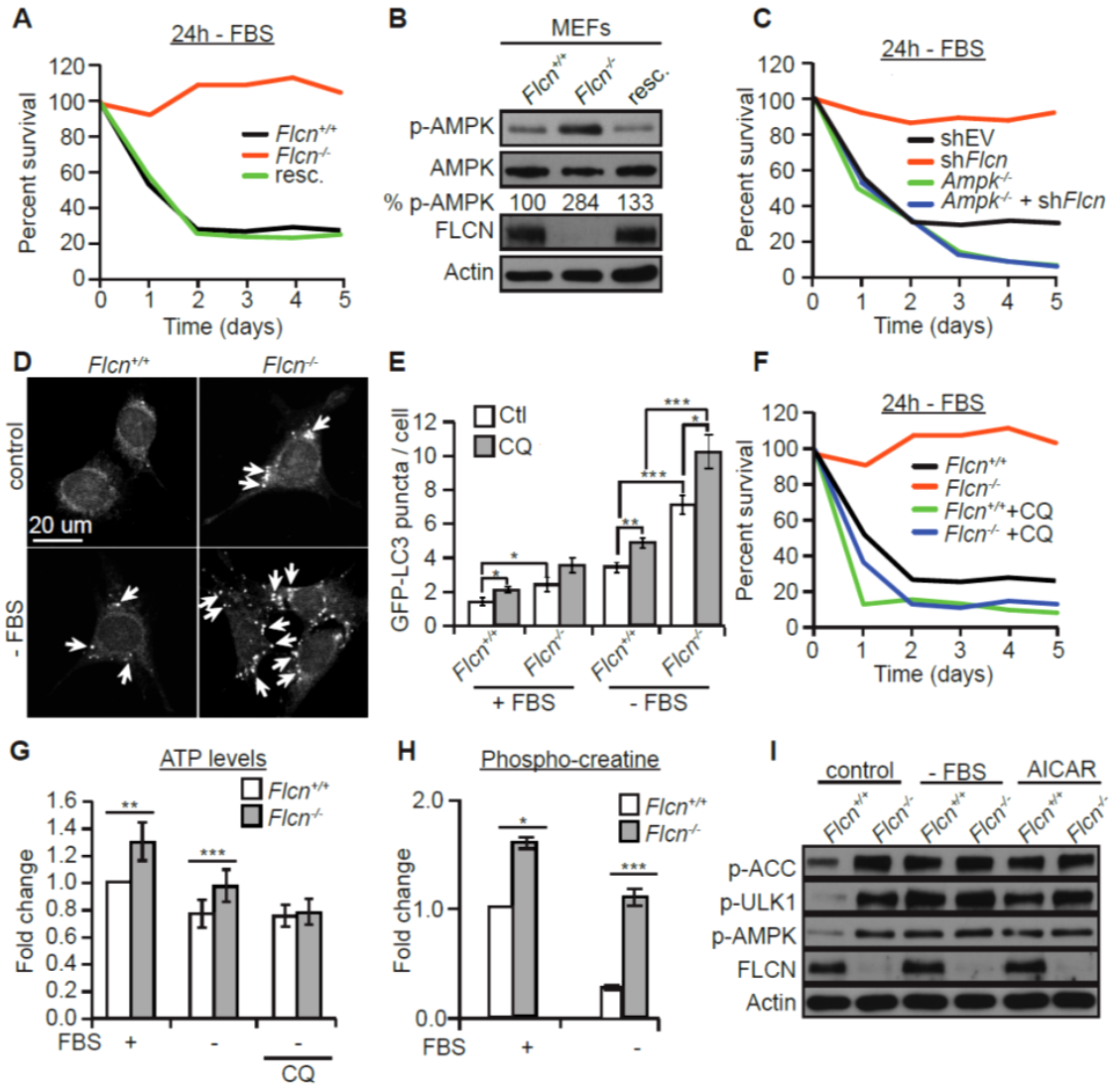

Figure 2.7: The FLCN-dependent regulation of AMPK, autophagy, and metabolic stress survival is evolutionary conserved

(A) Percent survival of wild-type, *Flcn*$^{-/-}$ and FLCN-rescued MEFs (resc.) upon serum starvation (-FBS). (B) Western blot analysis of pAMPK (Thr172) and AMPK protein levels in indicated MEFs lines. (C) Percent survival of the indicated MEF cell lines upon serum starvation. Data represent the means ± SEM, n≥3. (D and E) Representative immunofluorescence pictures (D) and quantification (E) of LC3 positive GFP puncta (arrows) in wild-type or *Flcn*$^{-/-}$ MEFs under basal or 24 h serum starvation conditions (-FBS). When indicated, cells were pretreated with chloroquine (CQ) 12 h prior to serum starvation, N>200 cells for every trial. (F) Percent survival of indicated cell lines upon serum starvation, treated with or without 10μM CQ. Data represent the mean ± SEM, n≥3. (G) Relative ATP levels measured in the indicated MEFs lines, pretreated with or without 10μM CQ prior to serum starvation. (H) Relative phosphocreatine levels in the indicated MEFs lines with or without 24 hours FBS starvation. (I) Western blot analysis of indicated antibodies with indicated treatments and MEFs lines.

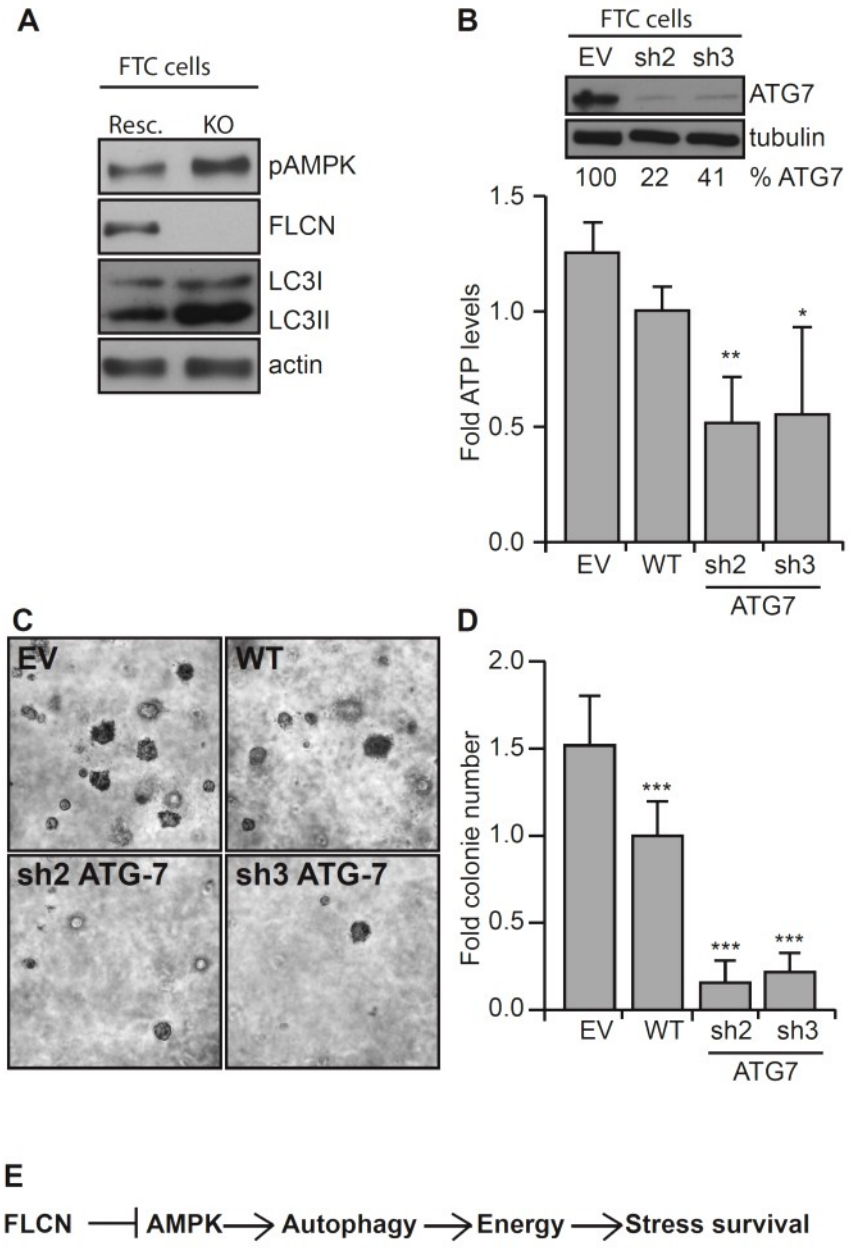

Figure 2.8: Loss of FLCN in tumor cells confers higher cellular energy levels dependent on increased autophagy.

(A) Western blot analysis of LC3 and AMPK phosphorylation levels on Threonine 172 (pAMPK) revealed in the indicated FTC cell lines. Folliculin (FLCN) and actin expression levels are shown as controls. (B) Western blot analysis of ATG7 in the indicated FTC cell lines. Tubulin expression level is shown as control. The percent downregulation is quantified using ImageJ software and is normalized for the tubulin levels. Data represent the means of at least three independent experiments. Relative ATP levels measured in the indicated FTC cell lines. Data represent the means ± S.D. (C) Soft agar colonies assays in the indicated FTC cell lines. (D) Quantification relative to control in the indicated FTC cell lines. Data represent the mean ± S.D. (E) Graphical model that summarizes findings in this study.

Table 2.1: Lifespan results and statistical analysis

Strain	Mean survival (days±SEM)	p-value	Number of Experiments(n)	Number of Nematodes(n)
N2	14.20 ± 0.3		5	384
flcn-1(ok975)	14.80 ± 0.5	n.s.[a]	5	378
N2 (100µM FUDR)	16.28 ± 0.9		5	273
flcn-1(ok975)(100µM FUDR)	21.01 ± 0.7	<0.0001[b]	5	302

(a) Compared to N2 animals grown on NGM plates
(b) Compared to N2 animals grown on NGM plates supplemented with FUDR.

Table 2.2: Percent survival upon mild oxidative stress (4mM): results and statistical analysis

Strain, RNAi, treatment	Mean survival (days±SEM)	p-value	Number of Experiments(n)	Number of Nematodes(n)
N2-PQ	3.2 ± 0.06		3	193
flcn-1(ok975)-PQ	4.6 ± 0.3	<0.0001[a]	3	116
flcn-1(ok975); flcn-1::GFP line1-PQ	3.4 ± 0.2	<0.05[b] /n.s.[a]	3	102
flcn-1(ok975); flcn-1::GFP line2-PQ	3.1 ± 0.03	<0.05[b] /n.s.[a]	3	88
N2-NT (non treated)	7.2 ± 0.3	<0.0001[a]	5	384
flcn-1(ok975)-NT (non treated)	7.8 ± 0.5	<0.0001[b]	5	378
N2-PQ	3.1 ± 0.07		3	92
flcn-1(ok975)- PQ	4.3 ± 0.32	<0.0001[c]	3	88
aak-2(ok524)- PQ	1.2 ± 0.06	<0.0001[c]	3	80
aak-2(ok524); flcn-1 (ok975)-PQ	1.2 ± 0.03	<0.0001[d] /n.s.[e]	3	81
aak-2(ok524)-NT	3.8+0	<0.0001 [e]	1	126
aak-2(ok524); *flcn-1 (ok975)*-NT	3.5+0	<0.0001 [f]	1	89
N2 (control RNAi)-PQ	3.0 ± 0.16		3	96
flcn-1(ok975) (control RNAi)-PQ	4.3 ± 0.40	<0.0001[g]	3	113
N2 (*bec-1*RNAi)-PQ	1.1 ± 1.14	<0.0001[g]	3	94
flcn-1(ok975)(*bec-1* RNAi)-PQ	1.5 ± 0.12	<0.0001[h] /n.s.[i]	3	81
N2 (control RNAi)-NT	7.4± 0.44	<0.0001[g]	3	266
flcn-1(ok975) (control RNAi)-NT	5.8± 0.06	<0.05 [h]	3	193
N2 (*bec-1*RNAi)-NT	4.7 ± 0.37	<0.0001[i]	3	307
flcn-1(ok975)(*bec-1* RNAi)-NT	3.9 ± 0.78	<0.05 [j]	3	313
N2 (control RNAi)-PQ	4.1 ± 0.18		3	87
flcn-1(ok975) (control RNAi)-	5.5 ± 0.23	<0.0001[k]	3	97

PQ				
N2 (*atg-7* RNAi)-PQ	3.0 ± 0.15	<0.0001[k]	3	84
flcn-1(ok975)(*atg-7* RNAi)-PQ	2.9 ±0.22	<0.0001[l] /n.s.[m]	3	80
N2 (control RNAi)-NT	7.4± 0.44	<0.0001[k]	3	266
flcn-1(ok975) (control RNAi)-NT	5.8± 0.06	<0.0001[l]	3	193
N2 (*atg-7*RNAi) NT	6.6 ± 0.38	<0.0001[m]	3	266
flcn-1(ok975)(*atg-7*RNAi) NT	5.9 ±0.32	<0.0001[n]	3	272
N2 (control RNAi)-PQ	3.5 ± 0.22		3	97
flcn-1(ok975) (control RNAi)-PQ	5.7 ± 0.43	<0.0001[o]	3	102
N2*(flcn-1* RNAi*)*-PQ	5.0 ± 0.30	<0.0001[o] /n.s[p]	3	86
flcn-1(ok975)(*flcn-1* RNAi*)*-PQ	5.2 ± 0.45	<0.0001[o] /n.s.[p]/n.s.[q]	3	88

(a) Compared to N2 animals treated with 4mM PQ.
(b) Compared to *flcn-1(ok975)* animals treated with 4mM PQ.
(c) Compared to N2 animals treated with 4mM PQ.
(d) Compared to *flcn-1(ok975)* animals treated with 4mM PQ.
(e) Compared to *aak-2(ok524)* animals treated with 4mM PQ.
(f) Compared to *flcn-1(ok975); aak-2(ok524)* animals treated with 4mM PQ.
(g) Compared to N2 animals treated with controlRNAi and 4mM PQ.
(h) Compared to *flcn-1(ok975)* animals treated with controlRNAi and 4mM PQ.
(i) Compared to N2 animals treated with *bec-1*RNAi and 4mM PQ.
(j) Compared to *flcn-1(ok975)* animals treated with *bec-1*RNAi and 4mM PQ.
(k) Compared to N2 animals treated with controlRNAi and 4mM PQ.
(l) Compared to *flcn-1(ok975)* animals treated with controlRNAi and 4mM PQ.
(m) Compared to N2 animals treated with *atg-7* RNAi and 4mM PQ.
(n) Compared to *flcn-1(ok975)* animals treated with *atg-7* RNAi and 4mM PQ.
(o) Compared toN2 animals treated with control RNAi and 4mM PQ.
(p) Compared to *flcn-1(ok975)* animals treated with control RNAi and 4mM PQ.
(q) Compared toN2 animals treated with *flcn-1*RNAi and 4mM PQ.

Table 2.3: Percent survival upon acute oxidative stress (100mM): results and statistical analysis

Strain, RNAi	Percent Survival (4h) (±SEM)	p-value	Number of experiments (n)	Number of worms (n)
N2	40.06 ± 3.29		3	94
flcn-1(ok975)	64.64 ± 0.47	<0.01 [a]	3	175
flcn-1(ok975); flcn-1::GFP line1	42.67 ± 8.28	<0.05 [b] / n.s.[a]	3	106
flcn-1(ok975); flcn-1::GFP line2	41.03 ± 8.9	<0.05 [b] / n.s.[a]	3	152
N2	35.08 ± 3.36		4	235
flcn-1(ok975)	53.00 ± 3.32	<0.05 [c]	4	227
aak-2(ok524)	22.57 ± 2.22	<0.01 [c] <0.001 [d]	4	203
flcn-1(ok975); aak-2(ok524)	21.68 ± 4.23	< 0.01 [d] /n.s. [e]	4	215
N2	46.13 ± 7.83		3	167
flcn-1(ok975)	66.00 ± 1.37	<0.05 [f]	3	163
aak-1(tm144)	46.91 ± 7.38	n.s. [f]	3	183
flcn-1(ok975); aak1(tm1944)	61.71 ± 3.58	n.s. [g] / <0.05 [h]	3	203
N2	25.78 ± 6.72			163
flcn-1(ok975)	50.58 ± 9.82	<0.05[i]	3	173
par-4(it57)	20.54 ± 0.095		3	167
flcn-1(ok975); par-4(it57)	35.03 ± 4.365	<0.01 [J]	3	177
N2	30.31 ± 2.44		3	169
flcn-1(ok975)	50.17 ± 2.67	<0.05 [k]	3	134
daf-2(e1370)	59.26 ± 0.1	<0.05 [k]	3	177
flcn-1(ok975); daf-2(e1370)	75.43 ± 0.43	<0.05 [l]	3	162
N2	40.90 ± 9.76		3	184
flcn-1(ok975)	54.71 ± 8.89	<0.01 [m]	3	193
daf-16(mu86)	28.62 ± 6.96	<0.05 [m]	3	188
daf-16(mu86); flcn-1(ok975)	50.00 ± 5.92	<0.01 [n]	3	193
N2 (control RNAi)	28.53 ± 8.55		5	292
flcn-1 (ok975) (control RNAi)	56.63 ± 8.89	<0.05 [o]	5	269

N2 (*atg-7* RNAi)	33.97 ± 5.14		5	294
flcn-1(ok975)(*atg-7* RNAi)	30.70 ± 10	<0.05 [p] / n.s. [q]	5	280
N2 (control RNAi)	28.53 ± 8.55		3	292
flcn-1(ok975) (control RNAi)	56.63 ± 8.89	<0.05 [o]	3	269
N2 (*bec-1*RNAi)	26.58 ± 8.40		3	272
flcn-1(ok975)(*bec-1*RNAi)	26.62 ± 4.70	<0.05 [p] / n.s. [r]	3	257
N2 (control RNAi)	47.17 ± 7.07		5	300
flcn-1(ok975) (control *RNAi*)	66.15 ± 4.23	<0.001 [s]	5	339
N2 *(ced-3* RNAi*)*	67.36 ± 5.18	<0.01 [s]	5	339
flcn-1(ok975)(*ced-3* RNAi*)*	70.39 ± 5.20	n.s. [t]	5	324
N2 (control RNAi)	52.52 ± 1.67		3	173
flcn-1(ok975) (control RNAi)	71.06 ± 3.73	<0.01 [u]	3	223
N2 (*ced-9* RNAi)	49.07 ± 2.44	n.s. [u]	3	170
flcn-1(ok975)(*ced-9* RNAi)	57.62 ± 4.72	<0.05 [v] / n.s. [w]	3	184
N2 (control RNAi)	47.51 ± 6.42		3	196
flcn-1(ok975) (control RNAi)	67.12 ± 4.51	<0.05 [x]	3	225
N2 (*egl-1* RNAi)	68.50 ± 1.22	<0.05 [x]/ n.s. [y]	3	213
flcn-1(ok975)(*egl-1* RNAi)	70.28 ± 7.53	n.s. [z] / n.s. [y]	3	218
N2 (control RNAi)	52.52 ± 7.23		3	203
N2 (*ced-3* RNAi)	74.96 ± 1.69	<0.05 [aa]	3	171
aak-2(ok 524) (control RNAi)	55.09 ± 10.61		3	165
aak-2(ok 524)(*ced-3* RNAi)	54.33 ± 7.76	n.s. [bb]	3	216
N2 (control RNAi)	51.21 ± 2.25		3	202
flcn-1(ok975) (control RNAi)	70.50 ± 9.15	<0.05 [cc]	3	207
N2 (*let-363* RNAi)	63.73 ± 1.53	<0.01 [cc]	3	187
flcn-1(ok975)(*let-363*RNAi)	83.18 ± 3.42	<0.01 [dd]	3	221

(a) Compared to *N2* animals.
(b) Compared to *flcn-1*(ok975) animals.
(c) Compared to N2 animals.
(d) Compared to *flcn-1(ok975)* animals.
(e) Compared to *aak-2(ok524)* animals.
(f) Compared to N2 animals.
(g) Compared to *flcn-1(ok975)* animals.
(h) Compared to *aak-1(tm1944)* animals.
(i) Compared to N2 animals.
(j) Compared to *par-4(it57)* animals.

(k) Compared to N2 animals.
(l) Compared to *daf-2(e1370)* animals.
(m) Compared to N2 animals.
(n) Compared to *daf-16(mu86)* animals.
(o) Compared to N2 animals.
(p) Compared to *flcn-1(ok975)* animals treated with control RNAi.
(q) Compared to N2 animals treated with *atg-7* RNAi.
(r) Compared to N2 animals treated with *bec-1* RNAi.
(s) Compared to N2 animals treated with control RNAi.
(t) Compared to N2 animals treated with *ced-3* RNAi.
(u) Compared to N2 animals treated with control RNAi.
(v) Compared to *flcn-1(ok975)* treated with control RNAi.
(w) Compared to N2 animals treated with *ced-9* RNAi.
(x) Compared to N2 animals treated with control RNAi.
(y) Compared to *flcn-1(ok975)* animals treated with control RNAi.
(z) Compared to N2 animals treated with *egl-1* RNAi
(aa) Compared to N2 animals treated with control RNAi.
(bb) Compared to *aak-2(ok524)* animals treated with control RNAi.
(cc) Compared to N2 animals treated with control RNAi.
(dd) Compared to N2 animals treated with *let-363* RNAi.

Table 2.4: Mean survival to heat stress: results and statistical analysis

Strain	Mean survival (hours±SEM)	p-value	Number of experiments (n)	Number of worms(n)
N2	7.09 ± 0.39		4	312
flcn-1(ok975)	9.51 ± 0.47	<0.001	4	261

Table 2.5: Percent recovery (1 hour) after anoxic stress: results and statistical analysis

Strain	Percent recovery (±SEM)	p-value	Number of Experiments (n)	Number of worms (n)
N2	35.04 ± 7.42		4	154
flcn-1(ok975)	81.40 ± 8.12	<0.01	4	143

Table 2.6: Strain list

Genotype	Strain Number	Additional information
wild-type Bristol (N2)		
flcn-1(ok975) II		RB1035 strain was outcrossed 8 times with wild-type Bristol (N2)
aak-1(tm1944) III	FX1944	from CGC
aak-2(ok524) X	RB754	from CGC
daf-16(mu86) I	CF1038	from CGC
daf-2(e1370) III	CB1370	from CGC
adIs2122[lgg-1::GFP + rol-6(su1006)]	DA2123	from CGC
par-4(it57)V	KK184	from CGC
flcn-1(ok975); flcn::GFP(1)		Overexpression of FLCN-1 co-injected with *rol-6(su1006)gf*
flcn-1(ok975); flcn::GFP(2)		Overexpression of FLCN-1 co-injected with *rol-6(su1006)gf*

flcn-1(ok975) II; aak-2(ok524) X
flcn-1(ok975) II; par-4(it54) V
flcn-1(ok975) II; daf-2(e1370) III
daf-16(mu86) I; flcn-1(ok975) II

Table 2.7: Primer sequences

Gene symbol	Forward primer	Reverse primer
ctl-1	GCGGATACCGTACTCGTGAT	AATCCGGATGAACTTTCGTG
ctl-2	CATCCGTGACCTGTTCAATG	TGGATTTCTGTTCAGCACCA
ctl-3	CTGGGAGAAAGTGCTCAAGG	TTCTTCTGGCAGAGCTGATG
sod-1	ACGCTTTACGGTCCAAACAC	CTTCTGCCTTGTCTCCGACT
sod-2	TGGACTTGTTCCACTGTTCG	CTCGCTGACGTTCTTCCAGT
sod-3	CTATTGCGGTTCAAGGCTCT	TGGCAAATCTCTCGCTGATA
sod-4	TCCGACTCTCTTGCCTCATT	AGGGATGCTGTCGTTGTTTC
sod-5	ACGTTGGTGACCTTGGAAAC	GAGCAATGACTCCACAAGCA
cdc-42	GGCAAAGGAATTGAAAGCAG	GGGGGCTAAGAAAATTTGGA
pmp-3	GTTCCCGTGTTCATCACTCAT	ACACCGTCGAGAAGCTGTAGA
y45f10d.4	GTCGCTTCAAATCAGTTCAGC	GTTCTTGTCAAGTGATCCGACA
aak-1	TTGGAAAAGGAGCATTTGGA	AACACGGAAGAGACGTGTGA
aak-2	ATAGGAAGGAGGACGGTGGT	CTTCGTCGACGTTTCTCCTC
lgg-1	GAAAACGCATCCAACTTCGT	TCGGCGGATAATACATGACA

CHAPTER 3

FLCN AND AMPK CONFER RESISTANCE TO HYPEROSMOTIC STRESS VIA REMODELING OF GLYCOGEN STORES

Plos Genetics (In press)

Elite Possik[1,2], Andrew Ajisebutu[1,2], Sanaz Manteghi[1,2], Marie-Claude Gingras [1,2], Tarika Vijayaraghavan[1,2], Mathieu Flamand[1], Barry Coull[3], Kathrin Schmeisser[1,2], Thomas Duchaine[1,2], Maurice van Steensel[3], David H. Hall[4] and Arnim Pause[1,2]

[1]Goodman Cancer Research Center, McGill University, Montréal, Québec, H3A 1A3, Canada.

[2]Department of Biochemistry, McGill University, Montréal, Québec, H3G 1Y6, Canada.

[3]College of Life Sciences, University of Dundee, Dundee, DD1 4HN, UK.

[4]Department of Neuroscience, Albert Einstein College of Medicine, NY10461, New York, USA.

3.1 Preface to chapter 3

The ability of an organism to adapt to sudden changes in environmental osmolarity is critical to ensure growth, propagation, and survival. The synthesis of organic osmolytes is a common adaptive strategy to survive hyperosmotic stress. However, it was not well understood, which biosynthetic pathways and storage strategies were used by organisms to rapidly generate osmolytes upon acute hyperosmotic stress. Here, we demonstrate that glycogen is an essential reservoir that is used upon acute hyperosmotic stress to generate the organic osmolyte glycerol promoting fast and efficient protection. Importantly, we show that this pathway is regulated by FLCN-1, an ortholog of the human tumor suppressor Folliculin responsible for the Birt-Hogg-Dubé cancer syndrome, and by AMPK, the master regulator of energy homeostasis.

3.2 Abstract

Mechanisms of adaptation to environmental changes in osmolarity are fundamental for cellular and organismal survival. Here we identify a novel osmotic stress resistance pathway in *Caenorhabditis elegans (C. elegans),* which is dependent on the metabolic master regulator 5'AMP-activated protein kinase (AMPK) and its negative regulator Folliculin (FLCN). FLCN-1 is the nematode ortholog of the tumor suppressor FLCN, responsible for the Birt-Hogg-Dubé (BHD) tumor syndrome. We show that *flcn-1* mutant nematodes exhibit increased resistance to hyperosmotic stress via constitutive AMPK-dependent accumulation of glycogen reserves. Upon hyperosmotic stress exposure, glycogen stores are rapidly degraded, leading to a significant accumulation of the organic osmolyte glycerol through transcriptional upregulation of glycerol-3-phosphate dehydrogenase enzymes (*gpdh-1* and *gpdh-2*). Importantly, the hyperosmotic stress resistance in *flcn-1* mutant and wild-type animals is strongly suppressed by loss of AMPK, glycogen synthase, glycogen phosphorylase, or simultaneous loss of *gpdh-1* and *gpdh-2* enzymes. Our studies show for the first time that animals normally exhibit AMPK-dependent glycogen stores, which can be utilized for rapid adaptation to either energy stress or hyperosmotic stress. Importantly, we show that glycogen accumulates in kidneys from mice lacking FLCN and in renal tumors from a BHD patient. Our findings suggest a dual role for glycogen, acting as a reservoir for energy supply and osmolyte production, and both processes might be supporting tumorigenesis.

3.3 Introduction

Water is a fundamental molecule for life and the ability of an organism to adapt to changes in water content is essential to ensure survival. Hyperosmotic stress promotes water efflux, causing cellular shrinkage, protein and DNA damage, cell cycle arrest and cell death. All living organisms encounter hyperosmotic environments [213,214]. In humans, both renal and non renal tissues are exposed to hyperosmotic stress, a condition that is regarded as a major cause for many chronic and fatal human diseases including diabetes, inflammatory bowel disease, hypernatremia, dry eye syndrome, and cancer [213]. Cells/tissues/organisms have evolved adaptive strategies to cope with threatening hyperosmotic environments [213,214]. Among adaptive strategies, the synthesis of compatible organic osmolytes, which keeps cellular osmotic pressure equal to that of the external environment, is widely used by all organisms [216]. In yeast and *C. elegans*, hyperosmotic stress triggers glycerol production via transcriptional upregulation of glycerol-3-phosphate dehydrogenase-1 *(gpdh-1)*, a rate-limiting enzyme in glycerol synthesis [217,219]. Moreover, several osmotic stress resistance mutants of divergent signaling pathways exhibit a constitutive transcriptional upregulation of gpdh-1, leading to increased glycerol content [220-224].

Here we define a novel hyperosmotic stress resistance pathway mediated by AMPK, a key regulator of cellular energy balance [304], which is chronically inactivated by the worm ortholog of the renal tumor suppressor Folliculin (FLCN-1). In humans, *FLCN* is a tumor suppressor gene responsible for the BHD disease, an autosomal dominantly-inherited syndrome associated with increased susceptibility to the development of several cancerous and non cancerous lesions including kidney cancer, pulmonary, renal, pancreatic and hepatic cysts and skin fibrofolliculomas [13-26]. FLCN has been shown to bind AMPK via the scaffold FLCN-interacting proteins FNIP1 and FNIP2 [38,81]. We have recently

demonstrated that FLCN negatively regulates AMPK signaling in the nematode *C. elegans* and in mammalian cells (chapter 2) [77,101]. Moreover, loss of FLCN increased ATP levels via heightened flux of glycolysis, oxidative phosphorylation, and autophagy, which resulted in an AMPK-dependent resistance to several metabolic stresses in *C. elegans* and mammalian cells (chapter 2) [77,101].

Here we identify a pathway involved in the physiological response to hyperosmotic stress resistance in *C. elegans* mediated by FLCN-1 and AMPK. We demonstrate that glycogen is an essential reservoir that is used upon acute hyperosmotic stress to generate glycerol and promote fast and efficient adaptation to prevent water loss and ensure survival. We show that in *flcn-1(ok975)* mutant animals, this phenotype is significantly enhanced, due to the robust AMPK-mediated accumulation of glycogen, which is rapidly converted to the osmolyte glycerol upon salt stress. Our results also suggest that the FLCN/AMPK pathway might be an evolutionarily conserved key regulator of glycogen metabolism and stress resistance.

3.4 Results

3.4.1 Loss of flcn-1 confers resistance to hyperosmotic stress in C. elegans

Since we have previously observed that loss of *flcn-1* in *C. elegans* increases AMPK-dependent resistance to metabolic stresses including oxidative stress, heat, and anoxia [101], we asked whether it could also increase resistance to hyperosmotic stress. We measured the survival of wild-type and *flcn-1(ok975)* animals on plates supplemented with 400mM and 500mM NaCl. Loss of *flcn-1* conferred a significant increase in resistance to hyperosmotic stress (Figures 3.1A-B and Table 3.1). The mean survival of *flcn-1(ok975)* animals increased by ~2 and ~3 fold upon treatment with 400mM and 500mM NaCl respectively, as compared

to wild-type animals (Figures 3.1A-C). Importantly, NaCl treatment leads to shrinkage and paralysis in both wild-type and *flcn-1(ok975)* animals. However, *flcn-1(ok975)* mutant nematodes recover significantly faster than wild-type animals after 2 hours of NaCl treatment suggesting that the mechanism of adaptation to salt is more robust upon loss *flcn-1* (Figure 3.1D). We also observed a significantly higher number of wild-type animals with more than 30% reduction of body size as compared to *flcn-1* suggesting that loss of *flcn-1* activates pathways that favor body size recovery after hyperosmotic stress (Figure 3.1E). Importantly, the hyperosmotic stress resistance phenotype can be rescued by transgenic re-expression of *C. elegans flcn-1* (Figure 3.1F and Table 3.1).

In addition, we used Agilent whole genome *C. elegans* microarrays to determine transcriptional profile differences between wild-type and *flcn-1(ok975)* mutant animals [305]. This data is presented with more details in chapter 4. We compared our data to published transcriptional profiles and found a significant overlap between genes upregulated in untreated *flcn-1(ok975)* animals and genes upregulated in wild-type animals treated with NaCl, or in osmotic stress resistant strains including *osm-7* and *osm-11* [220] (Figure 4.4A-C and Tables 4.3-4.6). Altogether, this data supports that *flcn-1* is involved in a mechanism of resistance to hyperosmotic stress.

3.4.2 Loss of flcn-1 increases glycogen content which mediates resistance to hyperosmotic stress

To determine how loss of *flcn-1(ok975)* increases resistance to hyperosmotic stress, we assessed the morphological differences between wild-type and *flcn-1(ok975)* using electron microscopy with or without NaCl treatment. Interestingly, we observed an increase in the size and number of glycogen stores in *flcn-1(ok975)* mutant worms as compared to

wild-type (Figure 3.2Ai,ii). Importantly, the glycogen stores after NaCl treatment in wild-type and *flcn-1(ok975)* animals were barely detectable after NaCl treatment suggesting that glycogen might be degraded to protect the animals from hyperosmotic stress (Figure 3.2Aiii, iv). We validated and quantified the increase in glycogen levels conferred by loss of *flcn-1* using iodine staining (Figures 3.2B, C). In accordance with the electron microscopy results, glycogen levels were significantly increased in untreated *flcn-1(ok975)* animals as compared to wild-type, and NaCl treatment severely reduced glycogen content in both wild-type and *flcn-1(ok975)* animals (Figures 3.2B, C).

We next asked whether glycogen is used to protect wild-type and *flcn-1(ok975)* animals from damage during hyperosmotic stress. Glycogen synthase (*gsy-1)* is responsible for the synthesis of glycogen from UDP-glucose molecules and glycogen phosphorylase (*pygl-1)* catalyzes glycogen breakdown to form glucose-1-phosphate [231]. Importantly, the inhibition of glycogen synthesis or degradation using RNAi against *gsy-1* and *pygl-1* respectively, strongly reduced the survival in both wild-type and *flcn-1(ok975)* animals to an equal level, suggesting that the accumulation of glycogen and its degradation are both required for the resistance of wild-type and *flcn-1(ok975)* mutant animals to hyperosmotic stress (Figures 3.2D, E and Table 3.1).

Additionally, transcript levels of *gsy-1* and *pygl-1* at normal condition and after 2 hours of 400mM NaCl stress did not reveal any significant changes suggesting that the regulation of glycogen metabolism might be via allosteric regulation (Figure 3.2F). Altogether, these results demonstrate that the degradation of glycogen reserves is essential to survive hyperosmotic stress in wild-type animals, and that the prominent accumulation of glycogen in *flcn-1(ok975)* mutant animals is responsible for their advantageous survival upon acute exposure to high salt conditions.

3.4.3 Hyperosmotic stress resistance of flcn-1(ok975) animals requires AMPK

Next we aimed to determine whether this phenotype is dependent on AMPK similarly to what we have previously reported with oxidative stress [101]. AMPK is activated by hyperosmotic stress in mammalian systems [306] and its deletion confers sensitivity to NaCl stress in yeast [307]. *C. elegans* nematodes have two catalytic α subunits *aak-1* and *aak-2.* Loss of *aak-2* was shown to mediate lifespan extension and resistance to various stresses including oxidative stress, anoxia, nutrient deprivation, and dietary restriction [41,74,80,264,266]. Interestingly, *aak-2* mutation strongly reduced hyperosmotic stress resistance. Despite, neither loss of *aak-2 (ok524* and *gt33)* nor *aak-1(tm1044)* alone were able to fully suppress the increased survival to hyperosmotic stress conferred by loss of *flcn-1* (Figures 3.3A-C and Table 3.1). To control for compensatory effects, we generated the *flcn-1(ok975); aak-1(tm1944); aak-2(ok524)* triple mutant and compared its survival under high salt conditions to *aak-1(tm1944); aak-2(ok524)* double mutant animals. Simultaneous loss of *aak-1* and *aak-2* completely abolished the increased osmotic stress resistance upon loss *flcn-1* demonstrating that this phenotype requires AMPK (Figure 3.3D and Table 3.1).

3.4.4 The accumulation of glycogen in flcn-1 mutant worms depends on AMPK.

AMPK has been shown to regulate glycogen metabolism in different organisms [65,308-319]. In fact, acute activation of AMPK leads to glycogen degradation [65,308-310], while chronic AMPK activation results in glycogen accumulation [311-313]. Since we observed an increased constitutive phoshorylation of AMPK upon loss of *flcn-1* in worms and mammalian cells [77,101], we hypothesized that the chronic AMPK activation in *flcn-1(ok975)* mutants is increasing glycogen levels. We determined glycogen levels in *aak-1(tm1944); aak-2(ok524)* animals compared to *flcn-1(ok975); aak-1(tm1944); aak-2(ok524)*

triple mutant worms and found that loss of AMPK strongly reduced glycogen levels in both strains (Figures 3.3E, F). This suggests that the chronic AMPK activation in *flcn-1* animals is leading to glycogen accumulation. Interestingly, the survival and glycogen accumulation in *aak-1(tm1944); aak-2(ok524)* mutant animals was also severely reduced as compared to wild-type, suggesting an important role for AMPK in maintaining glycogen stores, which are used for hyperosmotic stress resistance.

3.4.5 Autophagy is not fully required for the hyperosmotic stress resistance conferred by loss of flcn-1

Autophagy is a biological process through which cellular components and damaged organelles are recycled [137]. Based on our previous work where we show a requirement for autophagy to the resistance of *flcn-1(ok975)* mutant animals to energy stresses, we asked whether the increased autophagy at basal level in *flcn-1(ok975)* animals is protecting the animals via degradation of damaged proteins and organelles or through enhanced energy supply. Importantly, *atg-18(gk378)* mutant animals were hypersensitive to high salt concentrations suggesting that autophagy is a process involved in the resistance to hyperosmotic stress. However, loss of *flcn-1* significantly increased the resistance of *atg-18(gk378)* animals suggesting that the *flcn-1*-dependent hyperosmotic stress resistance does not require autophagy, and that this resistance pathway is different than the mechanism of resistance to the previously published stresses [101] (Figure 3.4 and Table 3.1).

3.4.6 Glycogen degradation leads to heightened glycerol levels and protects animals from hyperosmotic stress

Degradation of glycogen polymers leads to the formation of glucose-1-phosphate which is converted to glucose-6-phosphate, an important metabolite used in multiple pathways including glycolysis and glycerol production (Figure 3.5A) [231]. We hypothesized that glycogen degradation is leading to heightened glycerol levels that could protect the animals from hyperosmotic stress. To address this, we measured the mRNA levels of *gpdh-1* and *gpdh-2*. Interestingly, we observed a significant 2-fold increase in *gpdh-1* but not *gpdh-2* at normal conditions in *flcn-1(ok975)* mutant animals compared to wild-type consistently with our microarray results (Figures 3.5B, C and Table 4.3). Strikingly, after 2 hour treatment with 400mM NaCl, we detected a significantly enhanced induction of *gpdh-1* and *gpdh-2* mRNA levels in *flcn-1(ok975)* mutant animals compared to wild-type (Figures 3.5B, C). Accordingly, *flcn-1(ok975)* mutant animals exhibit higher glycerol content at basal level as compared to wild-type animals which was further increased upon NaCl treatment (Figure 3.5D).

To determine the importance of glycerol in the protection against hyperosmotic stress, we inhibit *gpdh-1* and *gpdh-2* using RNAi and using mutant strains. Importantly, treatment of *flcn-1(ok975)* animals with RNAi against either *gpdh-1* or *gpdh-2* alone did not fully suppress the increased resistance of *flcn-1(ok975)* animals to hyperosmotic stress (Table 3.1). We then compared the resistance of *flcn-1(ok975); gpdh-1(kb24); gpdh-2(kb33)* triple mutant animals to *gpdh-1(kb24); gpdh-2(kb33)* mutant nematodes. Simultaneous loss of *gpdh-1* and *gpdh-2* strongly reduced the survival of *flcn-1(ok975)* mutant animals demonstrating an important role for the osmolyte glycerol in the survival of *flcn-1(ok975)* and wild-type animals (Figure 3.5E and Table 3.1). Altogether, this data suggests that loss of *flcn-1*

increases resistance to hyperosmotic stress via enhanced transcriptional upregulation of *gpdh* enzymes which results in a more robust glycerol production.

3.4.7 Loss of pmk-1 does not fully suppress the hyperosmotic stress resistance conferred by loss of flcn-1

HOG/p38/PMK-1 MAP kinase signaling is widely known to control adaptation to hypertonic stresses in multiple organisms [217,218,222]. As expected, *pmk-1(km25)* mutant worms were highly sensitive to osmotic stress. However, loss of *pmk-1* in *flcn-1(ok975)* mutant animals reduced but did not fully suppress the increased resistance conferred by *flcn-1* depletion (Figure 3.6A and Table 3.1). Supporting this result, the expression of *gpdh-1* is ~2-fold higher in *flcn-1(ok975); pmk-1(km25)* mutant animals as compared to *pmk-1(km25)* alone (Figure 3.6B). Altogether, this suggests that *pmk-1* is not involved in the transcriptional upregulation of *gpdh-1* upon loss of *flcn-1* and that it acts in parallel to *flcn-1* and *ampk*.

3.4.8 The increased accumulation of glycogen content conferred by loss of FLCN is conserved from C. elegans to humans

Glycogen is linked to the progression and the aggressiveness of multiple cancer types in humans [251,255]. To determine whether loss of FLCN also leads to the accumulation of glycogen in mammalian systems, we used the *Flcn*$^{flox/flox}$/*Pax8-Cre* mouse model where *Flcn* is specifically deleted in the kidney and determined glycogen content using Periodic-Acid-Schiff (PAS) staining. The *Flcn*$^{flox/flox}$/*Pax8-Cre* mouse was generated by mating *Pax8-Cre* mice with the *Flcn* $^{flox/flox}$ C57BL/6 mice. By six months of age, all mice developed visible macroscopic lesions confirmed as cysts that later developed into tumors. Strikingly, kidneys from *Flcn*$^{flox/flox}$/*Pax8-Cre* mice accumulated higher glycogen levels as compared to normal

kidneys from *Flcn*$^{flox/flox}$ mouse littermates (Figure 3.7A). Our data show a stronger glycogen accumulation in the kidney cortex, which is due to the fact that *Pax8* is expressed in the epithelial cells of the proximal and distal renal tubules, loops of Henle, collecting ducts and the parietal epithelial cells of Bowman's capsule [320]. Importantly, PAS staining of tumors from BHD patients also indicate a strong accumulation of glycogen as compared to adjacent unaffected kidneys (Figures 3.7B). We also compared the expression level of glycogen biosynthesis and degradation genes in 3 different subtypes of kidney cancer, kidney renal papillary cell carcinoma (KIRP), kidney renal clear cell carcinoma (KIRC), and kidney chromophobe (KICH) tumors. Strikingly, we observed a significant upregulation of genes involved in the synthesis and degradation of glycogen (Figure 3.7C and Table 3.2). We also observed that the expression of 46% of these genes are negatively correlated with FLCN expression (Figure 3.7D). Overall, our data indicate that the accumulation of glycogen upon loss of FLCN is conserved from nematodes to mammals, and that it might play a role in tumorigenesis.

3.5 Discussion

A common mechanism to survive hyperosmotic stress is the synthesis of compatible osmolytes [216]. In yeast and in *C. elegans*, the rapid accumulation of glycerol after hyperosmotic stress has been demonstrated [217,219]. However, it is not clear what fuels glycerol production upon acute hyperosmotic stress. Here we show that animals have evolved an interesting strategy to maintain glycogen stores, which can serve as fuel for glycerol production to ensure survival to acute hyperosmotic stress (Figure 3.9). While storage of soluble glucose molecules in cells would lead to hyperosmotic stress, the storage of glucose in the form of insoluble glycogen polymers ensures osmotic homeostasis. Importantly, our

data uncover that glycogen stores have a dual role: they can serve as a reservoir for production of energy or osmolytes. Indeed, pretreatment of wild-type and *flcn-1(ok975)* animals with oxidative and energy stressor paraquat, depletes glycogen stores rapidly and suppresses survival upon treatment with 400mM NaCl (Figure 3.8).

The regulation of glycogen metabolism by AMPK has long been a paradox [65,308-313]. Acute activation of AMPK, by in vitro short term treatment of the AMP mimetic drug 5-Aminoimidazole-4-Carboxamide Riboside (AICAR), leads to the phosphorylation and inhibition of glycogen synthase, which favors glycogen degradation for supply of short term energy [65,308-310]. However, chronic AMPK activation induced by a long term AICAR treatment or by genetic manipulation of AMPK regulatory subunits, results in glycogen accumulation via glucose-6-phosphate-dependent allosteric activation of glycogen synthase, which bypasses the inhibitory effect of the AMPK-mediated phosphorylation [311-313]. In agreement, constitutive AMPK activation through transgenic expression of activating mutations in the γ2 and γ3 subunits in mice and pigs leads to substantial glycogen accumulation in cardiac and skeletal muscles [306,313-316,318,319]. In light of these results, our data indicate that chronic AMPK activation upon loss of *flcn-1* leads to glycogen accumulation. Similarly to what has been shown in yeast [317], we demonstrate that AMPK-deficient strains exhibit reduced glycogen content as compared to wild-type. We further show that the accumulation of glycogen in wild-type and *flcn-1(ok975)* mutant animals depends on AMPK. Based on the data presented here together with our recently published reports [77,101], we propose that FLCN is a key regulatory component of AMPK.

Flcn muscle-specific knockout mice and *Fnip1* knockout mice exhibited increased glycogen accumulation in muscles and liver, respectively [83,111]. Here we show that loss of FLCN leads to glycogen accumulation in kidneys of mice and in the tumors of BHD patients,

suggesting that this pathway is evolutionarily conserved. In agreement with the important role for glycogen in organismal survival to stress, glycogen can be used by tumor cells to survive harsh microenvironments such as hypoxia [251,253]. In fact, glycogen accumulates in many cancer types [253] and inhibition of its degradation led to induction of apoptosis and impaired *in vivo* growth of tumor xenografts [251].

Importantly, our data might impinge on a novel role for glycogen in tumorigenesis. In addition to its critical role as an energy supplier, we speculate that glycogen degradation might lead to higher osmolyte levels to help survive hyperosmotic tumor microenvironments. In fact, we found that taurine and sorbitol synthesis genes, CSAD and AKR1B1 respectively, are upregulated in many kidney tumors (Table 3.2). Supporting this idea, recent evidence shed light on an important role of the nuclear factor of activated T cells 5 (NFAT5), a major transcription factor that regulates osmotic stress resistance genes, in promoting tumorigenesis and metastasis of several cancer types [214,228,229,321]. In summary, we speculate that the increased glycogen stores in tumors might lead to extended survival of cells under hyperosmotic stress, which could ultimately lead to neoplastic transformation by accumulation of DNA damage [1, 2].

3.6 Material and methods

C. elegans strains, maintenance, and RNAi treatments

C. elegans strains were obtained from the *Caenorhabditis* Genetics Center (Table 3.3). Nematodes were maintained and synchronized using standard culture methods [128]. The RNAi feeding experiments were performed as described in [132], and bacteria

transformed with empty vector were used as control. For all RNAi experiments, phenotypes were scored with the F1 generation.

Osmotic stress resistance assay

To measure osmotic stress resistance, synchronized 1 day adult worms were transferred to high concentration NaCl plates. Survival was measured daily. Worms that responded by movement to touch with the platinum wire were considered as alive.

Percent recovery assay

To measure the percentage of animals that recovered after hyperosmotic shock, 1 day adult animals were transferred to high NaCl plates. Animals shrink and paralyse shortly after exposure to NaCl. After 2 hours, animals that were able to move their entire body forward or backward in response to touch with a platinum wire were considered as "recovered". Paralyzed animals often look straight and are unable to move.

RNA extraction and real-time PCR

Synchronized young adult nematodes were harvested and total RNA was extracted with Trizol. Reverse transcription and qRT-PCRs were performed as previously described [101]. Transcripts were normalized to *cdc-42*. Primers sequences are indicated in Table 3.4.

Transmission electron microscopy

Synchronized 1 day adult nematodes were transferred to 400mM NaCl plates for 16 hours. Recovering animals were picked and transferred for TEM. Immersion fixation and embedding was performed according to [322]. Thin sections were cut on an RMC Powertome XL (Boeckler Instruments) using a diamond knife (DDK) and collected on Pioloform-coated

copper slot grids. Grids were post-stained with 4% uranyl acetate and lead citrate and viewed using a Philips CM10 electron microscope (FEI) equipped with a Morada digital camera (Olympus) and iTEM software (Olympus SIS).

Glycogen quantification in *C. elegans*

Synchronized young adult animals were transferred to agarose pads. For comparisons between strains, different conditions were transferred to the same agarose pad and were exposed to iodine vapor for 30 seconds. Animals were rapidly imaged individually. Quantification of the intensity of the staining was performed using ImageJ software.

Periodic Acid Schiff staining

For human normal kidney and BHD tumor samples, slides were rehydrated after deparaffination and treated with 1% periodic acid for 10 minutes. Periodic acid was washed off with H_2O and slides were then incubated in Schiff reagent for 20 min. Slides were then rinsed with H_2O, counterstained with hematoxylin and embedded in entellan. Images were taken as described in [97].

Glycerol determination in *C. elegans*

Synchronized L4/young adult animals exposed or not to 400mM NaCl for 2 hours and were harvested and washed with M9 buffer adjusted to match plate salinity. Pellets were flash frozen in liquid nitrogen. Extraction was performed according to [219]. Briefly, frozen pellets were ground using a cold mortar and pestle on dry ice. The worm powder was then resuspended in 1N perchloric acid, and solutions were transferred to 15ml conical tubes and kept on ice for 1 hour. The lysate was then centrifuged and the supernatant was neutralized with 5N KOH containing 61.5mM K_2HPO_4 and 38.5mM KH_2PO_4. Glycerol levels were

determined using a glycerol determination kit (R-Biopharm, Marshall, MI). Pellets were solubilized in 0.1N NaOH and protein content was determined using BCA. Glycerol levels were normalized to protein content.

Gene expression analysis in kidney cancers from patients

TCGA data including 91 kidney chromophobe gene expression RNASeq (IlluminaHiSeq), 604 kidney renal clear cell carcinoma gene expression RNASeq (IlluminaHiSeq), and 258 kidney renal papillary cell carcinoma gene expression RNASeq (IlluminaHiSeq), were extracted from cancer Genomics Browser (https://genome-cancer.ucsc.edu/proj/site/hgHeatmap). For expression analysis, data were expressed as median fold change and the Mann-Whitney test was used to calculate the p-values between normal and tumor samples. P-values less than 0.05 were considered to be statistically significant. For correlation analysis TCGA expression data (same as expression analysis) were used to calculate the Pearson correlation coefficient, and generate a heat map, using R software 3.1.1 (http:// www.r-project.org/). P-values less than 0.05 were considered to be statistically significant.

Statistical Analyses

Data are expressed as means ±SEM. Statistical analyses for all data were performed by student's t-test, using Excel (Microsoft, Albuquerque, NM, USA). For hyperosmotic stress survival curve comparisons we used the Log-rank Mantel Cox test using GraphPad software. Statistical significance is indicated in figures (* $P<0.05$, ** $P<0.01$, *** $P<0.001$) or included in the supplemental tables.

3.7 Acknowledgements

We thank Kevin Strange for the *gpdh-1(kb24); gpdh-2(kb33)* double mutant strain and Todd Lamitina for *gpdh-2(kb33)* strain. We thank Mr. Ken Nguyen for his help in processing animals for electron microscopy. We acknowledge the *Caenorhabditis* Genetic Center for *C. elegans* strains and salary support to E.P. from the Rolande and Marcel Gosselin Graduate Studentship and the CIHR/FRSQ training grant in cancer research of the McGill Integrated Cancer Research Training Program (MICRTP). This work was supported by grants to A.P. from *Myrovlytis* Trust and Terry Fox Research Foundation.

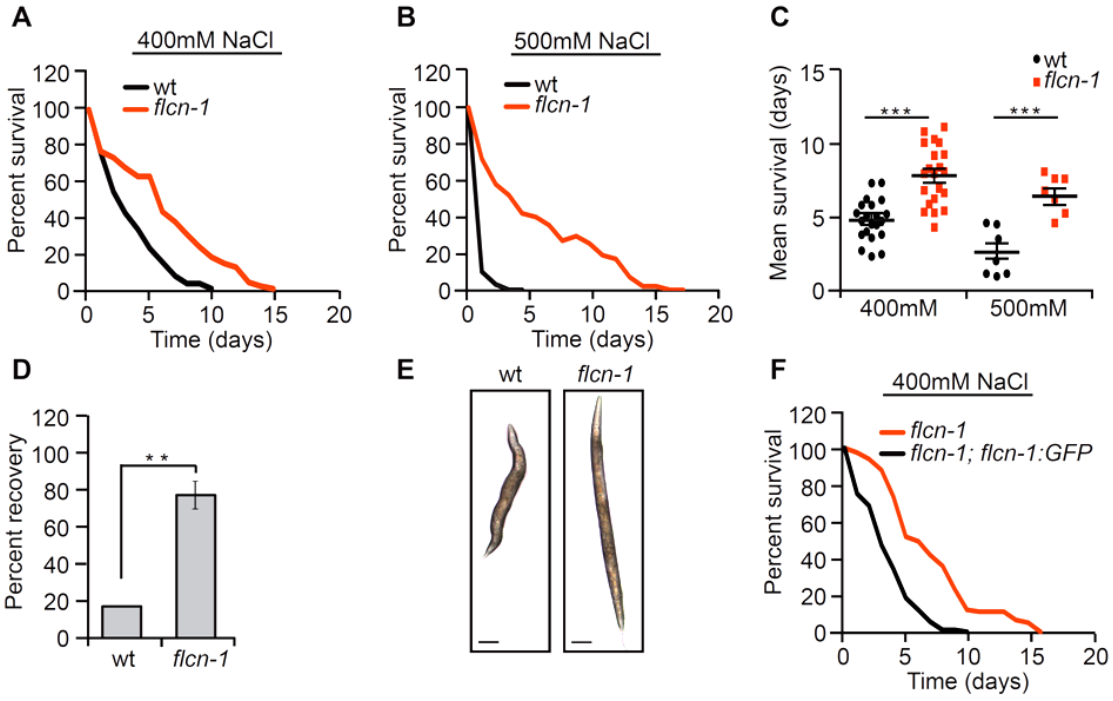

Figure 3.1: Loss of *flcn-1* confers resistance to hyperosmotic stress in *C. elegans*.

(A, B, F) Percent survival of indicated worm strains exposed to indicated NaCl concentration. Also see Table 3.1. (C) Dot plot showing the mean survival of wild-type and *flcn-1(ok975)* animals to 400mM NaCl. (D) Percent recovery of wild-type and *flcn-1(ok975)* animals after 2 hours from exposure to 400mM NaCl. Data represent mean ± SEM, n≥ 3. (E) Representative images of wild-type and *flcn-1(ok975)* animals treated or not with 400mM NaCl for 48 hours. (F) Percent survival of indicated worm strains to 400mM. Also see Table 3.1.

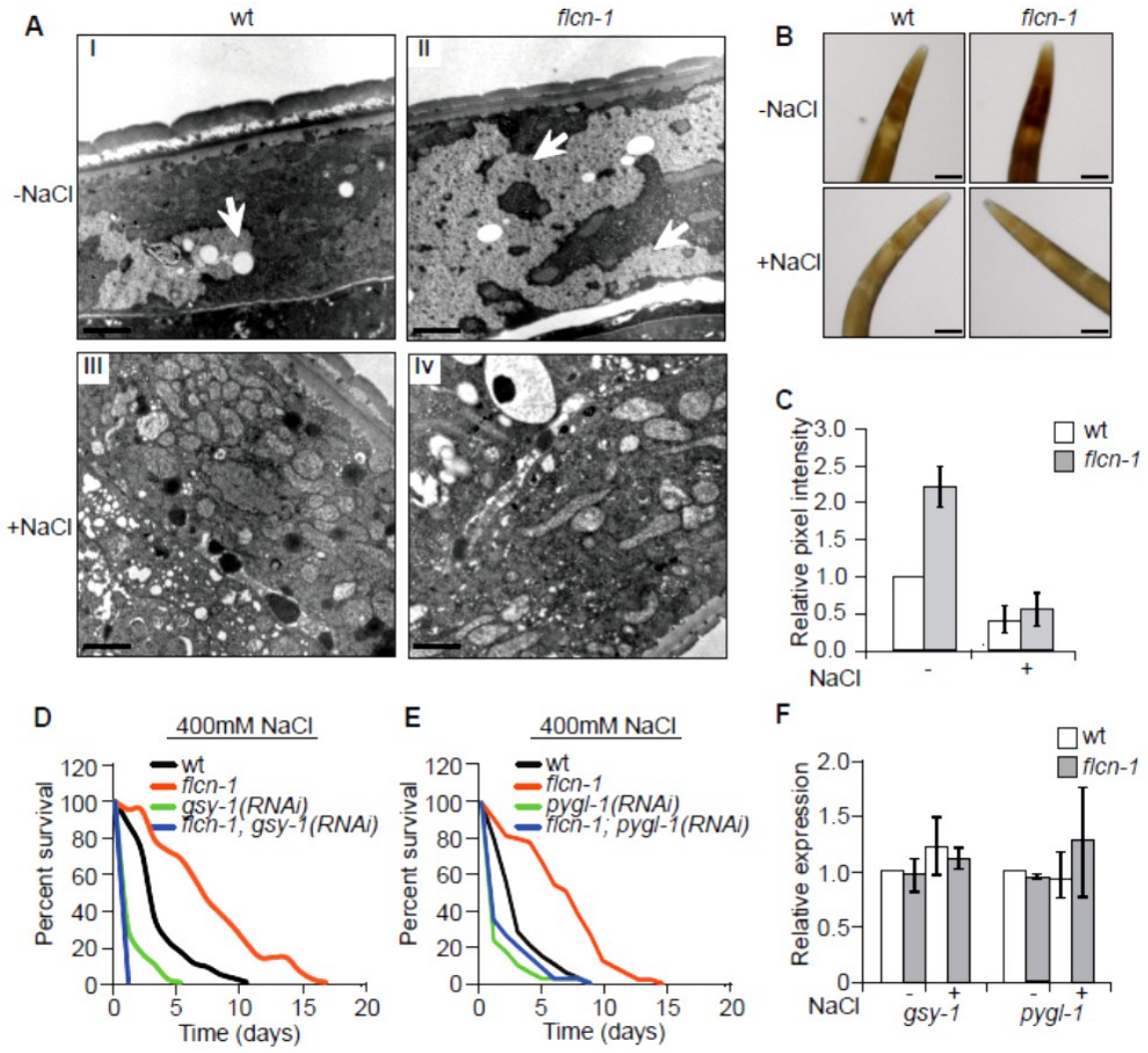

Figure 3.2: Loss of *flcn-1* increases glycogen content in *C. elegans* which mediates resistance to hyperosmotic stress.

(A) Representative electron micrographs from longitudinal sections of the hypodermis in indicated nematodes strains exposed or not to 400mM NaCl for 16 hours. Arrows represent glycogen stores. Scale bars indicate 2µm. (B, C) Iodine staining (B) and quantification of staining intensities (C) of indicated worm strains treated or not with 400mM NaCl for 16 hours. Data represent mean ± SEM, n≥ 3. (D, E) Percent survival to 400mM NaCl of indicated worm strains treated with indicated RNAi. Also see Table 3.1. (F) Relative mRNA levels of indicated target genes in indicated strains with or without 400mM NaCl treatment for 2 hours. Data represent mean ± SEM, n≥ 3.

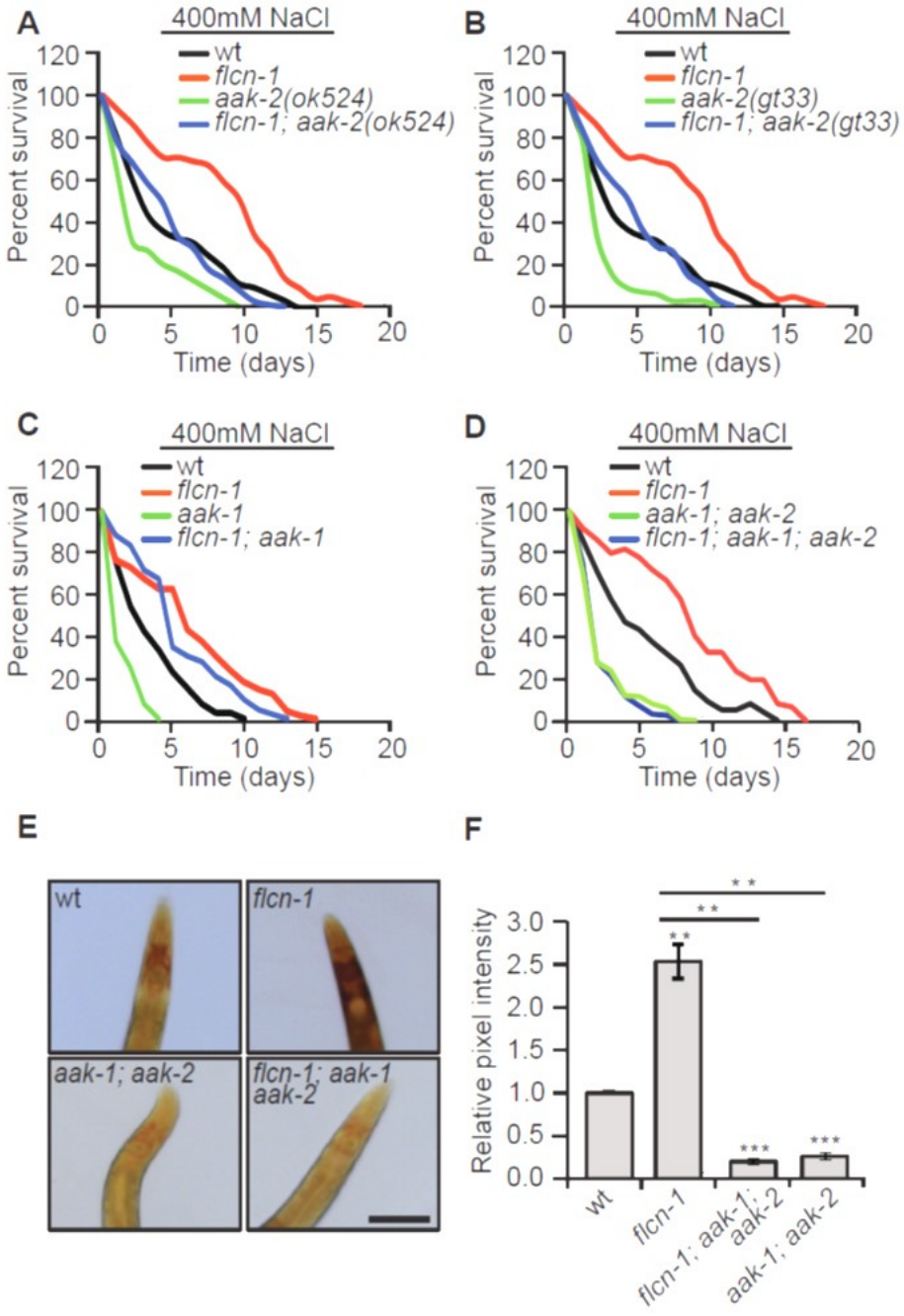

Figure 3.3: The increased survival to hyperosmotic stress and the accumulation of glycogen in *flcn-1* mutant worms require AMPK.

(A, B, C, D) Percent survival of indicated worm strains exposed to 400mM NaCl. (A) *aak-2(ok524)*, (B) *aak-2(gt33)*, (C) *aak-1(tm1944)*, (D) *aak-1(tm1944)*; *aak-2(ok524)*. Also see Table 3.1. (E, F) Iodine staining (E) and quantification of staining intensities (F) of indicated worm strains. Data represent mean ± SEM of at least 3 independent trials.

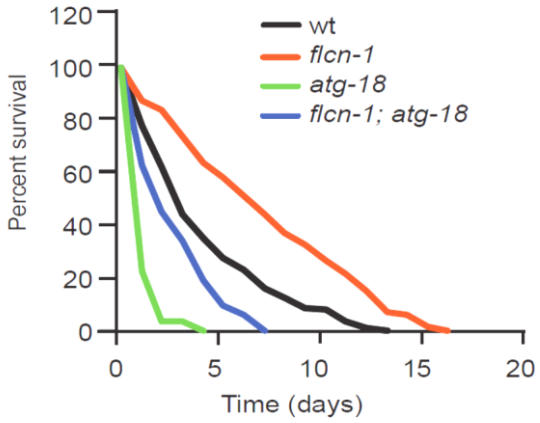

Figure 3.4: The increased resistance of *flcn-1(ok975)* animals to NaCl does not fully require autophagy.

Percent survival of indicated worm strains exposed to 400mM NaCl. Also see Table 3.1.

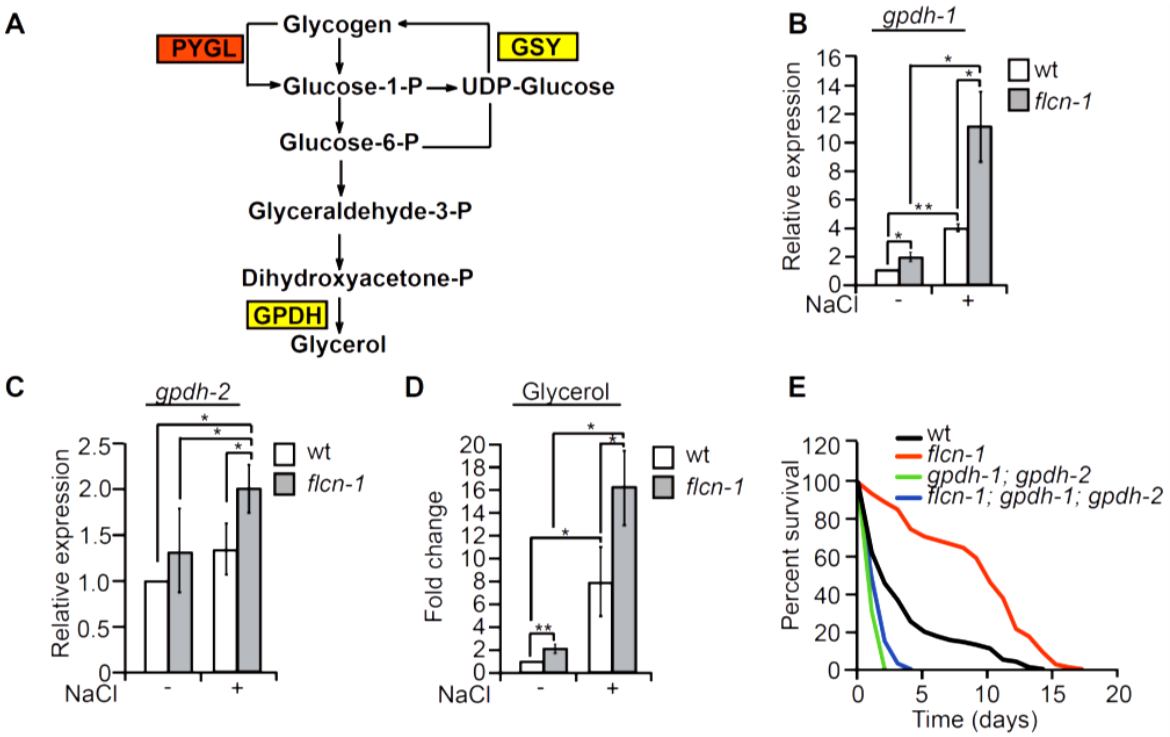

Figure 3.5: Enhanced glycogen degradation leads to higher levels of glycerol which protects animals against stress.

(A) Representative scheme of glycogen metabolism and osmolyte production in worms. Yellow squares indicate synthesis enzymes while orange squares indicate enzymes involved in degradation pathways. (B, C) Relative mRNA levels of *gpdh-1* (B) and *gpdh-2* (C) in wild-type and *flcn-1(ok975)* L4/young adult animals treated or not with 400mM NaCl for 2 hours. Data represent mean ± SEM, n ≥3. (D) Glycerol levels in wild-type and *flcn-1(ok975)* L4/young adult animals treated or not with 400mM NaCl for 2 hours. (E) Percent survival to 400mM NaCl of indicated worm strains. Also see Table 3.1.

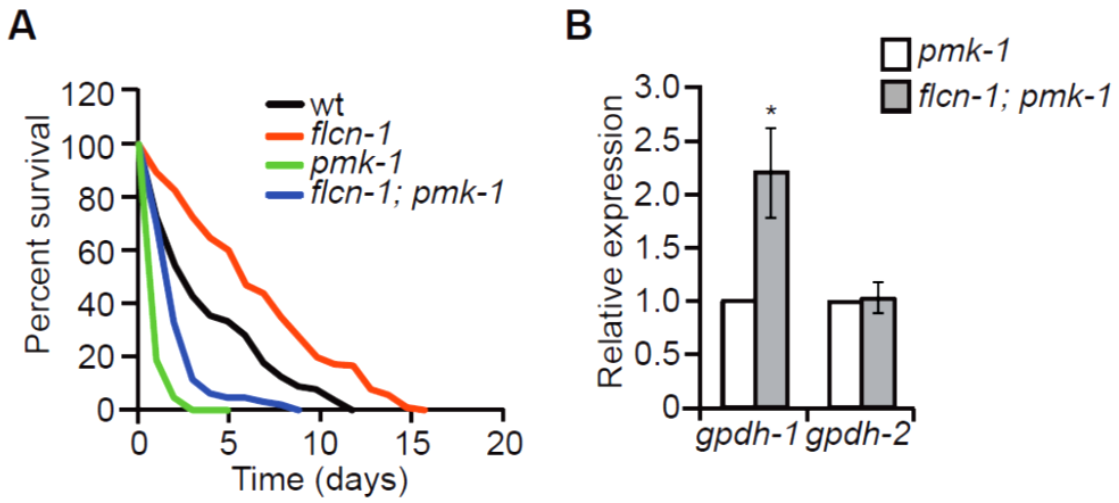

Figure 3.6: Involvement of PMK-1 in the transcriptional response of *gpdh-1* and response to hyperosmotic stress.

(A) Percent survival of indicated worm strains exposed to 400mM NaCl, *pmk-1(km25)*. Also see Table 3.1. (B) Relative mRNA levels of *gpdh-1* in indicated worm strains.

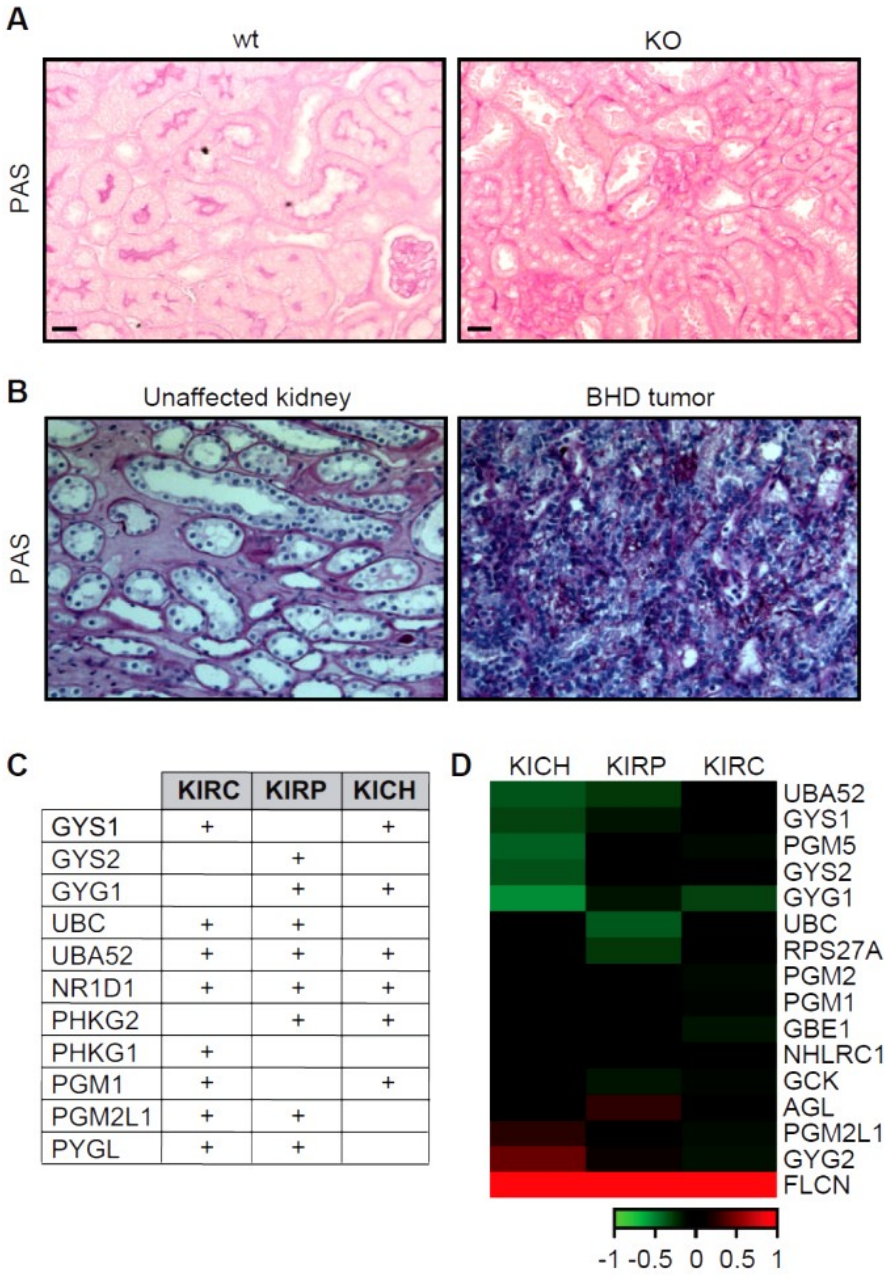

	KIRC	KIRP	KICH
GYS1	+		+
GYS2		+	
GYG1		+	+
UBC	+	+	
UBA52	+	+	+
NR1D1	+	+	+
PHKG2		+	+
PHKG1	+		
PGM1	+		+
PGM2L1	+	+	
PYGL	+	+	

Figure 3.7: The increased accumulation of glycogen content conferred by loss of FLCN is conserved from *C. elegans* to humans.

(A-B) PAS staining of kidney sections from wt and *Flcn* kidney-specific KO mice (A) and human BHD kidney tumor in comparison with an adjacent region from the same individual (B). Scale bars:100µm. (C) Table indicating the upregulated glycogen metabolism genes in kidney tumors (KIRC, KIRP, and KICH) as compared to normal kidney. The sign (+) indicates genes that are upregulated in these tumors. The values are indicated in Table S5. (D) Heat map indicating correlation of expression between glycogen metabolism genes and *FLCN* in KIRC, KIRP, and KICH tumors. Green and red colors indicate genes that are negatively or positively correlated with FLCN expression, respectively.

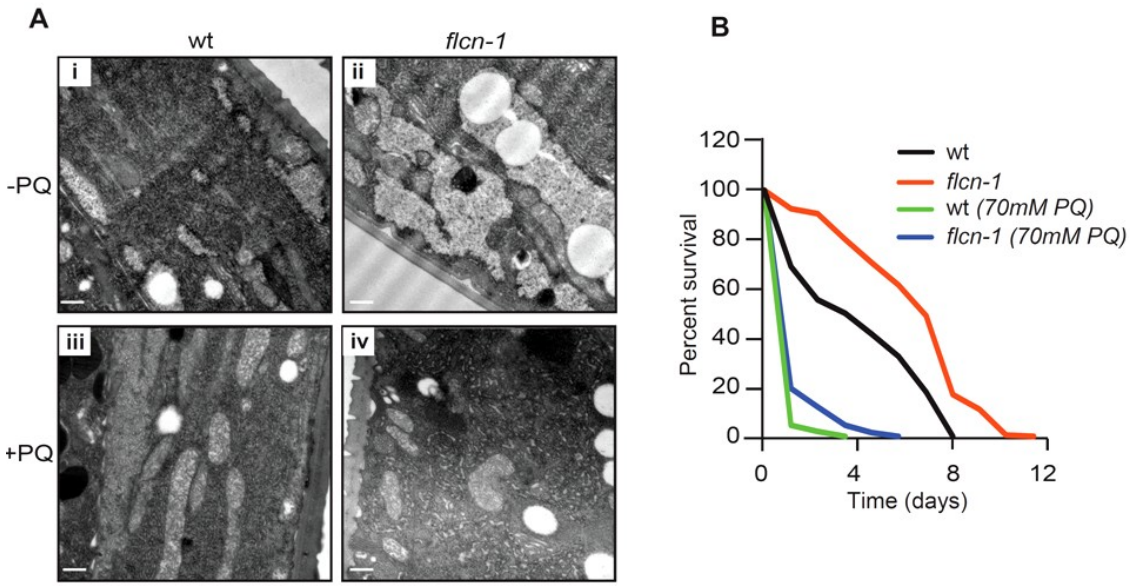

Figure 3.8: Pretreatment of wild-type and *flcn-1(ok975)* animals with paraquat suppresses hyperosmotic stress resistance.

(A) Electron micrographs showing glycogen stores in wild-type and *flcn-1(ok975)* L4/young adult animals with or without 50mM paraquat treatment for 2 hours. Scale bars indicate 0.5 µm. (B) Percent survival of indicated worm strains to 400mM NaCl treated or untreated with 70mM paraquat for 5 hours.

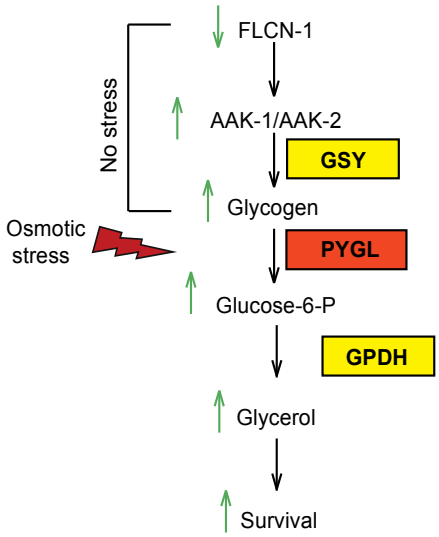

Figure 3.9: Graphical representation of FLCN-1/AMPK hyperosmotic stress resistance pathway.

Loss of *flcn-1* chronically activates AMPK and leads to glycogen accumulation under normal conditions. Upon exposure to hyperosmotic stress, glycogen is rapidly degraded leading to the production of glycerol and animal survival.

Table 3.1: Mean survival on NaCl plates: results[a] and statistical analysis[b]

Strain, RNAi	Percent Survival (4h) (±SEM)	p-value	Number of experiments (n)
N2	4.79 ± 1.11		21
flcn-1(ok975)	7.89 ± 1.70	<0.0001[c]	21
N2 (500mM NaCl)	2.58 ± 1.38		7
flcn-1(ok975) (500mM NaCl)	6.46 ± 1.03	<0.0001[d]	7
flcn-1(ok975)	7.15 ± 0.83		3
flcn-1(ok975); flcn-1:GFP	4.60 ± 1.17	<0.0001[e]	3
aak-2(ok524)	2.37 ± 0.77	<0.0001[f]	3
flcn-1(ok975); aak-2(ok524)	3.81 ± 1.05	<0.0001[g, h]	3
aak-1(tm144)	1.79 ± 0.09	<0.0001[i]	3
flcn-1(ok975); aak1(tm1944)	5.20 ± 0.38	<0.0001[j, k]	3
aak-1(tm1944); aak-2(ok524)	2.64 ± 0.64	<0.0001[l]	5
flcn-1(ok975);aak-1(tm1944);aak-2(ok524)	2.51 ± 0.60	<0.0001[m]/n.s. [n]	5
atg-18(gk378)	1.40 ± 0.24	<0.0001[o]	4
flcn-1(ok975);atg-18(gk378)	3.12 ± 0.50	<0.0001[p, q]	4
aak-2(gt-33)	2.14 ± 0.54	<0.0001[r]	3
flcn-1(ok975);aak-2(gt-33)	4.36 ± 0.64	<0.0001[s, t]	3
pmk-1(km25)	1.34 ± 0.26	<0.0001[u]	5
flcn-1 (ok975); pmk-1(km25)	2.43 ± 0.23	<0.0001[v, w]	5
gpdh-1(kb24); gpdh-2(kb33)	1.25 ± 0.09	<0.0001[x]	3
flcn-1; gpdh-1(kb24); gpdh-2(kb33)	1.59 ± 0.16	<0.0001[y, z]	3
N2 (*ev*)	3.24 ± 1.03		7
flcn-1 (ev)	5.74 ± 1.74	<0.0001[aa]/0.0069[bb]	7
N2 (*gsy-1* RNAi)	1.20 ± 0.19	<0.0001[cc]	4
flcn-1(ok975)(*gsy-1* RNAi)	1.22 ± 0.22	<0.0001[dd]/n.s. [ee]	4
N2 (*gpdh-1* RNAi)	1.64 ± 0.09	<0.0001[ff]	3
flcn-1(ok975)(*gpdh-1* RNAi)	2.68 ± 1.03	<0.0001[gg, hh]	3
N2 *(pygl-1* RNAi*)*	1.37 ± 0.37	<0.0001[ii]	4

flcn-1(ok975)(*pygl-1* RNAi)	1.47 ± 0.37	<0.0001[jj]/n.s. [kk]	4
N2 (*gpdh-2* RNAi)	3.43 ± 1.08	<0.0001[ll]	3
flcn-1(ok975)(*gpdh-2* RNAi)	7.42 ± 0.07	<0.0001[mm, nn]	3

(a) Survival on 400mM NaCl have been performed unless noted otherwise
(b) Mantel-Cox statistics on pooled results unless noted otherwise
(c) Compared to N2 animals
(d) Compared to *N2* animals
(e) Compared to *flcn-1(ok975)* animals
(f) Compared to N2 animals
(g) Compared to *aak-2 (ok524)* animals
(h) Compared to *flcn-1(ok975)* animals
(i) Compared to N2 animals
(j) Compared to *aak-1 (tm1944)* animals
(k) Compared to *flcn-1(ok975)* animals
(l) Compared to N2 animals
(m) Compared to *flcn-1(ok975)* animals
(n) Compared to *aak-1(tm1944); aak-2(ok524)* animals
(o) Compared to N2 animals
(p) Compared to *atg-18 (gk378)* animals
(q) Compared to *flcn-1(ok975)* animals
(r) Compared to N2 animals
(s) Compared to *aak-2(gt33)* animals
(t) Compared to *flcn-1(ok975)* animals
(u) Compared to N2 animals
(v) Compared to *pmk-1(ku25)* animals
(w) Compared to *flcn-1(ok975)* animals
(x) Compared to N2 animals
(y) Compared to *flcn-1(ok975)* animals
(z) Compared to *gpdh-1(kb24); gpdh-2(kb33)* animals
(aa) Compared to N2 animals (Mantel-Cox)
(bb) Compared to N2 animals (t-test for means)
(cc) Compared to N2 animals treated with control RNAi
(dd) Compared to *flcn-1(ok975)* animals treated with control RNAi
(ee) Compared to N2 animals treated with *gsy-1* RNAi
(ff) Compared to N2 animals treated with control RNAi
(gg) Compared to *flcn-1(ok975)* animals treated with control RNAi
(hh) Compared to N2 animals treated with *gpdh-1* RNAi
(ii) Compared to N2 animals treated with control RNAi
(jj) Compared to *flcn-1(ok975)* animals treated with control RNAi
(kk) Compared to N2 animals treated with *pygl-1* RNAi
(ll) Compared to N2 animals treated with control RNAi
(mm) Compared to *flcn-1(ok975)* animals treated with control RNAi
(nn) Compared to N2 animals treated with *gpdh-2* RNAi

Table 3.2: Glycogen metabolism gene regulation in KIRC, KIRP and KICH kidney tumors

Genes	KICH			KIRC			KIRP		
	Median of tumor samples	Median of normal samples	P value	Median of tumor samples	Median of normal samples	P value	Median of tumor samples	Median of normal samples	P value
GYS1	0.2794	-0.6122	<0.0001	0.02552	-0.7864	<0.0001	ns	ns	0.84
GYS2	ns	Ns	0.42	ns	ns	0.5	0.1384	-0.6196	<0.0001
GYG1	0.336	-0.9145	<0.0001	ns	ns	0.2	0.07869	-0.1943	<0.001
UBC	0.1075	-0.8703	0.192	0.1075	-0.8703	<0.0001	0.02744	-0.4162	<0.0001
UBA52	0.0913	-0.2527	<0.001	0.063	-0.5169	<0.0001	0.04811	-0.3756	<0.0001
NR1D1	0.3206	-0.8421	<0.0001	0.157	-0.8631	<0.0001	0.2355	-1.224	<0.0001
PHKG2	0.153	-0.3173	<0.0001	ns	ns	0.34	0.04544	-0.4429	<0.0001
PHKG1	ns	Ns	0.098	0.1104	-1.118	<0.0001	ns	ns	0.2
PGM1	0.1682	-0.1728	<0.001	0.0742	-0.1665	<0.0001	0.1336	0.07823	0.55
PGM2L1	ns	Ns	0.5	0.1793	-0.9215	<0.0001	0.09386	-0.8117	<0.0001
PYGL	-0.8172	1.78	<0.0001	0.3953	-1.85	<0.0001	0.3386	-1.08	<0.0001

Table 3.3: Strain list

Genotype	Strain Number	Additional information
wild-type Bristol (N2)		
flcn-1(ok975) II	RB1035	RB1035 strain was outcrossed 8 times with wild-type Bristol (N2)
aak-1(tm1944) III	FX1944	from CGC
aak-2(ok524) X	RB754	from CGC
aak-2(gt33)X	TG38	from CGC
atg-18(gk378) V	VC893	from CGC
pmk-1(km25) IV	KU25	from CGC
flcn-1(ok975); aak-1(tm1944)		
flcn-1(ok975); aak2 (gt33)		
flcn-1(ok975); atg-18(gk378)		
aak-1(tm1944); aak-2(ok524)		
flcn-1(ok975); aak-1(tm1944); aak-2(ok524)		
flcn-1(ok975); pmk-1(km25)		
gpdh-1(kb24); gpdh-2(kb33)		
flcn-1(ok975); gpdh-1(kb24) I ; gpdh-2(kb33) III		
flcn-1(ok975); flcn::GFP		Overexpression of FLCN-1 co-injected with pRF4 (*rol-6*) and pCFJ90 (*Pmyo-2::mCherry::unc-54utr*)

Table 3.4: Primer sequences

Gene symbol	Forward primer	Reverse primer
gpdh-1	CTTGCTATGGAGGTCGCAAT	CTTATGCACTGACGCGAAGA
gpdh-2	GTGGTAGCCGTCACTGACCT	GCCAAATTAGCTCCCATCAA
gsy-1	TCGTCAACGCATCATTCTTC	ATCGTCCTCTCCATCACTGG
pygl-1	TGGCATGTTCACTCCAGAAG	CCCAGATTTCACGAGCGTAT
cdc-42	GGCAAAGGAATTGAAAGCAG	GGGGGCTAAGAAAATTTGGA

CHAPTER 4

TRANSCRIPTIONAL REGULATION DOWNSTREAM FLCN-1 IN C. ELEGANS

Manuscript in preparation

4.1 Preface to chapter 4

We have shown in chapter 2 and chapter 3 that loss of *flcn-1* leads to increased resistance to energy stresses and hyperosmotic stress. We also showed that the increased survival to metabolic stresses relies on AMPK-dependent induction of autophagy while the resistance to hyperosmotic stress requires remodeling of glycogen stores. However, we did not investigate whether there is a gene expression profile that contributes to the increased stress survival upon loss of *flcn-1*. In this chapter, we determined the gene expression profile in *flcn-1* mutant animals as compared to wild-type at basal level. Importantly, we found that *flcn-1* deficiency leads to the transcriptional upregulation of stress response genes prior to stress and that this signature overlaps with divergent stress response signatures including oxidative stress, hyperosmotic stress, and infection with pathogens. Accordingly, we also showed that in addition to the stresses tested previously, loss of *flcn-1* leads to resistance to pathogens. Importantly, our data indicates a significant overlap with genes regulated by the transcription factor HLH-30, the worm homolog of TFEB. Supporting this, we show that loss of *hlh-30* abrogates resistance to hyperosmotic stress which might imply a potential role of *hlh-30* downstream *flcn-1/ampk*.

4.2 Abstract

Signaling through the FLCN-1/AMPK axis modulates metabolism and stress response in *Caoenorhabditis elegans*. FLCN-1 is the worm homolog of the tumor suppressor FLCN and its deficiency predisposes to renal tumors and cysts in humans. To understand and fully dissect the molecular basis of this stress response pathway in *C. elegans*, we compared changes in mRNA levels in wild-type and *flcn-1* mutant animals using wide-genome microarrays. We find that genes upregulated by loss of *flcn-1* are C-type lectins, stress response genes including heat-shock proteins, and metabolite biosynthesis, transport, and catabolism genes. Importantly, we found that the gene expression profile upon loss of *flcn-1* overlaps significantly with stress response signatures, including oxidative stress, hyperosmotic stress, and pathogen resistance, supporting the stress resistance phenotypes. We also found a significant overlap with genes regulated by the transcription factor HLH-30, a master regulator of lysosomal pathways, autophagy, and stress response. Our data also indicate a requirement for *hlh-30* in the increased resistance of *flcn-1* animals to hyperosmotic stress. The microarray data presented herein define FLCN-1 as a regulator of stress response gene expression. This could explain how loss of FLCN drives tumorigenesis in humans: by helping tumor cells resist stressful microenvironments.

4.3 Introduction

It is firmly established that metabolic pathways play important roles in the regulation of lifespan and stress resistance. In many organisms, mutations in the insulin signaling pathway, TOR signaling, mitochondrial respiration, feeding, and autophagy correspondingly modulate lifespan and resistance to various stresses (Zhou et al., 2011; Ristow and Zarse, 2010). The 5' AMP-activated protein kinase (AMPK) is a master regulator of cellular metabolism and stress response [65]. In *C. elegans,* like in most organisms, AMPK is

required for lifespan extension and survival to many stresses including oxidative stress, heat, dietary restriction [41,74,78,80,265]. We have shown in chapter 2 that AMPK is required for the resistance to oxidative stress, heat, and anoxia and in chapter 3 that it is required for survival to hyperosmotic stress in *C. elegans*.

Upon exposure to stress, several cellular processes are regulated by AMPK to enhance organismal/cellular survival. For instance, AMPK negatively regulates mTORC1 to suppress cellular growth and energy consuming pathways [43,57]. AMPK also regulates autophagy to manage cellular damage and recycle building blocks for energy production [57,59-61,262]. Among various tasks, AMPK orchestrates several cellular pathways through phosphorylation of transcription factors and co-activators [57]. In *C. elegans*, AMPK activates DAF-16/FOXO3a which induces the transcription of genes involved in stress response such as heat shock proteins and ROS detoxifying enzymes [78,323]. The AMPK/DAF-16 axis mediates lifespan extension and resistance to oxidative stress in nematodes [78]. AMPK also activates the transcription factors of the CREB family in *C. elegans* to mediate lifespan and in mammalian systems [74,75].

Folliculin (FLCN) is a 64kDa tumor suppressor protein that binds AMPK [38]. In humans, loss of FLCN causes the Birt-Hogg-Dubé syndrome, a disease characterized by the formation of renal cysts and tumors [3,12]. We have previously shown that loss of FLCN negatively regulates AMPK in *C. elegans* and in mammalian cells and that its deficiency enhances resistance to various stresses in both systems (Chapters 2 and 3) [77]. Since loss of FLCN chronically activates AMPK and based on the fact that AMPK activation induces stress response transcriptional programs, we hypothesized that the survival advantage conferred by FLCN loss might be due to an AMPK-dependent activation of a stress response transcriptional profile prior to stress. Microarray experiments aiming to understand the FLCN

function and determine FLCN-regulated downstream genes have linked FLCN to TGF beta signaling and Wnt signaling in mammalian systems [106,108]. Despite, it remains unclear which transcription factors are activated by FLCN deficiency and how loss of FLCN causes tumor and cyst formation in humans.

Since transcriptional signaling networks of stress response are highly evolutionarily conserved, we aimed to determine target genes regulated downstream of *flcn-1/ampk* in *C. elegans*. Here we show that *flcn-1* deficiency in *C. elegans* initiates a stress response transcriptional program prior to stress. Specifically, we demonstrate that C-type lectins, heat shock proteins, cytochrome P450 genes, and lysosymes are transcriptionally upregulated in *flcn-1(ok975)* animals at normal conditions. Importantly, we highlight that the transcriptional profile conferred by loss of *flcn-1* overlaps with many stress response signatures including oxidative stress, hyperosmotic stress, and infection with pathogens. We also show a significant overlap between genes upregulated upon loss of *flcn-1* and genes downregulated in *hlh-30* mutant animals and showed a requirement of *hlh-30* in the protection of *flcn-1(ok975)* against hyperosmotic stress.

4.4 Results

4.4.1 Transcriptional profile of flcn-1(ok975) nematodes

To understand the functional role of FLCN-1, we compared gene expression profiles of wild-type and *flcn-1(ok975)* animals using DNA microarray analysis (Agilent oligo microarrays). Among differentially expressed genes, 296 transcripts were up-regulated and 535 transcripts were downregulated significantly in *flcn-1(ok975)* mutant animals compared to wild-type at basal level. We did not analyze the downregulated list of genes since it encompasses a lot of hypothetical proteins. The up-regulated transcripts were then classified

according to their biological functions using DAVID (Database for Annotation, Visualization and Intergrated discovery). Strikingly, C-type lectins, stress response genes, as well as genes involved in secondary metabolites biosynthesis and catabolism were induced in *flcn-1(ok975)* unstressed animals compared wild-type animals. Specifically, 18 C-type lectin genes, 6 heat-shock transcripts, 9 cytochrome P450 family members, and 4 lysozyme genes were induced in *flcn-1(ok975)* mutants (Table 4.1). Microarray data were validated using quantitative real time PCR (qRT-PCR) of selected genes (Figure 4.1A). Specifically, *lys-3*, *lys-10*, *clec-60*, *clec-74*, *hsp-16.41*, *thn-2*, *cyp-13A5*, *cyp-35A4*, and *gpdh-1* were induced by qRT-PCR in *flcn-1(ok975)* mutant nematodes. This result indicates that a differential gene expression might be providing advantage to the *flcn-1* worms prior to stress. This is in accordance with our previously reported result where loss of *flcn-1(ok975)* confers resistance to oxidative stress, heat stress, anoxia, and hyperosmotic stress in *C. elegans* (chapters 2 and 3).

4.4.2 Autophagy and ROS-detoxification genes are not transcriptionally induced in flcn-1 animals

Since we observed in chapter 2 that autophagy is induced in *flcn-1(ok975)* animals at basal level, we asked whether this activation is the result of a transcriptional upregulation of autophagy genes. First, none of the *C. elegans* autophagy genes were found to be differentially regulated between wild-type and *flcn-1(ok975)* animals in our microarray. Supporting this result, using qRT-PCR performed, we did not observe a significant change in autophagy gene expression between wild-type and *flcn-1(ok975)* nematodes validating the microarray result (Figure 4.2). Moreover, in accordance with the qRT-PCR data presented in chapter 2 (Figure 2.3C), our microarray data also did not reveal ROS-detoxification genes upregulated in *flcn-1(ok975)* animals as compared to wild-type. Altogether, these data suggest first that the autophagy activation upon loss of *flcn-1* is not regulated transcriptionally, and that ROS-detoxification genes are not induced upon *flcn-1* loss.

4.4.3 Comparisons with other relevant stress response transcriptional profiles

Next we asked whether the transcriptional profile in *flcn-1* is a general stress response signature or is specific to the type of stress. We compared our results with other stress response transcriptional profiles to find significant overlaps. Importantly, out of 296 genes upregulated by loss of *flcn-1* and 133 genes upregulated by oxidative stress, 16 genes are overlapping, which is more than expected by chance [205]. This could also explain the increased resistance of *flcn-1(ok975)* mutant animals to oxidative stress that we reported in chapter 2 (Figure 4.3). Since loss of *flcn-1* also conferred resistance to hyperosmotic stress, we compared the transcriptional profile of the *flcn-1* mutant animals to the profiles of wild-type animals exposed to hyperosmotic stress and to hyperosmotic stress resistant mutant strains such as *osm-7* and *osm-11* and also observed a significant overlap [220] (Figures 4.4A-C). Importantly, *gpdh-1* is upregulated in all *flcn-1(ok975)*, *osm-7(n1515)*, and *osm-11(n1604)* mutant strains and in wild-type animals exposed to NaCl (Tables 4.3-4.5). Moreover, since it was demonstrated that the osmosensitive gene expression mimics the transcriptional profiles of pathogen infection [220], we compared the overlap between genes upregulated in *flcn-1(ok975)* animals and genes induced by infection of *C. elegans* nematodes with pathogens [324,325], and also found a significant overlap (Figures 4.5A-C and Tables 4.6-4.8). Altogether, this supports that loss of *flcn-1* increases stress response genes prior to stress and that the transcriptional profile overlaps with diverse stress response signatures.

4.4.4 Loss of flcn-1 increases resistance to pathogen infection

Since we observed a significant overlap between genes upregulated in *flcn-1* and genes induced by pathogen infection, we wondered if *flcn-1(ok975)* mutant animals are also resistant to pathogens. We measured the survival of wild-type and *flcn-1(ok975)* animals upon infection with *Staphylococcus aureus* and *Pseudomonas aeruginosa*. Strikingly, we found

that the *flcn-1(ok975)* animals are more resistant than wild-type to pathogens, especially to *Staphylococcus aureus (*Figures 4.5D-E).

4.4.5 Loss of flcn-1 controls protein homeostasis

We also looked for overlaps between genes regulated by *flcn-1* and genes that change during aging and that are upregulated in longevity mutant strains (Figure 4.6A) [326]. Although we did not observe a difference in lifespan between wild-type and *flcn-1(ok975)* animals as mentioned in chapter 2, the overlap between the longevity transcriptome and the *flcn-1*-dependent expression was significant (Figure 4.6A). This result might imply that loss of *flcn-1* increases healthy lifespan or healthspan without affecting lifespan. Supporting this, loss of *flcn-1* increased resistance to oxidative, heat, anoxia, and osmotic stresses (chapters 2 and 3), which are hallmarks of healthspan since they assess the ability of an organism to respond to perturbations [327].

Maintaining cellular homeostasis is another important factor for healthy lifespan. We aimed to determine whether loss of *flcn-1* has a role in protein homeostasis. We used the *polyQ-35:YFP* transgene, which is expressed in the body wall muscle of *C. elegans* nematodes, where polyQ residues mimic the glutamine repeats that are found in the mutated Huntington gene, which predisposes for Huntington disease. The accumulation of protein aggregates leads to nematode paralysis and can be scored over time. To determine whether *flcn-1* is involved in protein homeostasis, we generated the *flcn-1; polyQ-35* double mutant strain and measured paralysis and motility over time as compared to *polyQ-35* animals. Importantly, our results demonstrate that loss of *flcn-1* decreased worm paralysis and increased motility with age, suggesting that *flcn-1* deficiency improves the control of protein homeostasis (Figure 4.6C-D). Overall, our results demonstrate that loss of *flcn-1* improves healthspan.

4.4.6 Comparison with the hlh-30 transcriptional profile and requirement of hlh-30 in the resistance of flcn-1 animals to hyperosmotic stress.

HLH-30 (the worm ortholog of TFEB transcription factor) is involved in many longevity pathways and has been shown to modulate stress responses such as starvation in *C. elegans* via autophagy [328,329]. Based on this, we asked whether loss of FLCN-1 leads to the activation of HLH-30 at basal level in *C. elegans* leading to a transcriptional upregulation of stress response genes prior to stress. Importantly, we find a significant overlap between genes that are upregulated in *flcn-1* animals and downregulated in *hlh-30(jin1375)* mutant animals (Figure 4.7A and Table 4.9) [330]. To follow up on this result, we used a *flcn-1(ok975); hlh-30(jin1375)* double mutant strain and compared its hyperosmotic stress survival to *hlh-30* mutants alone. Loss of *hlh-30* significantly reduced the increased survival conferred by loss of *flcn-1* suggesting its involvement in the hyperosmotic stress resistance response (Figure 4.7B).

4.5 Discussion

Here we performed gene expression-profiling in wild-type and *flcn-1(ok975)* animals under normal conditions. In accordance with the stress resistance phenotypes that we previously reported, gene classification indicates that loss of *flcn-1* induced the expression of C-type lectins, stress response genes, and genes involved in metabolite transport and catabolism.

C-type lectins are carbohydrate-binding proteins which play an important role in pathogen recognition and are involved in the cross-talk with other signaling receptors including the Toll receptors. For instance, in *C. elegans*, the *clec-60* gene is used as an

infection marker because of its prominent induction upon infection with *Staphylococcus aureus* and is highly expressed in *flcn-1* animals prior to stress [324].

Up-regulated genes also include heat-shock proteins which are involved in protein homeostasis upon stress. They are upregulated in most organisms not only upon heat shock, but also during other stressful situations such as UV exposure, cold, oxidative stress, infection, hypoxia, starvation, and others [331]. Many heat shock proteins act as chaperones to others. They assist protein folding and monitor protein quality control by repairing misfolded ones or by sending damaged ones for degradation in the proteasome[331]. We report the upregulation of six heat shock proteins in *flcn-1* animals as compared to wild-type at basal level, *hsp-16.1*, *hsp-16.11, hsp-16.2*, *hsp-16.41*, *hsp-16.48* and *hsp-16.49*. In *C. elegans*, *hsp-16.2* has been shown to be upregulated upon several stresses [332,333]. Heat shock proteins are also important under non stressful conditions. The fact that they are upregulated in *flcn-1* at basal level correlates well with the delayed accumulation of age-related protein damage conferred by loss of *flcn-1* as we reported herein. Specifically, we show that the *polyQ-35* transgenic strains undergo slower age-dependent paralysis upon *flcn-1* deficiency reflecting lower protein damage and suggesting that *flcn-1* regulates protein homeostasis in *C. elegans*. This might also imply that *flcn-1* deficiency increases healthspan and not overall lifespan in *C. elegans.*

Loss of *flcn-1* also induced the expression of cytochrome P450 family proteins which are heme-containing monooxygenases that play an important role in xenobiotic metabolism and oxidative stress response [333,334]. The *C. elegans* genome contains 80 cytochrome P450 genes. Importantly, *cyp-35* has been shown to be a strongly xenobiotic inducible [333]. Our data indicates the upregulation of nine genes encoding CYP 450 proteins encompassing three genes of the *cyp-35* group, *cyp-35A2*, *cyp-35A3*, and *cyp-35A4*. Lysosymes are another

set of genes upregulated in *flcn-1* animals at normal conditions. Lysosymes are glycoside hydrolases that "degrade" bacterial cell walls by catalyzing the breakdown of 1,4-beta-linkages between N-acetylmuramic acid and N-acetyl-D-glucosamine residues and between N-acetyl-D-glucosamine residues in apeptidoglycan and in chitodextrins respectively.

What transcription factor is responsible for the stress response transcriptional profile acquired by loss of *flcn-1* in *C. elegans* is still not clear. Data presented herein suggest a potential involvement of HLH-30, the worm homolog of TFEB and master regulator of lysosomal biogenesis and stress response [328-330]. HLH-30 has been shown to play an important role in the transcriptional induction of autophagy and lysosomal genes, mediating resistance to pathogen infection and starvation [328-330]. Here we show that a significant number of stress response genes upregulated in *flcn-1(ok975)* animals are downregulated in the *hlh-30(jin1375)* mutant strain and that HLH-30 plays a pivotal role in resistance to hyperosmotic stress. The existence of a FLCN-1/HLH-30 axis is not surprising and could be evolutionary conserved. In fact, it has been shown that members of the TFE family are induced by loss of FLCN in mammalian cells [85,104]. On the other hand, we have previously shown that the FLCN-dependent AMPK activation induces the transcriptional coactivator PGC-1α and the hypoxia-inducible factor HIF-1, to drive the Warburg metabolic reprogramming and tumorigenesis [77]. These are other pathways that could be involved in the stress response signature mediated by *flcn-1* absence in *C. elegans*. In fact, it is highly likely that a network of transcription factors is induced by *flcn-1* loss to coordinate the expression of stress response genes prior to stress, enabling *flcn-1(ok975)* mutant nematodes to better survive acute stress conditions.

Notably, it remains unknown whether this stress response signature is conserved from worms to mammals and whether it contributes to the initiation and progression of BHD

disease. In chapters 2 and 3, we propose that the activation of autophagy, increased energy, and osmolyte production could be driving tumorigenesis in BHD kidneys. Although heat shock proteins, cytochrome P450 proteins and lysosymes protect cells/tissues from damage upon acute stress exposure, recent findings suggest their involvement in helping tumors survive harsh microenvironments [335-338]. Future work would aim to determine (1) whether this stress response transcriptional profile is linked to AMPK and TFEB signaling in *C. elegans* and mammalian systems, (2) whether it is conserved from worms to humans, and (3) whether it contributes to the initiation and progression of BHD disease. These perspectives will be detailed in the overall discussion of this thesis.

4.6 Material and methods

C. elegans strains and maintenance

The following strains were used: N2 Bristol (wild-type), *flcn-1(ok975),* rmIs132[*Punc-54*::Q35::YFP], *hlh-30(jin1375)* and *flcn-1(ok975); hlh-30(jin1375)* Unless noted otherwise, nematodes were maintained and synchronized using standard culture methods [128].

RNA extraction and real-time PCR

Synchronized L4/young adult nematodes were harvested and total RNA was extracted with Trizol and purified using the RNeasy kit (Qiagen). Quantitative real-time PCR (qRT-PCR) was performed using Express SYBR Green qPCRsupermix (Invitrogen) and LightCycler480 system (Roche). Genes were normalized to housekeeping gene *cdc-42* [302]. For primer sequences see Table 4.9.

Microarray experiment and gene overlap analysis

Synchronized L4/young adult wild-type and *flcn-1(ok975)* animals were harvested and RNA was extracted using Trizol and cleaned up on Qiagen RNeasy columns. Total RNA samples were then hybridized onto Agilent gene chips. Fold change values are calculated using the mean of both data sets. Agilent files were uploaded into the FlexArray software at Genome Quebec for analysis. Three replicates were normalized and analyzed for each condition. Fold change was determined and p-value was obtained using t-test. Differentially expressed genes were compared to other studies, oxidative stress, hyperosmotic stress [220], pathogen infection[324], *osm-7*[220], *osm-11*[220], and aging using compare two lists from nemates. The overlapping genes were determined using the "compare two lists" online tool at http://www.nemates.org/MA/progs/Compare.html. The significance of the overlap and enrichment scores were determined via hypergeometric distribution method using http://nemates.org/MA/progs/overlap_stats.html. The number of genes in the *C. elegans* genome was considered 19,735.

Paralysis assay

Aging-induced *polyQ-35* toxicity was measured by transferring synchronized one day adult animals to normal media growth plates. Adult animals were transferred every two days to new plates to separate them from their progeny. Paralysis was monitored and scored over time. Animals that did not move their bodies in response to touch with a platinum wire were considered paralyzed.

Body movement assay

Synchronized adult polyQ-35 animals were used for this assay. Briefly, animals are transferred individually onto fresh plates and poked using a platinum wire. The number of

sinusoidal tracks on the bacterial lawn in response to touch was recorded. At least 25 animals were used for every condition during a single repeat.

Statistical Analyses

Data are expressed as means ±SEM. Statistical analyses for all data were performed by student's t-test, using Excel (Microsoft, Albuquerque, NM, USA). Statistical significance is indicated in figures (* $P<0.05$, ** $P<0.01$, *** $P<0.001$) or included in the supplemental tables.

4.7 Acknowledgements

We thank Malene Hansen for the *hlh-30(jin1375)* mutant strain. We thank Javier Irazoqui and his lab for the *flcn-1(ok975); hlh-30(jin1375)* double mutant strain and for performing the pathogen resistance assays. We thank Greg Voisin for his help in the analysis of the microarray data. We acknowledge the *Caenorhabditis* Genetic Center for *C. elegans* strains and salary support to E.P. from the Rolande and Marcel Gosselin Graduate Studentship and the CIHR/FRSQ training grant in cancer research of the McGill Integrated Cancer Research Training Program (MICRTP).

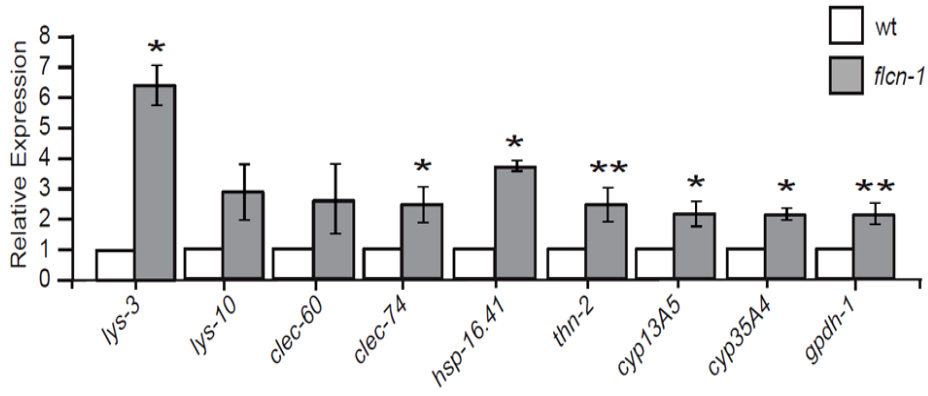

Figure 4.1: Validation of the microarray.

Relative mRNA expression of indicated target genes in wild-type and *flcn-1(ok975)* L4 animals.

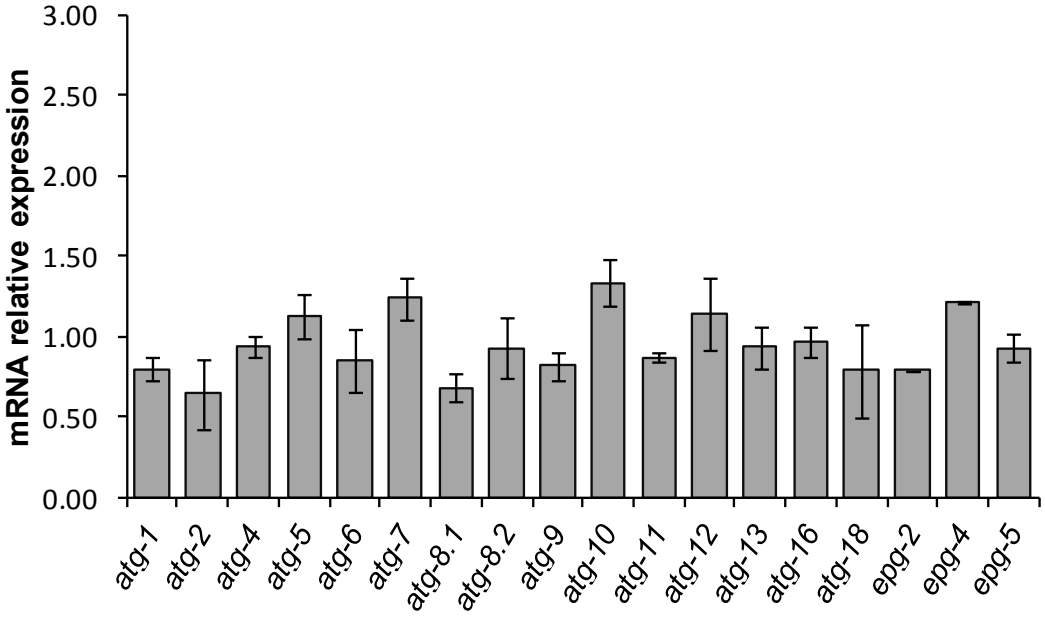

Figure 4.2: Autophagy genes are not transcriptionally up-regulated in *flcn-1(ok975)* animals.

Relative mRNA expression of indicated autophagy genes in wild-type and *flcn-1(ok975)* L4 animals.

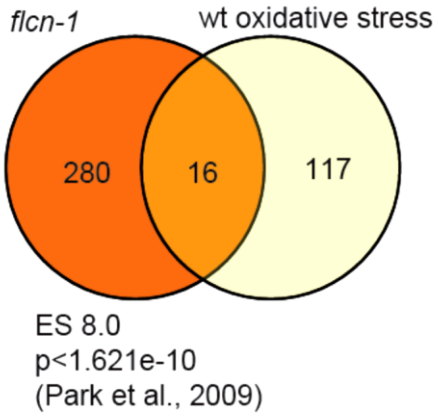

Figure 4.3: Transcriptional profile of *flcn-1* prior to stress overlaps with profiles of wild-type animals exposed to oxidative stress.

(A) Ven diagrams showing the overlap of genes upon indicated strains and treatments.

Figure 4.4: Transcriptional profile of *flcn-1* prior to stress overlaps with profiles of wild-type animals exposed to NaCl and to osmotic stress resistant mutants.

(A, B, C) Ven diagrams showing the overlap of genes upon indicated strains and treatments.

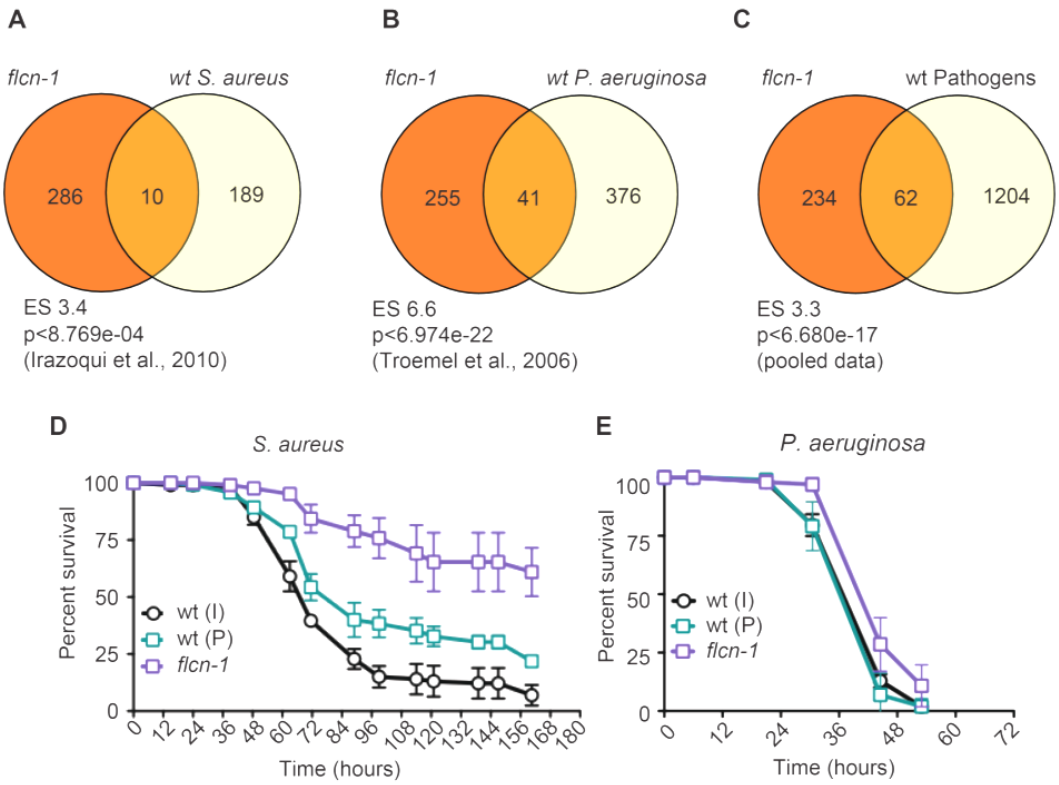

Figure 4.5: Transcriptional profile of *flcn-1* prior to stress overlaps with profiles of wild-type animals infected with pathogens and correlates with a pathogen resistance phenotype.

(A, B, C) Ven diagrams showing the overlap of genes upon indicated strains and treatments. (D, E) Percent survival of indicated strains upon infection with indicated pathogens. I indicates Irazoqui and P indicates Pause.

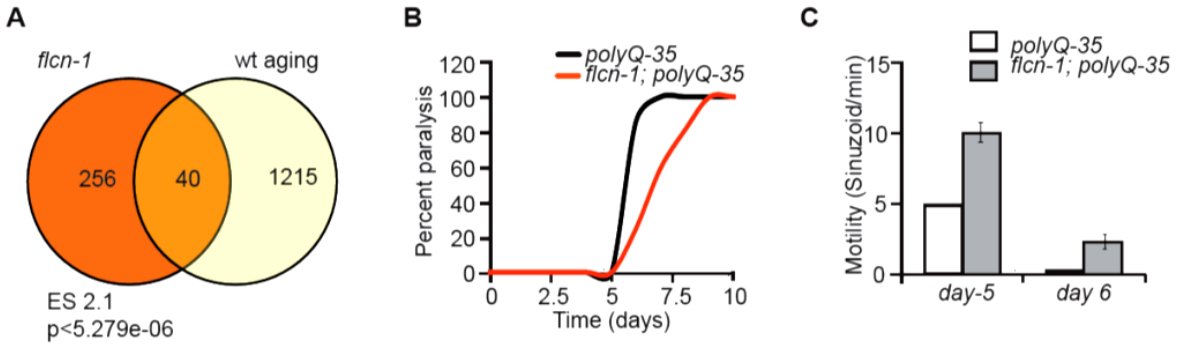

Figure 4.6: Transcriptional profile of *flcn-1* prior to stress overlaps with longevity signatures and correlates with improved protein homeostasis.

(A) Ven diagrams showing the overlap of genes upon indicated strains and conditions.

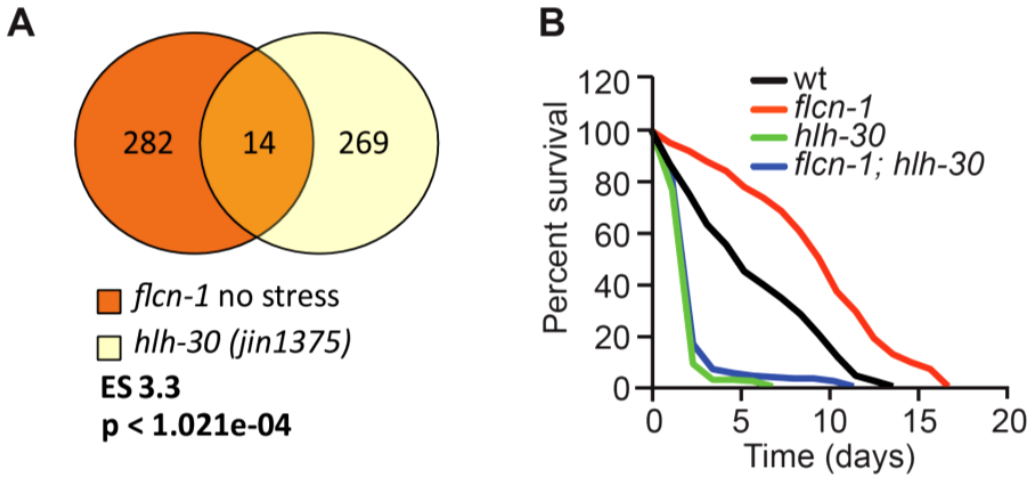

Figure 4.7: Role of *hlh-30* downstream of *flcn-1*.

(A) Ven diagrams showing the overlap of genes upon indicated strains. (B) Percent survival of indicated strains to 400mM NaCl stress.

Table 4.1: Functional classification of genes up-regulated in *flcn-1(ok975)* animals

Gene ID	Gene	Sequence description	Fold change	P value	ES
C-type lectins					3.91
H16D19.1	*clec-13*	C-type lectin	8.77	7.37×10^{-7}	
T07D10.4	*clec-15*	C-type lectin			
E03H4.10	*clec-17*	C-type lectin	2.52	7.07×10^{-5}	
F49A5.4	*clec-24*	C-type lectin	2.32	0.00299	
T20B3.16	*clec-36*	C-type lectin	1.69	0.00219	
T20B3.13	*clec-40*	C-type lectin	2.68	0.000341	
ZK666.6	*clec-60*	C-type lectin	3.1018	0.000705	
ZK666.7	*clec-61*	C-type lectin	2.67	0.00221	
F35C5.6.2	*clec-63*	C-type lectin	1.426	0.000774	
F35C5.8.1	*clec-65*	C-type lectin	1.36	0.0010	
Y46C8L.8	*clec-74*	C-type lectin	3.486	3.16×10^{-5}	
Y45G2A.8a	*clec-82*	C-type lectin	2.04	0.001072	
Y54G2A.6	*clec-85*	C-type lectin			
C54D1.2	*clec-86*	C-type lectin	1.79	9.79×10^{-5}	
Y54G2A.6	*clec-85*	C-type lectin	1.592	0.000105	
R13F6.2	*clec-159*	C-type lectin	2.566	0.002786	
F38A1.5	*clec-166*	C-type lectin	1.62	0.000868	
F59A7.5	*clec-206*	C-type lectin	2.36	0.001348	
F01D4.1	*ugt-43*	UDP-glucoronosyltransferase	2.28	7.07×10^{-5}	
F38A5.3a	*lec-11*	galectin	1.64	0.000287	
Stress response					3.31
T27E4.2	*hsp-16.1*	Heat shock protein			
T27E4.8	*hsp-16.11*	Heat shock protein	1.76	1.65×10^{-5}	
Y46H3A.3	*hsp-16.2*	Heat shock protein	2.83	1.01×10^{-5}	
Y46H3A.2	*hsp-16.41*	Heat shock protein	3.39	5.58×10^{-7}	
T27E4.3	*hsp-16.48*	Heat shock protein	1.81	1.01×10^{-5}	
T27E4.9	*hsp-16.49*	Heat shock protein			

F47G4.3	*gpdh-1*	Glycerol-3-phsophate dehydrogenase	1.724	1.47 x 10^{-5}	
Secondary metabolites biosynthesis, transport, and catabolism					3.31
T10B9.1	*cyp-13A4*	Cytochrome P450 family	2.308	0.001429	
T10B9.2	*cyp-13A5*	Cytochrome P450 family	2.103	0.000459	
K09A11.3	*cyp-14A2*	Cytochrome P450 family	1.602	0.001237	
C36A4.1	*cyp-25A1*	Cytochrome P450 family	1.880	0.000518	
B0213.14	*cyp-34A8*	Cytochrome P450 family	1.48	0.001729	
B0213.15b	*cyp-34A9*	Cytochrome P450 family	1.613	0.002954	
C03G6.15	*cyp-35A2*	Cytochrome P450 family	1.818	7.40 x 10^{-6}	
K09D9.2	*cyp-35A3*	Cytochrome P450 family	1.92	4.18 x 10^{-5}	
C49G7.8	*cyp-35A4*	Cytochrome P450 family	2.04	0.000106	
Y22F5A.5	*lys-2*	Lysosyme	1.406	0.001077	
Y22F5A.6	*lys-3*	Lysosyme	6.155	6.96 x 10^{-6}	
C02A12.4	*lys-7*	Lysosyme	2.54	5.96 x 10^{-10}	
F17E9.11	*lys-10*	Lysosyme	3.086	0.000372	

Table 4.2: Overlapping genes upregulated in *flcn-1(ok975)* animals at basal level and genes induced by oxidative stress

Gene ID	Gene	Sequence description	Fold change	P value	ES
C24B9.9	*dod-3*	Downstream of *daf-16*	1.88	2.83E-06	8.0
C52E4.1	*cpr-1*	Cysteine protease	1.56	0.002228	
F01D5.1	F01D5.1		1.58	0.000173	
F01D5.5	F01D5.5		1.50	0.000916	
F15E6.4	F15E6.4		1.36	0.001732	
F28D1.5	*thn-2*	Thaumatin family	2.72	2.16E-11	
F55G11.4	F55G11.4	Contains a CUB-like domain	2.53	5.64E-09	
H17B01.3	*lips-14*	Lipase related	1.79	1.78E-05	
R07E3.4	R07E3.4	Ortholog of the human solute carrier SLC25A6	1.64	0.000572	
R09B5.9	*cnc-4*	Caenanin family	1.98	2.08E-07	
R10D12.9	*swt-6*	Ortholog of the human solute carrier SLC50A1	1.63	0.002343	
T24B8.5	T24B8.5	ShK-like toxin peptide	1.43	0.000901	
T27E4.8	*hsp16.1*	Heat shock protein	1.76	1.65E-05	
W04B5.1	W04B5.1		1.54	0.00092	
Y22F5A.5	*lys-2*	Lysosyme	1.40	0.001077	
ZK1251.2	*ins-7*	Insulin related	2.03	2.52E-05	

Table 4.3: Overlapping genes upregulated in *flcn-1(ok975)* animals at basal level and wild-type animals treated with NaCl

Gene ID	Gene	Sequence description	Fold change	P value	ES
C31A11.5	*oac-6*	O-acyltransferase homolog	2.86	0.00026	3.0
C49G7.10	C49G7.10		1.64	0.0030	
F10F2.2	F10F2.2	Ortholog of human phosphoribosylformylglycinamidine synthase	1.50	0.00015	
F13A7.11	F13A7.11		1.98	0.0021	
F15B9.1	*far-3*	Fatty Acid/Retinol binding protein	1.39	0.0028	
F15E11.12	F15E11.12		2.19	6.29E-07	
F47G4.3	*gpdh-1*	Glycerol -3- phosphate dehydrogenase 1	1.72	1.47E-05	
F53A9.2	F53A9.2	Ortholog of human histidine-rich glycoprotein	2.22	4.74E-05	
F53B2.8	F53B2.8		2.25	0.00087	
H17B01.3	*lips-14*	Lipase related	1.79	1.78E-05	
R09B5.9	*cnc-4*	Caenanin family	1.98	2.08E-07	
T12D8.5	T12D8.5		2.14	0.00019	
T24C4.4	T24C4.4		2.78	0.0012	

Table 4.4: Overlapping genes upregulated in *flcn-1(ok975)* animals and *osm-7(n1515)* animals

Gene ID	Gene	Sequence description	Fold change	P value	ES
B0213.14	*cyp-34A8*	Cytochrome P450 family	1.48	0.0017	6.1
C14C6.5	C14C6.5	Contains a Methridin like shK toxin domain	1.90	1.48E-06	
F01D5.5	F01D5.5		1.50	0.0009	
F10F2.2	F10F2.2	Ortholog of human phosphoribosylformylglycinamidine synthase	1.50	0.00015	
F15B9.1	*far-3*	Fatty Acid/Retinol binding protein	1.39	0.0028	
F17E9.11	*lys-10*	Lysozyme	3.08	0.00037	
F28D1.5	*thn-2*	Thaumatin family	2.72	2.16E-11	
F41C3.1	F41C3.1		2.02	0.00306	
F47G4.3	*gpdh-1*	Glycerol -3- phosphate dehydrogenase 1	1.72	1.47E-05	
F53A9.1	F53A9.1	Ortholog of human histidine-rich glycoprotein	1.55	8.20E-05	
F55G11.4	F55G11.4	Contains a CUB-like domain	2.53	5.64E-09	
F59A7.2	F59A7.2		1.62	0.00067	
K08C7.5	*fmo-2*	Flavin-containing Mono-oxygenase family	3.01	0.0011	
R09B5.9	*cnc-4*	Caenacin family	1.98	2.08E-07	
T03D3.1	T03D3.1	UDP-GlucuronosylTransferase	1.61	0.0014	
T19B10.2	*phi-59*		1.64	1.91E-05	
Y43C5A.2	Y43C5A.2		1.37	0.0030	
Y9C9A.16	Y9C9A.16	Ortholog of human sulfide quinonereductase-like	2.77	0.0001	
ZC204.12	ZC204.12		1.58	0.0014	
ZK970.7	ZK970.7		1.41	0.0007	

Table 4.5: Overlapping genes upregulated in *flcn-1(ok975)* animals and *osm-11(n1604)* animals

Gene ID	Gene	Sequence description	Fold change	P value	ES
C01B10.6	C01B10.6		1.42	0.0027	4.1
C03G6.15	*cyp-35A2*	Cytochrome P450 family	1.81	7.40E-06	
C08E3.13	C08E3.13		5.61	2.94E-11	
C14C6.5	C14C6.5	Contains a Metridin-like ShK toxin domain	1.90	1.48E-06	
C31A11.5	*oac-6*	O-acyltransferase homolog	2.86	0.00026	
C54D1.2	*clec-86*	C-type lectin	1.79	9.79E-05	
F01D5.5	F01D5.5		1.50	0.0009	
F09B9.1	*oac-14*	O-acyltransferase homolog	2.44	0.00087	
F10F2.2	F10F2.2	Ortholog of human phosphoribosylformylglycin amidine synthase	1.50	0.00015	
F17E9.11	*lys-10*	Lysozyme	3.08	0.00037	
F28D1.5	*thn-2*	Thaumatin family	2.72	2.16E-11	
F47G4.3	*gpdh-1*	Glycerol-3-phosphate dehydrogenase	1.72	1.47E-05	
F53A9.1	F53A9.1	Ortholog of human histidine-rich glycoprotein	1.55	8.20E-05	
F53A9.2	F53A9.2	Ortholog of human histidine-rich glycoprotein	2.22	4.74E-05	
F55G11.4	F55G11.4	Contains a CUB-like domain	2.53	5.64E-09	
F59A7.2	F59A7.2	hypothetical protein	1.62	0.00067	
K08C7.5	*fmo-2*	Flavin-containing Mono-oxygenase family	3.01	0.0011	
R08E3.1	R08E3.1		1.42	0.00095	
R09B5.9	*cnc-4*	Caenacin family	1.98	2.08E-07	
T12D8.5	T12D8.5		2.14	0.00019	
T19B10.2	*phi-59*		1.64	1.91E-05	
Y43C5A.2	Y43C5A.2		1.37	0.0030	
ZK1251.2	*ins-7*	Insulin related	2.03	2.52E-05	
ZK666.6	*clec-60*	C-type lectin	2.41	0.00040	
ZK970.7	ZK970.7		1.41	0.0007	

Table 4.6: Overlapping genes upregulated in *flcn-1(ok975)* animals and animals infected with *Staphylococcus aureus*

Gene ID	Gene	Sequence description	Fold change	P value	ES
F41C3.1	F41C3.1		2.02	0.00306	3.4
49H6.13	F49H6.13		3.66	0.000276	
F53A9.1	F53A9.1	Ortholog of human histidine-rich glycoprotein	1.55	8.20E-05	
F53A9.2	F53A9.2	Ortholog of human histidine-rich glycoprotein	2.22	4.74E-05	
K08C7.5	*fmo-2*	Flavin-containing Mono-oxygenase family	3.01	0.0011	
R09D1.11	*chil-23*	Chitinase-like	1.85	0.001132	
T27C5.8	T27C5.8		3.705	0.001911	
ZK666.6	*clec-60*	C-type lectin	2.41	0.00040	
ZK666.7	*clec-61*	C-type lectin	2.68	0.002212	
Y53F4B.45	Y53F4B.45		1.71	0.000234	

Table 4.7: Overlapping genes upregulated in *flcn-1(ok975)* animals and animals infected with *Pseudomonas aeruginosa*

Gene ID	Gene	Sequence description	Fold change	P value	ES
B0024.4	B0024.4		2.14	0.0023	6.6
C02F5.11	*tsp-2*	Tetraspanin family	2.66	6.48E-05	
C02F5.8	*tsp-1*	Tetraspanin family	4.10	3.71E-06	
C03G6.15	*cyp-35A2*	Cytochrome P450 family	1.82	7.40E-06	
C09F12.1	*clc-1*	Claudin-like	1.79	1.90E-06	
C13D9.1	*srr-6*	Serpentine receptor	5.74	4.95E-06	
C31A11.5	*oac-6*	O-acetyltransferase homolog	2.86	0.00026	
C33H5.13	C33H5.13		1.50	0.00031	
C49G7.10	C49G7.10		1.64	0.003074	
C54D1.2	*clec-86*	C-type lectin	1.79	9.79E-05	
C56A3.2	*ttr-44*	Transthyretin-related	1.61	1.52E-05	
E03H4.10	*clec-17*	C-type lectin	2.52	7.07E-05	
F01D5.5	F01D5.5		1.50	0.000916	
F09B9.1	*oac-14*	O-acetyl transferase homolog	2.44	0.00087	
F10A3.3	*fbxa-18*	F-box A protein	2.14	0.001788	
F13A7.11	F13A7.11		1.98	0.002178	
F15E6.4	F15E6.4		1.36	0.001732	
F22H10.2	F22H10.2	Ortholog of human histidine-rich glycoprotein	2.38	9.92E-05	
F47G4.3	*gpdh-1*	Glycerol-3-phosphate dehydrogenase	1.72	1.47E-05	
F49F1.5	F49F1.5		1.72	0.00041	
F49H6.13	F49H6.13		3.66	0.000276	
F53A9.2	*kreg-1*	Ortholog of human histidine-rich glycoprotein	2.22	4.74E-05	
F53B2.8	F53B2.8		2.25	0.000872	
F55C12.7	*tag-234*	Temporarily assigned gene name	1.67	0.000863	
H17B01.3	*lips-14*	Lipase-related	1.79	1.78E-05	
K09D9.1	K09D9.1		2.66	9.87E-05	
K09F5.2	*vit-1*	Vitellogenin structural gene	1.16	0.002931	
R09B5.9	*cnc-4*	Caenacin	1.98	2.08E-07	
T03D3.1	T03D3.1	UDP-GlucuronosylTransferase	1.61	0.0014	
T10B9.2	*cyp-13A5*	Cytochrome P450 family	2.02	0.000246	
T24C4.4	T24C4.4		2.78	0.0012	

T27F2.4	*zip-10*	bZIP transcription family factor	2.23	4.33E-05
W04B5.1	W04B5.1		1.54	0.00092
Y17D7B.2	Y17D7B.2		3.69	1.17E-05
Y22F5A.6	*lys-3*	Lysosyme	6.15	6.96E-06
Y40C7B.4	Y40C7B.4		1.84	0.001488
Y46C8AL.8	*clec-74*	C-type lectin	3.09	0.000111
Y47H10A.5	Y47H10A.5		2.10	0.002451
Y75B8A.28	Y75B8A.28		4.43	4.90E-07
ZK970.7	ZK970.7		1.41	0.0007

Table 4.8: Overlapping genes upregulated in *flcn-1(ok975)* animals and animals infected with *pathogens*

Gene ID	Gene	Sequence description	Fold change	P value	ES
B0024.4	B0024.4		2.14	0.0023	3.3
C02F5.11	*tsp-2*	Tetraspanin family	2.66	6.48E-05	
C02F5.8	*tsp-1*	Tetraspanin family	4.10	3.71E-06	
C03G6.15	*cyp-35A2*	Cytochrome P450 family	1.82	7.40E-06	
C09F12.1	*clc-1*	Claudin-like	1.79	1.90E-06	
C13D9.1	*srr-6*	Serpentine receptor	5.74	4.95E-06	
C31A11.5	*oac-6*	O-acetyltransferase homolog	2.86	0.00026	
C32H11.9	C32H11.9	Ortholog of human epoxide hydrolase 1 (xenobiotic)	2.48	7.22E-06	
C33H5.13	C33H5.13		1.50	0.00031	
C49G7.10	C49G7.10		1.64	0.003074	
C54D1.2	*clec-86*	C-type lectin	1.79	9.79E-05	
C56A3.2	*ttr-44*	Transthyretin-related	1.61	1.52E-05	
E03H4.10	*clec-17*	C-type lectin	2.52	7.07E-05	
F01D5.5	F01D5.5		1.50	0.000916	
F09B9.1	*oac-14*	O-acetyl transferase homolog	2.44	0.00087	
F10A3.3	*fbxa-18*	F-box A protein	2.14	0.001788	
F13A7.11	F13A7.11		1.98	0.002178	
F15B9.1	*far-3*	Fatty Acid/Retinol binding protein	1.39	0.0028	
F15E11.12	F15E11.12		2.19	6.29E-07	
F15E6.4	F15E6.4		1.36	0.001732	
F17E9.11	*lys-10*	Lysozyme	3.08	0.00037	
F22H10.2	F22H10.2	Ortholog of human histidine-rich glycoprotein	2.38	9.92E-05	
F41C3.1	F41C3.1		2.02	0.00306	
F47G4.3	*gpdh-1*	Glycerol-3-phosphate dehydrogenase	1.72	1.47E-05	
F49F1.5	F49F1.5		1.72	0.00041	
F49H6.13	F49H6.13		3.66	0.000276	
F53A9.1	F53A9.1	Ortholog of human histidine-rich glycoprotein	1.55	8.20E-05	
F53A9.2	*kreg-1*	Ortholog of human histidine-rich glycoprotein	2.22	4.74E-05	
F53B2.8	F53B2.8		2.25	0.000872	

F54C9.3	F54C9.3		1.51	0.000331
F55C12.7	*tag-234*	Temporarily assigned gene name	1.67	0.000863
F57H12.6	F57H12.6		2.10	8.30E-06
H16D19.1	*clec-13*		8.77	7.37E-07
H17B01.3	*lips-14*	Lipase-related	1.79	1.78E-05
K08C7.5	*fmo-2*	Flavin-containing Mono-oxygenase family	3.01	0.0011
K09D9.1	K09D9.1		2.66	9.87E-05
K09F5.2	*vit-1*	Vitellogenin structural gene	1.16	0.002931
R07C12.4	R07C12.4		2.09	0.001301
R09B5.9	*cnc-4*	Caenacin	1.98	2.08E-07
R09D1.11	*chil-23*	Chitinase-like	1.85	0.001132
R10D12.9	*swt-6*	Ortholog of the human solute carrier SLC50A1	1.63	0.002343
T03D3.1	T03D3.1	UDP-GlucuronosylTransferase	1.61	0.0014
T10B9.2	*cyp-13A5*	Cytochrome P450 family	2.02	0.000246
T19B10.2	*phi-59*		1.64	1.91E-05
T24B8.5	T24B8.5	ShK-like toxin peptide	1.43	0.000901
T24C4.4	T24C4.4		2.78	0.0012
T27C5.8	T27C5.8		3.705	0.001911
T27F2.4	*zip-10*	bZIP transcription family factor	2.23	4.33E-05
W03A5.3	W03A5.3		1.68	0.000488
W04B5.1	W04B5.1		1.54	0.00092
Y17D7B.2	Y17D7B.2		3.69	1.17E-05
Y22FA.6	*lys-3*	Lysosyme	6.15	6.96E-06
Y40C7B.4	Y40C7B.4		1.84	0.001488
Y46C8AL.8	*clec-74*	C-type lectin	3.09	0.000111
Y46H3A.3	*hsp-16.2*	Heat shock protein	2.83	1.01E-05
Y47H10A.5	Y47H10A.5		2.10	0.002451
Y53F4B.45	Y53F4B.45		1.71	0.000234
Y75B8A.28	Y75B8A.28		4.43	4.90E-07
ZK1320.3	ZK1320.3		1.40	0.001165
ZK666.6	*clec-60*	C-type lectin	2.41	0.00040
ZK666.7	*clec-61*	C-type lectin	2.68	0.002212
ZK970.7	ZK970.7		1.41	0.0007

Table 4.9: Overlapping genes upregulated in *flcn-1(ok975)* animals and downregulated in *hlh-30(jin1375)*

Gene ID	Gene	Sequence description	Fold change	P value	ES
C08E3.13	C08E3.13		5.61	2.94E-11	3.3
C52E4.1	C52E4.1		1.56	7.88E-05	
F28D1.5	*thn-2*	Thaumatin family	2.72	2.16E-11	
F41C3.2	F41C3.2	Ortholog of human solute carrier	1.93	0.002081	
F44E7.2	F44E7.2	Ortholog of human pyridoxal phosphate	2.12	4.47E-05	
K09F5.2	*vit-1*	Vitellogenin structural genes	1.16	0.002931	
T27E4.8	*hsp-16.1*	Heat shock protein	1.76	1.65E-05	
W06D12.3	*Fat-5*	Fatty acid desaturase	1.56	0.002228	
Y46H3A.2	*hsp-16.41*	Heat shock protein	1.98	5.44E-05	
Y46H3A.3	*hsp-16.2*	Heat shock protein	2.83	1.01E-05	
Y51H7BM.1	*math-54*	Meprin-associated traf homology domain containing	3.14	1.77E-06	
Y71H2AM.16	*pho-9*	Intestinal acid phosphatase	2.95	0.000437	
ZC84.3	*cls-3*	CLASP family of microtubule-binding protein	1.87	0.00027	
ZK1290.5			1.73	9.72E-05	

Table 4.9: Primer sequences

Gene symbol	Forward primer	Reverse primer
gpdh-1	CTTGCTATGGAGGTCGCAAT	CTTATGCACTGACGCGAAGA
cdc-42	GGCAAAGGAATTGAAAGCAG	GGGGGCTAAGAAAATTTGGA
lys-3	CCAATGGCTGTGAGAATTGA	CCTGTCTCCATGGTCCAAAT
lys-10	ATGGCCTGCTAATCATGCTC	GCCGAAAGCTACGAATTTTG
clec-60	ACGGTGCTCTTCTTGCAGAT	ACCGTAGCGGTAGGAGTGAA
clec-74	CCGCCTGTCCTAGCAGTAAG	GCCCAATCCAAAAGTTTTCA
thn-2	CCAACTTACGGCTGGACAAT	CTGGGAGGTTGTATCCATCG
cyp13a5	GCAAGTGCAAAAGGAAAAGC	AAAGGTAGTTTACGACCATCTTTGA
cyp35a4	GAAAACCCGCTGAAGTTTGA	ATGGTCTCTTTCCGATGCTG
hsp-16.41	TCTTGGACGAACTCACTGGA	TCCATGTTCCGATTTTGTTTC

CHAPTER 5

GENERAL DISCUSSION OF THE THESIS

5.1 Role of FLCN/AMPK in cellular and organismal stress response

One of the main goals of our research group is to characterize the role of the tumor suppressor FLCN and to determine the mechanism by which its loss leads to BHD renal neoplasm. Since 2001, the cellular role of FLCN has not been elucidated. FLCN has been linked to several cellular processes and signaling pathways. However, it is still unclear whether the reported effects are directly linked to the absence of FLCN or whether they are indirect effects. In 2006, FLCN has been shown to bind AMPK [38], a central regulator of energy homeostasis. We and other groups have shown that loss of FLCN in mice leads to embryonic lethality and kidney specific knock out (KO) of FLCN causes renal cysts and tumors [89,96]. Additionally, in regards to the AMPK and TOR signaling, confusing and inconsistent results have been reported by several groups; evidence for both activation and inhibition of AMPK/mTOR signaling pathways were presented depending on the context [38,89,95,96].

To gain insight into the functional role of FLCN, we used the nematode *C. elegans* as a powerful genetic tool to determine upstream and downstream pathways linked to FLCN/AMPK signaling. Strikingly, findings of this work demonstrate that the cellular role of FLCN is highly conserved from worms to mammals. In this work, we identify FLCN as an evolutionarily conserved negative upstream regulator of AMPK signaling. Specifically, we demonstrate that AMPK is induced upon loss of FLCN (Figures 2.2 and 2.7) and that it is required for the increased resistance of *flcn-1(ok975)* animals to energy stresses in both *C. elegans* and mammalian cells (Chapter 2: Figures 2.1, 2.6 and 2.7) and to hyperosmotic stress (Chapter 3: Figure 3.1) in *C. elegans*.

In the nematode *C. elegans,* like in most organisms, AAK-2/AMPK overexpression or activation by dietary restriction or treatment with metformin or 2-deoxy-glucose, extends lifespan and enhances resistance to several stresses including oxidative stress, heat, and starvation which are known to induce severe energy crisis [41,74,78,80,265]. In these cases, AMPK restores energy levels by suppressing ATP-consuming processes and activating ATP-producing processes [43]. In mammalian cells, AMPK plays diverse roles in cellular responses to stress by controlling life and death processes, mainly autophagy and apoptosis [57]. Importantly, how AMPK activation leads to increased stress resistance is complicated and context-dependent, and this is due to the versatile cellular roles of AMPK. For instance, AMPK activation leads to the transcriptional induction of stress response genes through phosphorylation of stress-controlled transcription factors including FOXO/DAF-16, p53, NRF2/SKN-1 and others [339]. AMPK activation also modulates mitochondrial biogenesis, improving bioenergetics and heightening ROS levels, which in this case, act as signaling molecules that activate cellular defense mechanisms that protect against excessive damaging stress-related ROS molecules [339]. Among the various tasks, AMPK also activates autophagy by directly binding and phosphorylating essential autophagy proteins as ULK1, BECLIN1, and VPS-34 [58,60,61,262]. In accordance we show in chapter 2, that the AMPK activation upon loss of FLCN induces autophagy and protects against deleterious energy stresses.

How AMPK is activated upon loss of FLCN is still not clear. Our data in chapter 2 indicate that PAR-4, the worm homolog of LKB1, is not fully required for the FLCN-dependent stress resistance phenotype and that the phosphorylation on the critical threonine residue of the AMPK α catalytic subunit is not completely lost upon PAR-4 mutation (Figure 2.2). Although LKB1 is the major evolutionarily conserved upstream kinase of AMPK, other upstream kinases have been also identified including Ca^{2+}/calmodulin-dependent protein

kinase kinase β (CaMKKβ) [285,340] transforming growth factor-β-activated kinase 1 (TAK1), [341] and the Ataxia telangiectasia mutated protein kinase ATM1 [342]. Importantly, our result in chapter 2 indicates that PAR-4/LKB1 mutation in *C. elegans* reduces but does not completely suppress AMPK phosphorylation on the threonine residue of the catalytic subunit (Figure 2.2). This suggests that mechanisms of AMPK phosphorylation independent of PAR-4/LKB1 are likely to exist in *C. elegans* similarly to what has been demonstrated in mammalian systems.

In this work, we demonstrate that AMPK is also involved in the resistance of *C. elegans* nematodes to hyperosmotic stress (Figure 3.1). We further show that the increased resistance of *flcn-1* mutant nematodes to hyperosmotic stress strictly depends on both AMPK catalytic subunits *aak-1* and *aak-2* (Figure 3.3). The involvement of AMPK in resistance to salt stress has been previously reported in yeast [307,343]. AMPK was shown to be also activated by salt stress in mammalian cell lines [306,344]. However, its role in regards to cell survival or cell death is not clearly defined since both processes have been reported [306,344]. How AMPK induction leads to increased survival to hyperosmotic stress has not been previously elucidated. Our results in chapter 3 suggest that AMPK plays a crucial role in glycogen remodeling prior and after hyperosmotic stress, which is essential for survival to stress. Specifically, we show that the chronic AMPK activation conferred by loss of FLCN leads to glycogen accumulation, which under acute hyperosmotic shock, is degraded to produce an essential organic osmolyte. Even though glycogen is usually degraded following acute AMPK activation [65,308-310], it is now firmly established that the chronic activation of AMPK leads to glycogen accumulation in many systems and organisms [311-313]. This result is discussed in more details in the discussion section of chapter 3.

AMPK activation has been also shown to increase lifespan in many organisms including *C. elegans*. Despite the fact that AMPK is chronically activated upon loss of *flcn-1*,

results in chapter 2 indicate that there is no difference in lifespan between wild-type and *flcn-1* animals (Figure 2.1). Several possibilities could explain this result. It is likely that the activation by different upstream kinases could result in different outcomes. Another possibility could be that the AMPK activation that leads to the extension of lifespan is tissue-specific. Results from chapters 2, 3 and 4, indicate that loss of *flcn-1* in *C. elegans* improves healthspan rather than overall lifespan. Specifically we show that loss of *flcn-1* increases resistance to anoxia (Figure 2.6), heat (Figure 2.6), oxidative stress (Figure 2.1) and hyperosmotic stress (Figure 3.1) which are damaging stresses. Additionally, we show in chapter 4 that loss of *flcn-1* decreases the age-related protein aggregation supporting that FLCN is involved in protein homeostasis control (Figure 4.6).

This last result opens new insight into a novel role for *flcn-1* in the regulation of protein homeostasis, which could be further investigated in *C. elegans* and mammalian systems. Experiments aiming to determine whether the resistance to polyQ aggregation upon loss of *flcn-1* depends on AMPK, autophagy, glycogen reserves, or other mechanisms in *C. elegans* are important. Additionally, it would be also relevant to determine whether this cellular role of FLCN is evolutionarily conserved. In fact, protein damage largely contributes to cancer initiation and progression and has been previously linked to AMPK and autophagy. Understanding the mechanism by which FLCN regulates protein homeostasis could be highly relevant to the role of FLCN in the kidney in humans, which is an organ constantly exposed to oxidative and osmotic stresses, where clearance of protein damage is essential. Moreover, the fact that FLCN modulates AMPK function and that AMPK is a versatile cellular complex involved in a wide range of cellular biological processes; it is likely that FLCN exerts multiple unknown physiological functions (ex. protein homeostasis) other than being a renal tumor suppressor depending on the level and tissue specific expression. Results of the future

work will help characterize these functions and this is essential to understand FLCN-dependent metabolic diseases that appear with age.

5.2 Role of FLCN/AMPK in the regulation of autophagy and cellular metabolism

In this work, we demonstrate in chapter 2 that the AMPK induction conferred by loss of FLCN activates autophagy (Figures 2.4 and 2.7), improves bioenergetics (Figures 2.6 and 2.7), and increases resistance to stress (Figure 2.1). The resistance to oxidative stress by induction of autophagy was observed across evolution from algae [345,346] and plants [347] to mammals [267,348]. However, it was still not clear how autophagy increases resistance to stress and specifically oxidative stress. The degradation of damaged macromolecular components and organelles and the increased energy availability through recycling of cellular material are valid possibilities. In *Arabidopsis thaliana*, autophagy has been shown to be required for degradation of oxidized proteins during oxidative stress [347]. Moreover, selective degradation of damaged mitochondria by autophagy has been also shown to protect against oxidative stress and mitochondrial dysfunction [349]. Furthermore, recent evidence support a role for autophagy in the maintenance of proper energy levels upon energy depletion triggered by oxidative stress [175]. Our data demonstrate that the amount of oxidized proteins in *flcn-1* mutant animals upon PQ treatment is not decreased (Figure 2.2), suggesting that the role of autophagy activation in *flcn-1(ok975)* mutant animals upon oxidative stress is unlikely to be through enhanced degradation of damaged macromolecules. Instead, we show that the ATP levels are heightened upon loss of FLCN in both *C. elegans* and mammalian cells (Figures 2.6 and 2.7). Importantly, we also demonstrate that downregulation of autophagy suppresses the increase in ATP levels conferred by loss of FLCN in *C. elegans* and mammalian cells (Figures 2.4 and 2.7), suggesting that autophagy

activation plays a key role in improving cellular bioenergetics, which is crucial to survive oxidative stress.

Importantly, we demonstrate in chapter 3 that autophagy is also required for the survival of wild-type animals to hyperosmotic stress (Figure 3.4). Although not much is known about the role of autophagy in resistance to hyperosmotic stress in lower organisms, autophagy was shown to be induced by hyperosmotic stress in mammalian cells [350-352]. Despite, our data indicate that autophagy is not required for the increased resistance of *flcn-1(ok975)* mutant animals to hyperosmotic stress, in contrast to its requirement for the resistance to energy stresses, indicating that the mechanism of resistance of *flcn-1* mutant animals to hyperosmotic stress is distinct from the mechanism of resistance to energy stresses. This could be explained by the fact that we observed by TEM, an accumulation of impaired autophagosomes in the intestine of the nematodes upon NaCl treatment, which was not observed upon PQ treatment, suggesting that autophagy is not functioning efficiently to degrade damaged cellular components and generate ATP upon exposure to salt stress (Appendix I). This also implies that the degradation of glycogen to produce glycerol requires pathways other than autophagy, which could be via *pygl-1* activation in this case.

Moreover, we show here that cells lacking *Flcn* store energy in the form of phosphocreatine and that *C. elegans* nematodes store energy in the form of glycogen. In parallel to this work, our lab demonstrates in a recent publication that loss of FLCN in MEFs and in human cancer cells leads to metabolic reprogramming and upregulation of amino acids such as serine and glutamine, as well as glycolysis intermediates and other metabolites involved in cellular proliferation [77]. This is consistent with other reports that show a requirement for autophagy in the maintenance of amino acid levels under stress and in the promotion of tumorigenesis [175,353].

The role of glycogen as an energy source has been widely demonstrated in multiple organisms. However, its role as a reservoir for the production of osmolytes upon acute exposure to hypertonic stress has not been clearly reported. In *Corynebacterium glutamicum,* the exposure to hyperosmotic shock was shown to result in glycogen degradation and the synthesis of the osmoprotectant trehalose [354]. In *C. elegans*, recent reports demonstrate an important role for glycogen in mediating survival to hyperosmotic-anoxic stress [238,239]. Our data might suggest that glycogen degradation leads to different outcomes depending on the type of stress. It is possible that the glycogen degraded by oxidative stress generates ATP while the glycogen degraded by hyperosmotic stress produces glycerol. In support to this, the pretreatment of wild-type and *flcn-1* mutant animals with PQ suppressed the increased resistance of *flcn-1* nematodes to NaCl, while the pretreatment of wild-type and *flcn-1* mutant worms with 200mM NaCl increased their resistance upon PQ exposure (Figure 3.8 and Appendix II). This could imply that the pretreatment of the animals with PQ depletes them from glycogen, generating ATP, and abrogating their ability to produce glycerol later on upon NaCl exposure. However, the pretreatment of the worms with NaCl depletes the glycogen stores and produces glycerol, a carbon source that could be used later on to produce ATP upon exposure to PQ.

Future experiments aiming to determine which osmolytes are produced following glycogen degradation in animals are necessary to understand the role of glycogen in hyperosmotic stress resistance. Although we show that glycerol is a major osmoprotectant, other osmolytes resulting from the hyperosmotic-stress dependent degradation of glycogen could also contribute to the survival of cells/organisms.

5.3 Conserved pathways involved in tumorigenesis

Cancer cells are often exposed to nutrient-poor and hypoxic microenvironments and their metabolic reprogramming to provide energy is crucial to promote tumor proliferation. AMPK activation and autophagy are essential mechanisms that could be used by cancer cells to survive [166,175,355]. In fact, while the chronic activation of AMPK suppresses energy-consuming pathways and induces energy-promoting processes, the activation of autophagy recycles damaged macromolecules and provides building blocks to produce ATP and promote cancer survival [166,175,355]. Results of this work imply important roles for AMPK and autophagy activation in BHD tumorigenesis. Specifically, we show in chapter 2 that ATP levels are heightened in FLCN-deficient cancer cells in an autophagy-dependent manner (Figure 2.8). Importantly, we also show that the inhibition of ATG7 suppresses the FLCN-dependent colony formation on soft agar supporting the requirement of AMPK/autophagy in cancer proliferation upon loss of FLCN (Figure 2.8). Although AMPK and autophagy have been suggested to acquire tumor suppressing functions, recent reports suggest that they both could have tumor-promoting functions, presumably by loading cancer cells with energy, helping them survive harsh microenvironments [166,175,355].

In analogy with the important role of glycogen in survival to stress, glycogen could also be an important molecule that fuels tumorigenesis. Similarly to the role of AMPK and autophagy, glycogen metabolism has been shown to sustain proliferation. Glycogen accumulates in many cancer types including ovarian cancer [356], kidney cancer [251], colorectal cancer [252], bladder cancer [357], and others [255]. In addition, higher glycogen levels were detected in breast, kidney, bladder, uterus, skin, ovary, and brain cancer cell lines [255] and recent studies have demonstrated a critical role for glycogen in the survival of cancer cells to hypoxic environments and glucose restriction [251,254]. Importantly,

inhibition of glycogen degradation induced apoptosis in pancreatic cancer cells and impaired the in vivo growth of tumor xenografts [251]. Glycogen phosphorylase appears to be transcriptionally induced in many cancer types including renal cancers and its inhibition has been shown to suppress cancer proliferation [251]. In light of these findings, we show in chapter 3, an evolutionary conserved role of FLCN/AMPK in the regulation of glycogen metabolism (Figures 3.2 and 3.7). Specifically, we show that glycogen accumulates in the tumors of BHD patients and in renal tissues of kidney-specific *Flcn* KO mice (Figure 3.7). This result implies that glycogen could play an important role in BHD tumorigenesis. In accordance, heightened glycogen levels were also reported in the livers of FNIP KO mice and in the muscle tissues of muscle-specific FLCN KO mice as compared to the controls [83,111].

In chapter 3, we also demonstrate an important role for glycogen in survival to hyperosmotic stress in *flcn-1(ok975)* mutant nematodes, via osmolyte production. In analogy with this finding, we speculate that glycogen plays a dual role in BHD neoplasm: it supplies cancer cells with energy and helps them resist the renal hyperosmotic environment.

The AMPK-dependent regulation of hyperosmotic stress is a very interesting aspect in regards to BHD disease, which is mostly manifested by enlarged renal cysts and tumors in all mammalian models including rats, mice, dogs, and men [15-17,19,23]. Since the kidney is an organ chronically and highly exposed to hyperosmotic stress, it is possible that the BHD renal tumors and cysts are formed because of an increased resistance to hyperosmotic conditions, which could lead to DNA damage. In support of this, loss of *FLCN* and *VHL*, which are both renal tumor suppressor genes, predispose to renal clear cell carcinomas which are glycogen-rich tumors.

The hyperosmotic stress regulation is tightly linked to the development and progression of kidney diseases. Although the relationship between osmotic stress and kidney

diseases is not well explored, a growing line of evidence from numerous studies demonstrate the importance of water intake in the treatment of nephrolithiasis, chronic kidney diseases, and ADPKD the most common form of polycystic kidney disease [358-362]. The increased water intake, which was shown to result in better clearance of urea, inhibited the development of renal cysts and reduced the growth of cysts [359,363]. Results of this work shed the light for the first time on a novel, previously uncharacterized, potential role for glycogen in tumorigenesis. Future experiments aiming to define the role of glycogen in hyperosmotic stress-mediated tumorigenesis are therefore necessary.

5.4 A role for TFEB in BHD syndrome

In chapter 4, we demonstrate an important role for FLCN-1 in the transcriptional regulation of stress response genes in *C. elegans*. Specifically, we show that cytochrome P450 proteins, heat shock proteins, lysozymes, and C-type lectins are transcriptionally induced in *flcn-1(ok975)* animals prior to stress (Table 4.1). Additionally, we show that this stress response signature overlaps with other stress response transcriptional profiles suggesting that *flcn-1* may regulate general stress response and not type-specific stresses.

Whether AMPK signaling is responsible for this stress response signature downstream of FLCN-1 has not been determined in this work. The measurement of mRNA expression of *flcn-1*-dependent genes in *flcn-1(ok975); aak-1(tm1944); aak-2(ok524)* mutant animals as compared to *aak-1(tm1944); aak-2*(ok524) double mutant nematodes is therefore important. AMPK plays an important role in the transcriptional regulation of stress response genes in many systems, either by direct nuclear translocation, or through activation of transcription factors or the modulation of corepressors' activities [57,339,364]. For instance, AMPK regulates mitochondrial biogenesis and function by phosphorylating PGC1α [69,77,365], an important transcriptional coactivator that controls key transcription factors including ERRα,

NRF1, NRF2, and PPARs [110,299,366,367]. Moreover, AMPK is an evolutionarily conserved regulator of the CREB and FOXO family of transcription factors, which play important roles in oxidative stress response, in both *C. elegans* and mammalian systems [74,75,78,339,368]. AMPK also modulates stress response-related cell fate by regulating p53 activity [55].

Among transcription factors involved in stress response, transcription factor EB TFEB plays a major role in regulating autophagy and lysosomal functions [90,328,329]. TFEB belongs to the microphtalmia-associated transcription factor subfamily of basic helix-loop-helix type of transcription factors [90]. Under normal conditions, TFEB is sequestered in the cytoplasm. However, upon stress such as starvation, it translocates to the nucleus and induces the transcription of genes involved lysosomal and autophagosomal biogenesis and substrate degradation [90,369]. Importantly, the role of TFEB is conserved across evolution. In *C. elegans*, the TFEB ortholog HLH-30 has been also shown to activate the transcription of autophagy and lysosomal genes and is required for resistance to starvation and extension of lifespan [328,329]. TFEB has been also shown to mediate resistance to pathogen infection via transcriptional activation of antimicrobial genes that function in the organismal defense against pathogens [330]. Our data suggest an important role for *hlh-30* in the resistance of wild-type animals to hyperosmotic stress (Figure 4.7). Furthermore, we demonstrate that *hlh-30* is required for the enhanced resistance of *flcn-1(ok975)* mutant animals to hyperosmotic stress (Figure 4.7). Supporting this, we show that there is a significant overlap between genes upregulated in *flcn-1(ok975)* mutant animals and downregulated in *hlh-30(jin1375)* animals suggesting that HLH-30 functions downstream FLCN-1 in *C. elegans* (Figure 4.7). These results are important because they shed the light on a possible link between FLCN and TFEB in mammalian cells, especially that TFEB is highly implicated in renal cancers. Specifically, chromosomal rearrangements resulting in the fusion of MiTF genes notably TFE3 and TFEB

have been widely reported in renal cell carcinomas [370,371]. Although it is not clear how these gene fusions contribute to tumorigenesis, TFE3 has been shown to translocate to the nucleus in cells lacking FLCN, and to induce the transcription of the lysosomal gene GPNMB [85,104].

As a follow up to the data presented in this work, the relationship between FLCN-1 and HLH-30 should be further investigated. Specifically, experiments aiming to determine if *hlh-30* is fully or partially responsible of the regulation of the *flcn-1*-dependent stress response transcriptional signature in *C. elegans* should be performed. The *hlh-30::GFP* reporter would be useful to validate the nuclear translocation of HLH-30 in *flcn-1* mutant animals upon stress exposure including oxidative stress, hyperosmotic stress, and pathogen infection. Additionally, the HLH-30 target genes should be identified. Furthermore, the relationship between HLH-30 and AMPK should be investigated and mammalian cell lines should be used to determine whether this pathway is evolutionarily conserved. Although TFEB has been shown to be regulated by mTOR, the relationship between TFEB and AMPK has not been clearly reported. It is likely that in BHD tumors, loss of FLCN may activate AMPK, resulting in the constitutive nuclear translocation of TFEB and the subsequent upregulation of genes involved in resistance to stress such as starvation and hypoxia, which fuels cancer progression.

5.5 Concluding remarks

The nematode *C. elegans* is an attractive model organism that could be used to genetically study the molecular pathways that are involved in kidney diseases in humans [372,373]. In this work, using *C. elegans*, we found that loss of *flcn-1* confers resistance to oxidative stress, anoxia, heat, hypertonic stress, and infection with pathogens. Importantly, the data of this work demonstrates an evolutionarily conserved role for FLCN in AMPK signaling, autophagy, and glycogen metabolism. Furthermore, our recent results suggest a transcriptional upregulation of stress response genes in *flcn-1(ok975)* mutant animals prior to stress and a potential involvement of the HLH-30 transcription factor downstream FLCN-1.

The work described in this thesis has helped and will help characterize the tumor suppression function of FLCN and has highlighted novel evolutionarily conserved signaling pathways linked to FLCN. As a continuation of this work, it will be important to assess these pathways in BHD mouse models and to target them in cancer models to determine potential therapeutic benefits in the treatment of BHD disease in specific and kidney cancers in general.

REFERENCE

1. Ferlay J, Shin HR, Bray F, Forman D, Mathers C, et al. (2010) Estimates of worldwide burden of cancer in 2008: GLOBOCAN 2008. Int J Cancer 127: 2893-2917.

2. Canadian Cancer Society http://www.cancer.ca/en/cancer-information/cancer-type/kidney/statistics/?region=on.

3. Linehan WM, Srinivasan R, Schmidt LS (2010) The genetic basis of kidney cancer: a metabolic disease. Nature Reviews Urology 7: 277-285.

4. Klatte T, Pantuck AJ, Said JW, Seligson DB, Rao NP, et al. (2009) Cytogenetic and Molecular Tumor Profiling for Type 1 and Type 2 Papillary Renal Cell Carcinoma. Clinical Cancer Research 15: 1162-1169.

5. Yamazaki K, Sakamoto M, Ohta T, Kanai Y, Ohki M, et al. (2003) Overexpression of KIT in chromophobe renal cell carcinoma. Oncogene 22: 847-852.

6. Cancer Genome Atlas Research N (2013) Comprehensive molecular characterization of clear cell renal cell carcinoma. Nature 499: 43-49.

7. Krieg M, Haas R, Brauch H, Acker T, Flamme I, et al. (2000) Up-regulation of hypoxia-inducible factors HIF-1alpha and HIF-2alpha under normoxic conditions in renal carcinoma cells by von Hippel-Lindau tumor suppressor gene loss of function. Oncogene 19: 5435-5443.

8. Maxwell PH, Wiesener MS, Chang GW, Clifford SC, Vaux EC, et al. (1999) The tumour suppressor protein VHL targets hypoxia-inducible factors for oxygen-dependent proteolysis. Nature 399: 271-275.

9. Ohh M, Park CW, Ivan M, Hoffman MA, Kim TY, et al. (2000) Ubiquitination of hypoxia-inducible factor requires direct binding to the beta-domain of the von Hippel-Lindau protein. Nat Cell Biol 2: 423-427.

10. Jaakkola P, Mole DR, Tian YM, Wilson MI, Gielbert J, et al. (2001) Targeting of HIF-alpha to the von Hippel-Lindau ubiquitylation complex by O2-regulated prolyl hydroxylation. Science 292: 468-472.

11. Greer SN, Metcalf JL, Wang Y, Ohh M (2012) The updated biology of hypoxia-inducible factor. EMBO J 31: 2448-2460.

12. Tee AR, Pause A (2013) Birt-Hogg-Dube: tumour suppressor function and signalling dynamics central to folliculin. Fam Cancer 12: 367-372.

13. Hornstein OP, Knickenberg M (1975) Perifollicular fibromatosis cutis with polyps of the colon--a cutaneo-intestinal syndrome sui generis. Arch Dermatol Res 253: 161-175.

14. Birt AR, Hogg GR, Dube WJ (1977) Hereditary multiple fibrofolliculomas with trichodiscomas and acrochordons. Arch Dermatol 113: 1674-1677.

15. Toro JR, Glenn G, Duray P, Darling T, Weirich G, et al. (1999) Birt-Hogg-Dube syndrome: a novel marker of kidney neoplasia. Arch Dermatol 135: 1195-1202.

16. Pavlovich CP, Walther MM, Eyler RA, Hewitt SM, Zbar B, et al. (2002) Renal tumors in the Birt-Hogg-Dube syndrome. Am J Surg Pathol 26: 1542-1552.

17. Zbar B, Alvord WG, Glenn G, Turner M, Pavlovich CP, et al. (2002) Risk of renal and colonic neoplasms and spontaneous pneumothorax in the Birt-Hogg-Dube syndrome. Cancer Epidemiol Biomarkers Prev 11: 393-400.

18. Tobino K, Gunji Y, Kurihara M, Kunogi M, Koike K, et al. (2011) Characteristics of pulmonary cysts in Birt-Hogg-Dube syndrome: thin-section CT findings of the chest in 12 patients. Eur J Radiol 77: 403-409.

19. Gupta P, Eshaghi N, Kamba TT, Ghole V, Garcia-Morales F (2007) Radiological findings in Birt-Hogg-Dube syndrome: a rare differential for pulmonary cysts and renal tumors. Clin Imaging 31: 40-43.

20. Kupres KA, Krivda SJ, Turiansky GW (2003) Numerous asymptomatic facial papules and multiple pulmonary cysts: a case of Birt-Hogg-Dube syndrome. Cutis 72: 127-131.

21. Furuya M, Tanaka R, Koga S, Yatabe Y, Gotoda H, et al. (2012) Pulmonary cysts of Birt-Hogg-Dube syndrome: a clinicopathologic and immunohistochemical study of 9 families. Am J Surg Pathol 36: 589-600.

22. Van Denhove A, Guillot-Pouget I, Giraud S, Isaac S, Freymond N, et al. (2011) [Multiple spontaneous pneumothoraces revealing Birt-Hogg-Dube syndrome]. Rev Mal Respir 28: 355-359.

23. Petersson F, Gatalica Z, Grossmann P, Perez Montiel MD, Alvarado Cabrero I, et al. (2010) Sporadic hybrid oncocytic/chromophobe tumor of the kidney: a clinicopathologic, histomorphologic, immunohistochemical, ultrastructural, and molecular cytogenetic study of 14 cases. Virchows Arch 456: 355-365.

24. Koga S, Furuya M, Takahashi Y, Tanaka R, Yamaguchi A, et al. (2009) Lung cysts in Birt-Hogg-Dube syndrome: histopathological characteristics and aberrant sequence repeats. Pathol Int 59: 720-728.

25. Toro JR, Wei MH, Glenn GM, Weinreich M, Toure O, et al. (2008) BHD mutations, clinical and molecular genetic investigations of Birt-Hogg-Dube syndrome: a new series of 50 families and a review of published reports. J Med Genet 45: 321-331.

26. Nickerson ML, Warren MB, Toro JR, Matrosova V, Glenn G, et al. (2002) Mutations in a novel gene lead to kidney tumors, lung wall defects, and benign tumors of the hair follicle in patients with the Birt-Hogg-Dube syndrome. Cancer Cell 2: 157-164.

27. Liaw D, Marsh DJ, Li J, Dahia PL, Wang SI, et al. (1997) Germline mutations of the PTEN gene in Cowden disease, an inherited breast and thyroid cancer syndrome. Nat Genet 16: 64-67.

28. Marsh DJ, Kum JB, Lunetta KL, Bennett MJ, Gorlin RJ, et al. (1999) PTEN mutation spectrum and genotype-phenotype correlations in Bannayan-Riley-Ruvalcaba syndrome suggest a single entity with Cowden syndrome. Hum Mol Genet 8: 1461-1472.

29. Toro JR, Shevchenko YO, Compton JG, Bale SJ (2002) Exclusion of PTEN, CTNNB1, and PTCH as candidate genes for Birt-Hogg-Dube syndrome. J Med Genet 39: E10.

30. Inoki K, Corradetti MN, Guan KL (2005) Dysregulation of the TSC-mTOR pathway in human disease. Nat Genet 37: 19-24.

31. Khoo SK, Bradley M, Wong FK, Hedblad MA, Nordenskjold M, et al. (2001) Birt-Hogg-Dube syndrome: mapping of a novel hereditary neoplasia gene to chromosome 17p12-q11.2. Oncogene 20: 5239-5242.

32. Schmidt LS, Warren MB, Nickerson ML, Weirich G, Matrosova V, et al. (2001) Birt-Hogg-Dube syndrome, a genodermatosis associated with spontaneous pneumothorax and kidney neoplasia, maps to chromosome 17p11.2. Am J Hum Genet 69: 876-882.

33. Vocke CD, Yang Y, Pavlovich CP, Schmidt LS, Nickerson ML, et al. (2005) High frequency of somatic frameshift BHD gene mutations in Birt-Hogg-Dube-associated renal tumors. J Natl Cancer Inst 97: 931-935.

34. Warren MB, Torres-Cabala CA, Turner ML, Merino MJ, Matrosova VY, et al. (2004) Expression of Birt-Hogg-Dube gene mRNA in normal and neoplastic human tissues. Mod Pathol 17: 998-1011.

35. Schmidt LS, Nickerson ML, Warren MB, Glenn GM, Toro JR, et al. (2005) Germline BHD-mutation spectrum and phenotype analysis of a large cohort of families with Birt-Hogg-Dube syndrome. Am J Hum Genet 76: 1023-1033.

36. Nookala RK, Langemeyer L, Pacitto A, Ochoa-Montano B, Donaldson JC, et al. (2012) Crystal structure of folliculin reveals a hidDENN function in genetically inherited renal cancer. Open Biol 2: 120071.

37. Marat AL, Dokainish H, McPherson PS (2011) DENN domain proteins: regulators of Rab GTPases. J Biol Chem 286: 13791-13800.

38. Baba M, Hong SB, Sharma N, Warren MB, Nickerson ML, et al. (2006) Folliculin encoded by the BHD gene interacts with a binding protein, FNIP1, and AMPK, and is involved in AMPK and mTOR signaling. Proc Natl Acad Sci U S A 103: 15552-15557.

39. Hedbacker K, Carlson M (2008) SNF1/AMPK pathways in yeast. Front Biosci 13: 2408-2420.

40. Narbonne P, Roy R (2006) Inhibition of germline proliferation during C. elegans dauer development requires PTEN, LKB1 and AMPK signalling. Development 133: 611-619.

41. Apfeld J, O'Connor G, McDonagh T, DiStefano PS, Curtis R (2004) The AMP-activated protein kinase AAK-2 links energy levels and insulin-like signals to lifespan in C. elegans. Genes Dev 18: 3004-3009.

42. Johnson EC, Kazgan N, Bretz CA, Forsberg LJ, Hector CE, et al. (2010) Altered metabolism and persistent starvation behaviors caused by reduced AMPK function in Drosophila. PLoS One 5.

43. Hardie DG, Ross FA, Hawley SA (2012) AMPK: a nutrient and energy sensor that maintains energy homeostasis. Nat Rev Mol Cell Biol 13: 251-262.

44. Oakhill JS, Steel R, Chen ZP, Scott JW, Ling N, et al. (2011) AMPK is a direct adenylate charge-regulated protein kinase. Science 332: 1433-1435.

45. Oakhill JS, Scott JW, Kemp BE (2009) Structure and function of AMP-activated protein kinase. Acta Physiologica 196: 3-14.

46. Xiao B, Sanders MJ, Underwood E, Heath R, Mayer FV, et al. (2011) Structure of mammalian AMPK and its regulation by ADP. Nature 472: 230-233.

47. Suter M, Riek U, Tuerk R, Schlattner U, Wallimann T, et al. (2006) Dissecting the role of 5'-AMP for allosteric stimulation, activation, and deactivation of AMP-activated protein kinase. J Biol Chem 281: 32207-32216.

48. Oakhill JS, Scott JW, Kemp BE (2012) AMPK functions as an adenylate charge-regulated protein kinase. Trends Endocrinol Metab 23: 125-132.

49. Woods A, Vertommen D, Neumann D, Turk R, Bayliss J, et al. (2003) Identification of phosphorylation sites in AMP-activated protein kinase (AMPK) for upstream AMPK kinases and study of their roles by site-directed mutagenesis. J Biol Chem 278: 28434-28442.

50. Hawley SA, Selbert MA, Goldstein EG, Edelman AM, Carling D, et al. (1995) 5'-AMP activates the AMP-activated protein kinase cascade, and Ca2+/calmodulin activates the calmodulin-dependent protein kinase I cascade, via three independent mechanisms. J Biol Chem 270: 27186-27191.

51. Shaw RJ, Kosmatka M, Bardeesy N, Hurley RL, Witters LA, et al. (2004) The tumor suppressor LKB1 kinase directly activates AMP-activated kinase and regulates apoptosis in response to energy stress. Proc Natl Acad Sci U S A 101: 3329-3335.

52. Hurley RL[1], Anderson KA, Franzone JM, Kemp BE, Means AR, Witters LA. (2005) The Ca2+/calmodulin-dependent protein kinase kinases are AMP-activated protein kinase kinases. J Biol Chem.Aug 12;280(32):29060-6. Epub 2005 Jun 24.

53. Hardie DG (2014) AMPK: positive and negative regulation, and its role in whole-body energy homeostasis. Curr Opin Cell Biol 33C: 1-7.

54. Gwinn DM, Shackelford DB, Egan DF, Mihaylova MM, Mery A, et al. (2008) AMPK phosphorylation of raptor mediates a metabolic checkpoint. Mol Cell 30: 214-226.

55. Jones RG, Plas DR, Kubek S, Buzzai M, Mu J, et al. (2005) AMP-activated protein kinase induces a p53-dependent metabolic checkpoint. Mol Cell 18: 283-293.

56. Liang J, Shao SH, Xu ZX, Hennessy B, Ding Z, et al. (2007) The energy sensing LKB1-AMPK pathway regulates p27(kip1) phosphorylation mediating the decision to enter autophagy or apoptosis. Nat Cell Biol 9: 218-224.

57. Mihaylova MM, Shaw RJ (2011) The AMPK signalling pathway coordinates cell growth, autophagy and metabolism. Nat Cell Biol 13: 1016-1023.

58. Egan D, Kim J, Shaw RJ, Guan KL (2011) The autophagy initiating kinase ULK1 is regulated via opposing phosphorylation by AMPK and mTOR. Autophagy 7: 643-644.

59. Kim J, Guan KL (2011) Regulation of the autophagy initiating kinase ULK1 by nutrients: Roles of mTORC1 and AMPK. Cell Cycle 10.

60. Kim J, Kundu M, Viollet B, Guan KL (2011) AMPK and mTOR regulate autophagy through direct phosphorylation of Ulk1. Nat Cell Biol 13: 132-141.

61. Kim J, Kim YC, Fang C, Russell RC, Kim JH, et al. (2013) Differential regulation of distinct Vps34 complexes by AMPK in nutrient stress and autophagy. Cell 152: 290-303.

62. Scott JW, Norman DG, Hawley SA, Kontogiannis L, Hardie DG (2002) Protein kinase substrate recognition studied using the recombinant catalytic domain of AMP-activated protein kinase and a model substrate. J Mol Biol 317: 309-323.

63. Merrill GF, Kurth EJ, Hardie DG, Winder WW (1997) AICA riboside increases AMP-activated protein kinase, fatty acid oxidation, and glucose uptake in rat muscle. Am J Physiol 273: E1107-1112.

64. Nielsen JN, Wojtaszewski JF, Haller RG, Hardie DG, Kemp BE, et al. (2002) Role of 5'AMP-activated protein kinase in glycogen synthase activity and glucose utilization: insights from patients with McArdle's disease. J Physiol 541: 979-989.

65. Carling D, Hardie DG (1989) The substrate and sequence specificity of the AMP-activated protein kinase. Phosphorylation of glycogen synthase and phosphorylase kinase. Biochim Biophys Acta 1012: 81-86.

66. Jorgensen SB, Honeyman J, Oakhill JS, Fazakerley D, Stockli J, et al. (2009) Oligomeric resistin impairs insulin and AICAR-stimulated glucose uptake in mouse skeletal muscle by inhibiting GLUT4 translocation. American Journal of Physiology-Endocrinology and Metabolism 297: E57-E66.

67. McGee SL, van Denderen BJ, Howlett KF, Mollica J, Schertzer JD, et al. (2008) AMP-activated protein kinase regulates GLUT4 transcription by phosphorylating histone deacetylase 5. Diabetes 57: 860-867.

68. Suwa M, Nakano H, Kumagai S (2003) Effects of chronic AICAR treatment on fiber composition, enzyme activity, UCP3, and PGC-1 in rat muscles. J Appl Physiol (1985) 95: 960-968.

69. Jager S, Handschin C, St-Pierre J, Spiegelman BM (2007) AMP-activated protein kinase (AMPK) action in skeletal muscle via direct phosphorylation of PGC-1alpha. Proc Natl Acad Sci U S A 104: 12017-12022.

70. Canto C, Gerhart-Hines Z, Feige JN, Lagouge M, Noriega L, et al. (2009) AMPK regulates energy expenditure by modulating NAD+ metabolism and SIRT1 activity. Nature 458: 1056-1060.

71. Puigserver P, Wu Z, Park CW, Graves R, Wright M, et al. (1998) A cold-inducible coactivator of nuclear receptors linked to adaptive thermogenesis. Cell 92: 829-839.

72. Canto C, Jiang LQ, Deshmukh AS, Mataki C, Coste A, et al. (2010) Interdependence of AMPK and SIRT1 for metabolic adaptation to fasting and exercise in skeletal muscle. Cell Metab 11: 213-219.

73. Canto C, Auwerx J (2010) AMP-activated protein kinase and its downstream transcriptional pathways. Cell Mol Life Sci 67: 3407-3423.

74. Mair W, Morantte I, Rodrigues AP, Manning G, Montminy M, et al. (2011) Lifespan extension induced by AMPK and calcineurin is mediated by CRTC-1 and CREB. Nature 470: 404-408.

75. Thomson DM, Herway ST, Fillmore N, Kim H, Brown JD, et al. (2008) AMP-activated protein kinase phosphorylates transcription factors of the CREB family. J Appl Physiol (1985) 104: 429-438.

76. Hwang AB, Ryu EA, Artan M, Chang HW, Kabir MH, et al. (2014) Feedback regulation via AMPK and HIF-1 mediates ROS-dependent longevity in Caenorhabditis elegans. Proc Natl Acad Sci U S A 111: E4458-4467.

77. Yan M, Gingras MC, Dunlop EA, Nouet Y, Dupuy F, et al. (2014) The tumor suppressor folliculin regulates AMPK-dependent metabolic transformation. J Clin Invest.

78. Greer EL, Dowlatshahi D, Banko MR, Villen J, Hoang K, et al. (2007) An AMPK-FOXO pathway mediates longevity induced by a novel method of dietary restriction in C. elegans. Curr Biol 17: 1646-1656.

79. Lee H, Cho JS, Lambacher N, Lee J, Lee SJ, et al. (2008) The Caenorhabditis elegans AMP-activated protein kinase AAK-2 is phosphorylated by LKB1 and is required for resistance to oxidative stress and for normal motility and foraging behavior. J Biol Chem 283: 14988-14993.

80. Schulz TJ, Zarse K, Voigt A, Urban N, Birringer M, et al. (2007) Glucose restriction extends Caenorhabditis elegans life span by inducing mitochondrial respiration and increasing oxidative stress. Cell Metab 6: 280-293.

81. Hasumi H, Baba M, Hong SB, Hasumi Y, Huang Y, et al. (2008) Identification and characterization of a novel folliculin-interacting protein FNIP2. Gene 415: 60-67.

82. Park H, Staehling K, Tsang M, Appleby MW, Brunkow ME, et al. (2012) Disruption of Fnip1 reveals a metabolic checkpoint controlling B lymphocyte development. Immunity 36: 769-781.

83. Baba M, Keller JR, Sun HW, Resch W, Kuchen S, et al. (2012) The folliculin-FNIP1 pathway deleted in human Birt-Hogg-Dube syndrome is required for murine B-cell development. Blood 120: 1254-1261.

84. Tsun ZY, Bar-Peled L, Chantranupong L, Zoncu R, Wang T, et al. (2013) The Folliculin Tumor Suppressor Is a GAP for the RagC/D GTPases That Signal Amino Acid Levels to mTORC1. Mol Cell 52: 495-505.

85. Petit CS, Roczniak-Ferguson A, Ferguson SM (2013) Recruitment of folliculin to lysosomes supports the amino acid-dependent activation of Rag GTPases. J Cell Biol 202: 1107-1122.

86. Takagi Y, Kobayashi T, Shiono M, Wang L, Piao X, et al. (2008) Interaction of folliculin (Birt-Hogg-Dube gene product) with a novel Fnip1-like (FnipL/Fnip2) protein. Oncogene 27: 5339-5347.

87. Sano S, Sakagami R, Sekiguchi M, Hidaka M (2013) Stabilization of MAPO1 by specific binding with folliculin and AMP-activated protein kinase in O(6)-methylguanine-induced apoptosis. Biochem Biophys Res Commun 430: 810-815.

88. Zhang D, Iyer LM, He F, Aravind L (2012) Discovery of Novel DENN Proteins: Implications for the Evolution of Eukaryotic Intracellular Membrane Structures and Human Disease. Front Genet 3: 283.

89. Hasumi Y, Baba M, Ajima R, Hasumi H, Valera VA, et al. (2009) Homozygous loss of BHD causes early embryonic lethality and kidney tumor development with activation of mTORC1 and mTORC2. Proc Natl Acad Sci U S A 106: 18722-18727.

90. Martina JA, Diab HI, Li H, Puertollano R (2014) Novel roles for the MiTF/TFE family of transcription factors in organelle biogenesis, nutrient sensing, and energy homeostasis. Cell Mol Life Sci 71: 2483-2497.

91. Dunlop EA, Seifan S, Claessens T, Behrends C, Kamps MA, Rozycka E, Kemp AJ, Nookala RK, Blenis J, Coull BJ, Murray JT, van Steensel MA,Wilkinson S, Tee AR (2014). FLCN, a novel autophagy component, interacts with GABARAP and is regulated by ULK1 phosphorylation. Autophagy.2014 Oct 1;10(10):1749-60.

92. Gaur K, Li J, Wang D, Dutta P, Yan SJ, et al. (2013) The Birt-Hogg-Dube tumor suppressor Folliculin negatively regulates ribosomal RNA synthesis. Hum Mol Genet 22: 284-299.

93. Nahorski MS, Seabra L, Straatman-Iwanowska A, Wingenfeld A, Reiman A, et al. (2012) Folliculin interacts with p0071 (plakophilin-4) and deficiency is associated with disordered RhoA signalling, epithelial polarization and cytokinesis. Hum Mol Genet 21: 5268-5279.

94. Medvetz DA, Khabibullin D, Hariharan V, Ongusaha PP, Goncharova EA, et al. (2012) Folliculin, the product of the Birt-Hogg-Dube tumor suppressor gene, interacts with the adherens junction protein p0071 to regulate cell-cell adhesion. PLoS One 7: e47842.

95. Piao X, Kobayashi T, Wang L, Shiono M, Takagi Y, et al. (2009) Regulation of folliculin (the BHD gene product) phosphorylation by Tsc2-mTOR pathway. Biochem Biophys Res Commun 389: 16-21.

96. Hudon V, Sabourin S, Dydensborg AB, Kottis V, Ghazi A, et al. (2010) Renal tumour suppressor function of the Birt-Hogg-Dube syndrome gene product folliculin. J Med Genet 47: 182-189.

97. Preston RS, Philp A, Claessens T, Gijezen L, Dydensborg AB, et al. (2011) Absence of the Birt-Hogg-Dube gene product is associated with increased hypoxia-inducible factor transcriptional activity and a loss of metabolic flexibility. Oncogene 30: 1159-1173.

98. Cash TP, Gruber JJ, Hartman TR, Henske EP, Simon MC (2011) Loss of the Birt-Hogg-Dube tumor suppressor results in apoptotic resistance due to aberrant TGFbeta-mediated transcription. Oncogene 30: 2534-2546.

99. Khabibullin D, Medvetz DA, Pinilla M, Hariharan V, Li C, et al. (2014) Folliculin regulates cell-cell adhesion, AMPK, and mTORC1 in a cell-type-specific manner in lung-derived cells. Physiol Rep 2.

100. Lim TH, Fujikane R, Sano S, Sakagami R, Nakatsu Y, et al. (2012) Activation of AMP-activated protein kinase by MAPO1 and FLCN induces apoptosis triggered by alkylated base mismatch in DNA. DNA Repair (Amst) 11: 259-266.

101. Possik E, Jalali Z, Nouet Y, Yan M, Gingras MC, et al. (2014) Folliculin regulates ampk-dependent autophagy and metabolic stress survival. PLoS Genet 10: e1004273.

102. Dunlop EA, Seifan S, Claessens T, Behrends C, Kamps MA, et al. (2014) FLCN, a novel autophagy component, interacts with GABARAP and is regulated by ULK1 phosphorylation. Autophagy 10: 1749-1760.

103. Luijten MN, Basten SG, Claessens T, Vernooij M, Scott CL, et al. (2013) Birt-Hogg-Dube syndrome is a novel ciliopathy. Hum Mol Genet 22: 4383-4397.

104. Hong SB, Oh H, Valera VA, Baba M, Schmidt LS, et al. (2010) Inactivation of the FLCN tumor suppressor gene induces TFE3 transcriptional activity by increasing its nuclear localization. PLoS One 5: e15793.

105. Betschinger J, Nichols J, Dietmann S, Corrin PD, Paddison PJ, et al. (2013) Exit from Pluripotency Is Gated by Intracellular Redistribution of the bHLH Transcription Factor Tfe3. Cell 153: 335-347.

106. Hong SB, Oh H, Valera VA, Stull J, Ngo DT, et al. (2010) Tumor suppressor FLCN inhibits tumorigenesis of a FLCN-null renal cancer cell line and regulates expression of key molecules in TGF-beta signaling. Mol Cancer 9: 160.

107. Reiman A, Lu X, Seabra L, Boora U, Nahorski MS, et al. (2012) Gene expression and protein array studies of folliculin-regulated pathways. Anticancer Res 32: 4663-4670.

108. Klomp JA, Petillo D, Niemi NM, Dykema KJ, Chen J, et al. (2010) Birt-Hogg-Dube renal tumors are genetically distinct from other renal neoplasias and are associated with up-regulation of mitochondrial gene expression. BMC Med Genomics 3: 59.

109. Lin J, Handschin C, Spiegelman BM (2005) Metabolic control through the PGC-1 family of transcription coactivators. Cell Metab 1: 361-370.

110. Austin S, St-Pierre J (2012) PGC1alpha and mitochondrial metabolism--emerging concepts and relevance in ageing and neurodegenerative disorders. J Cell Sci 125: 4963-4971.

111. Hasumi H, Baba M, Hasumi Y, Huang Y, Oh H, et al. (2012) Regulation of mitochondrial oxidative metabolism by tumor suppressor FLCN. J Natl Cancer Inst 104: 1750-1764.

112. Reyes NL, Banks GB, Tsang M, Margineantu D, Gu H, et al. (2015) Fnip1 regulates skeletal muscle fiber type specification, fatigue resistance, and susceptibility to muscular dystrophy. Proc Natl Acad Sci U S A 112: 424-429.

113. Kauffman EC, Ricketts CJ, Rais-Bahrami S, Yang Y, Merino MJ, et al. (2014) Molecular genetics and cellular features of TFE3 and TFEB fusion kidney cancers. Nat Rev Urol 11: 465-475.

114. Okimoto K, Sakurai J, Kobayashi T, Mitani H, Hirayama Y, et al. (2004) A germ-line insertion in the Birt-Hogg-Dube (BHD) gene gives rise to the Nihon rat model of inherited renal cancer. Proc Natl Acad Sci U S A 101: 2023-2027.

115. Hartman TR, Nicolas E, Klein-Szanto A, Al-Saleem T, Cash TP, et al. (2009) The role of the Birt-Hogg-Dube protein in mTOR activation and renal tumorigenesis. Oncogene 28: 1594-1604.

116. Chen J, Futami K, Petillo D, Peng J, Wang P, et al. (2008) Deficiency of FLCN in mouse kidney led to development of polycystic kidneys and renal neoplasia. PLoS One 3: e3581.

117. Baba M, Furihata M, Hong SB, Tessarollo L, Haines DC, et al. (2008) Kidney-targeted Birt-Hogg-Dube gene inactivation in a mouse model: Erk1/2 and Akt-mTOR activation, cell hyperproliferation, and polycystic kidneys. J Natl Cancer Inst 100: 140-154.

118. Lium B, Moe L (1985) Hereditary multifocal renal cystadenocarcinomas and nodular dermatofibrosis in the German shepherd dog: macroscopic and histopathologic changes. Vet Pathol 22: 447-455.

119. Lingaas F, Comstock KE, Kirkness EF, Sorensen A, Aarskaug T, et al. (2003) A mutation in the canine BHD gene is associated with hereditary multifocal renal cystadenocarcinoma and nodular dermatofibrosis in the German Shepherd dog. Hum Mol Genet 12: 3043-3053.

120. Bonsdorff TB, Jansen JH, Lingaas F (2008) Second hits in the FLCN gene in a hereditary renal cancer syndrome in dogs. Mamm Genome 19: 121-126.

121. Bonsdorff TB, Jansen JH, Thomassen RF, Lingaas F (2009) Loss of heterozygosity at the FLCN locus in early renal cystic lesions in dogs with renal cystadenocarcinoma and nodular dermatofibrosis. Mamm Genome 20: 315-320.

122. Liu W, Chen Z, Ma Y, Wu X, Jin Y, et al. (2013) Genetic characterization of the Drosophila birt-hogg-dube syndrome gene. PLoS One 8: e65869.

123. Gharbi H, Fabretti F, Bharill P, Rinschen M, Brinkkotter S, et al. (2013) Loss of the Birt-Hogg-Dube gene product Folliculin induces longevity in a hypoxia-inducible factor dependent manner. Aging Cell.

124. van Slegtenhorst M, Khabibullin D, Hartman TR, Nicolas E, Kruger WD, et al. (2007) The Birt-Hogg-Dube and tuberous sclerosis complex homologs have opposing roles in amino acid homeostasis in Schizosaccharomyces pombe. J Biol Chem 282: 24583-24590.

125. Van Raamsdonk JM, Hekimi S (2011) FUdR causes a twofold increase in the lifespan of the mitochondrial mutant gas-1. Mech Ageing Dev 132: 519-521.

126. Aitlhadj L, Sturzenbaum SR (2010) The use of FUdR can cause prolonged longevity in mutant nematodes. Mech Ageing Dev 131: 364-365.

127. Davies SK, Leroi AM, Bundy JG (2012) Fluorodeoxyuridine affects the identification of metabolic responses to daf-2 status in Caenorhabditis elegans. Mech Ageing Dev 133: 46-49.

128. Brenner S (1974) The genetics of Caenorhabditis elegans. Genetics 77: 71-94.

129. Poulin G, Nandakumar R, Ahringer J (2004) Genome-wide RNAi screens in Caenorhabditis elegans: impact on cancer research. Oncogene 23: 8340-8345.

130. Harris TW, Chen N, Cunningham F, Tello-Ruiz M, Antoshechkin I, et al. (2004) WormBase: a multi-species resource for nematode biology and genomics. Nucleic Acids Res 32: D411-417.

131. Fire A, Xu S, Montgomery MK, Kostas SA, Driver SE, et al. (1998) Potent and specific genetic interference by double-stranded RNA in Caenorhabditis elegans. Nature 391: 806-811.

132. Kamath RS, Martinez-Campos M, Zipperlen P, Fraser AG, Ahringer J (2001) Effectiveness of specific RNA-mediated interference through ingested double-stranded RNA in Caenorhabditis elegans. Genome Biology 2.

133. Timmons L (2006) Delivery methods for RNA interference in C. elegans. Methods Mol Biol 351: 119-125.

134. Fraser AG, Kamath RS, Zipperlen P, Martinez-Campos M, Sohrmann M, et al. (2000) Functional genomic analysis of C. elegans chromosome I by systematic RNA interference. Nature 408: 325-330.

135. Chen N, Lawson D, Bradnam K, Harris TW, Stein LD (2004) WormBase as an integrated platform for the C. elegans ORFeome. Genome Res 14: 2155-2161.

136. Rodriguez M, Snoek LB, De Bono M, Kammenga JE (2013) Worms under stress: C. elegans stress response and its relevance to complex human disease and aging. Trends Genet 29: 367-374.

137. Lapierre LR, Hansen M (2012) Lessons from C. elegans: signaling pathways for longevity. Trends Endocrinol Metab.

138. Baumeister R, Schaffitzel E, Hertweck M (2006) Endocrine signaling in Caenorhabditis elegans controls stress response and longevity. J Endocrinol 190: 191-202.

139. Lettre G, Hengartner MO (2006) Developmental apoptosis in C. elegans: a complex CEDnario. Nat Rev Mol Cell Biol 7: 97-108.

140. Sulston JE, Schierenberg E, White JG, Thomson JN (1983) The embryonic cell lineage of the nematode Caenorhabditis elegans. Dev Biol 100: 64-119.

141. Sulston JE, Horvitz HR (1977) Post-embryonic cell lineages of the nematode, Caenorhabditis elegans. Dev Biol 56: 110-156.

142. Kimble J, Hirsh D (1979) The postembryonic cell lineages of the hermaphrodite and male gonads in Caenorhabditis elegans. Dev Biol 70: 396-417.

143. Hengartner MO, Ellis RE, Horvitz HR (1992) Caenorhabditis elegans gene ced-9 protects cells from programmed cell death. Nature 356: 494-499.

144. Ellis HM, Horvitz HR (1986) Genetic control of programmed cell death in the nematode C. elegans. Cell 44: 817-829.

145. Desai C, Garriga G, McIntire SL, Horvitz HR (1988) A genetic pathway for the development of the Caenorhabditis elegans HSN motor neurons. Nature 336: 638-646.

146. Yuan J, Shaham S, Ledoux S, Ellis HM, Horvitz HR (1993) The C. elegans cell death gene ced-3 encodes a protein similar to mammalian interleukin-1 beta-converting enzyme. Cell 75: 641-652.

147. Xue D, Horvitz HR (1995) Inhibition of the Caenorhabditis elegans cell-death protease CED-3 by a CED-3 cleavage site in baculovirus p35 protein. Nature 377: 248-251.

148. Xue D, Shaham S, Horvitz HR (1996) The Caenorhabditis elegans cell-death protein CED-3 is a cysteine protease with substrate specificities similar to those of the human CPP32 protease. Genes Dev 10: 1073-1083.

149. Riedl SJ, Shi Y (2004) Molecular mechanisms of caspase regulation during apoptosis. Nat Rev Mol Cell Biol 5: 897-907.

150. Hengartner MO, Horvitz HR (1994) C. elegans cell survival gene ced-9 encodes a functional homolog of the mammalian proto-oncogene bcl-2. Cell 76: 665-676.

151. Hengartner MO, Horvitz HR (1994) Activation of C. elegans cell death protein CED-9 by an amino-acid substitution in a domain conserved in Bcl-2. Nature 369: 318-320.

152. Yang X, Chang HY, Baltimore D (1998) Essential role of CED-4 oligomerization in CED-3 activation and apoptosis. Science 281: 1355-1357.

153. Yuan J, Horvitz HR (1992) The Caenorhabditis elegans cell death gene ced-4 encodes a novel protein and is expressed during the period of extensive programmed cell death. Development 116: 309-320.

154. Judy ME, Nakamura A, Huang A, Grant H, McCurdy H, et al. (2013) A shift to organismal stress resistance in programmed cell death mutants. PLoS Genet 9: e1003714.

155. Yee C, Yang W, Hekimi S (2014) The intrinsic apoptosis pathway mediates the pro-longevity response to mitochondrial ROS in C. elegans. Cell 157: 897-909.

156. Cotter TG (2009) Apoptosis and cancer: the genesis of a research field. Nat Rev Cancer 9: 501-507.

157. Vazquez A, Bond EE, Levine AJ, Bond GL (2008) The genetics of the p53 pathway, apoptosis and cancer therapy. Nat Rev Drug Discov 7: 979-987.

158. Yip KW, Reed JC (2008) Bcl-2 family proteins and cancer. Oncogene 27: 6398-6406.

159. Mizushima N, Komatsu M (2011) Autophagy: renovation of cells and tissues. Cell 147: 728-741.

160. Mizushima N, Levine B, Cuervo AM, Klionsky DJ (2008) Autophagy fights disease through cellular self-digestion. Nature 451: 1069-1075.

161. Melendez A, Talloczy Z, Seaman M, Eskelinen EL, Hall DH, et al. (2003) Autophagy genes are essential for dauer development and life-span extension in C. elegans. Science 301: 1387-1391.

162. Jia K, Thomas C, Akbar M, Sun Q, Adams-Huet B, et al. (2009) Autophagy genes protect against Salmonella typhimurium infection and mediate insulin signaling-regulated pathogen resistance. Proc Natl Acad Sci U S A 106: 14564-14569.

163. Samokhvalov V, Scott BA, Crowder CM (2008) Autophagy protects against hypoxic injury in C. elegans. Autophagy 4: 1034-1041.

164. Hansen M, Chandra A, Mitic LL, Onken B, Driscoll M, et al. (2008) A role for autophagy in the extension of lifespan by dietary restriction in C. elegans. PLoS Genet 4: e24.

165. Zhang H, Kong X, Kang J, Su J, Li Y, et al. (2009) Oxidative stress induces parallel autophagy and mitochondria dysfunction in human glioma U251 cells. Toxicol Sci 110: 376-388.

166. Shintani T, Klionsky DJ (2004) Autophagy in health and disease: a double-edged sword. Science 306: 990-995.

167. Dwivedi M, Song HO, Ahnn J (2009) Autophagy genes mediate the effect of calcineurin on life span in C. elegans. Autophagy 5: 604-607.

168. Morselli E, Galluzzi L, Kepp O, Criollo A, Maiuri MC, et al. (2009) Autophagy mediates pharmacological lifespan extension by spermidine and resveratrol. Aging (Albany NY) 1: 961-970.

169. Morselli E, Maiuri MC, Markaki M, Megalou E, Pasparaki A, et al. (2010) Caloric restriction and resveratrol promote longevity through the Sirtuin-1-dependent induction of autophagy. Cell Death Dis 1: e10.

170. O'Rourke EJ, Kuballa P, Xavier R, Ruvkun G (2013) omega-6 Polyunsaturated fatty acids extend life span through the activation of autophagy. Genes Dev 27: 429-440.

171. Madeo F, Tavernarakis N, Kroemer G (2010) Can autophagy promote longevity? Nat Cell Biol 12: 842-846.

172. Juhasz G, Erdi B, Sass M, Neufeld TP (2007) Atg7-dependent autophagy promotes neuronal health, stress tolerance, and longevity but is dispensable for metamorphosis in Drosophila. Genes Dev 21: 3061-3066.

173. Pyo JO, Yoo SM, Ahn HH, Nah J, Hong SH, et al. (2013) Overexpression of Atg5 in mice activates autophagy and extends lifespan. Nat Commun 4: 2300.

174. Levine B (2007) Cell biology - Autophagy and cancer. Nature 446: 745-747.

175. Yang S, Wang X, Contino G, Liesa M, Sahin E, et al. (2011) Pancreatic cancers require autophagy for tumor growth. Genes Dev 25: 717-729.

176. Degenhardt K, Mathew R, Beaudoin B, Bray K, Anderson D, et al. (2006) Autophagy promotes tumor cell survival and restricts necrosis, inflammation, and tumorigenesis. Cancer Cell 10: 51-64.

177. Mathew R, White E (2011) Autophagy, stress, and cancer metabolism: what doesn't kill you makes you stronger. Cold Spring Harb Symp Quant Biol 76: 389-396.

178. Alfadda AA, Sallam RM (2012) Reactive oxygen species in health and disease. J Biomed Biotechnol 2012: 936486.

179. Schieber M, Chandel NS (2014) ROS function in redox signaling and oxidative stress. Curr Biol 24: R453-462.

180. Finkel T, Holbrook NJ (2000) Oxidants, oxidative stress and the biology of ageing. Nature 408: 239-247.

181. Di Carlo M, Giacomazza D, Picone P, Nuzzo D, San Biagio PL (2012) Are oxidative stress and mitochondrial dysfunction the key players in the neurodegenerative diseases? Free Radic Res 46: 1327-1338.

182. Gandhi S, Abramov AY (2012) Mechanism of oxidative stress in neurodegeneration. Oxid Med Cell Longev 2012: 428010.

183. Trushina E, McMurray CT (2007) Oxidative stress and mitochondrial dysfunction in neurodegenerative diseases. Neuroscience 145: 1233-1248.

184. Touyz RM, Briones AM (2011) Reactive oxygen species and vascular biology: implications in human hypertension. Hypertens Res 34: 5-14.

185. Gorrini C, Harris IS, Mak TW (2013) Modulation of oxidative stress as an anticancer strategy. Nat Rev Drug Discov 12: 931-947.

186. Sosa V, Moline T, Somoza R, Paciucci R, Kondoh H, et al. (2013) Oxidative stress and cancer: an overview. Ageing Res Rev 12: 376-390.

187. Moreno-Arriola E, Cardenas-Rodriguez N, Coballase-Urrutia E, Pedraza-Chaverri J, Carmona-Aparicio L, et al. (2014) Caenorhabditis elegans: A Useful Model for Studying Metabolic Disorders in Which Oxidative Stress Is a Contributing Factor. Oxid Med Cell Longev 2014: 705253.

188. Van Raamsdonk JM, Hekimi S (2010) Reactive Oxygen Species and Aging in Caenorhabditis elegans: Causal or Casual Relationship? Antioxid Redox Signal 13: 1911-1953.

189. Muller FL, Song W, Liu Y, Chaudhuri A, Pieke-Dahl S, et al. (2006) Absence of CuZn superoxide dismutase leads to elevated oxidative stress and acceleration of age-dependent skeletal muscle atrophy. Free Radic Biol Med 40: 1993-2004.

190. Sentman ML, Granstrom M, Jakobson H, Reaume A, Basu S, et al. (2006) Phenotypes of mice lacking extracellular superoxide dismutase and copper- and zinc-containing superoxide dismutase. J Biol Chem 281: 6904-6909.

191. Li Y, Huang TT, Carlson EJ, Melov S, Ursell PC, et al. (1995) Dilated cardiomyopathy and neonatal lethality in mutant mice lacking manganese superoxide dismutase. Nat Genet 11: 376-381.

192. Parkes TL, Elia AJ, Dickinson D, Hilliker AJ, Phillips JP, et al. (1998) Extension of Drosophila lifespan by overexpression of human SOD1 in motorneurons. Nat Genet 19: 171-174.

193. Celotto AM, Liu Z, Vandemark AP, Palladino MJ (2012) A novel Drosophila SOD2 mutant demonstrates a role for mitochondrial ROS in neurodevelopment and disease. Brain Behav 2: 424-434.

194. Van Raamsdonk JM, Hekimi S (2009) Deletion of the mitochondrial superoxide dismutase sod-2 extends lifespan in Caenorhabditis elegans. PLoS Genet 5: e1000361.

195. Van Raamsdonk JM, Hekimi S (2012) Superoxide dismutase is dispensable for normal animal lifespan. Proc Natl Acad Sci U S A 109: 5785-5790.

196. Zarse K, Schmeisser S, Groth M, Priebe S, Beuster G, et al. (2012) Impaired insulin/IGF1 signaling extends life span by promoting mitochondrial L-proline catabolism to induce a transient ROS signal. Cell Metab 15: 451-465.

197. Klaunig JE, Xu Y, Isenberg JS, Bachowski S, Kolaja KL, et al. (1998) The role of oxidative stress in chemical carcinogenesis. Environ Health Perspect 106 Suppl 1: 289-295.

198. Klaunig JE, Kamendulis LM (2004) The role of oxidative stress in carcinogenesis. Annu Rev Pharmacol Toxicol 44: 239-267.

199. Liou GY, Storz P (2010) Reactive oxygen species in cancer. Free Radic Res 44: 479-496.

200. Storz P (2005) Reactive oxygen species in tumor progression. Front Biosci 10: 1881-1896.

201. Klaunig JE, Kamendulis LM, Hocevar BA (2010) Oxidative stress and oxidative damage in carcinogenesis. Toxicol Pathol 38: 96-109.

202. Lemon JA, Rollo CD, Boreham DR (2008) Elevated DNA damage in a mouse model of oxidative stress: impacts of ionizing radiation and a protective dietary supplement. Mutagenesis 23: 473-482.

203. Schenk H, Klein M, Erdbrugger W, Droge W, Schulze-Osthoff K (1994) Distinct effects of thioredoxin and antioxidants on the activation of transcription factors NF-kappa B and AP-1. Proc Natl Acad Sci U S A 91: 1672-1676.

204. Honda Y, Honda S (1999) The daf-2 gene network for longevity regulates oxidative stress resistance and Mn-superoxide dismutase gene expression in Caenorhabditis elegans. FASEB J 13: 1385-1393.

205. Park SK, Tedesco PM, Johnson TE (2009) Oxidative stress and longevity in Caenorhabditis elegans as mediated by SKN-1. Aging Cell 8: 258-269.

206. Ventura N, Rea SL, Schiavi A, Torgovnick A, Testi R, et al. (2009) p53/CEP-1 increases or decreases lifespan, depending on level of mitochondrial bioenergetic stress. Aging Cell 8: 380-393.

207. Borrello S, De Leo ME, Galeotti T (1993) Defective gene expression of MnSOD in cancer cells. Mol Aspects Med 14: 253-258.

208. Borrelli A, Schiattarella A, Bonelli P, Tuccillo FM, Buonaguro FM, et al. (2014) The functional role of MnSOD as a biomarker of human diseases and therapeutic potential of a new isoform of a human recombinant MnSOD. Biomed Res Int 2014: 476789.

209. Kim A (2010) Modulation of MnSOD in Cancer:Epidemiological and Experimental Evidence. Toxicol Res 26: 83-93.

210. Glorieux C, Dejeans N, Sid B, Beck R, Calderon PB, et al. (2011) Catalase overexpression in mammary cancer cells leads to a less aggressive phenotype and an altered response to chemotherapy. Biochem Pharmacol 82: 1384-1390.

211. Markaki M, Tavernarakis N (2010) Modeling human diseases in Caenorhabditis elegans. Biotechnol J 5: 1261-1276.

212. Possik E, Pause A (2015) Measuring oxidative stress resistance of Caenorhabditis elegans in 96-well microtiter plates. J Vis Exp: e52746.

213. Brocker C, Thompson DC, Vasiliou V (2012) The role of hyperosmotic stress in inflammation and disease. Biomol Concepts 3: 345-364.

214. Burg MB, Ferraris JD, Dmitrieva NI (2007) Cellular response to hyperosmotic stresses. Physiol Rev 87: 1441-1474.

215. Christoph K, Beck FX, Neuhofer W (2007) Osmoadaptation of Mammalian cells - an orchestrated network of protective genes. Curr Genomics 8: 209-218.

216. Yancey PH (2005) Organic osmolytes as compatible, metabolic and counteracting cytoprotectants in high osmolarity and other stresses. J Exp Biol 208: 2819-2830.

217. O'Rourke SM, Herskowitz I, O'Shea EK (2002) Yeast go the whole HOG for the hyperosmotic response. Trends Genet 18: 405-412.

218. Sheikh-Hamad D, Gustin MC (2004) MAP kinases and the adaptive response to hypertonicity: functional preservation from yeast to mammals. Am J Physiol Renal Physiol 287: F1102-1110.

219. Lamitina ST, Morrison R, Moeckel GW, Strange K (2004) Adaptation of the nematode Caenorhabditis elegans to extreme osmotic stress. Am J Physiol Cell Physiol 286: C785-791.

220. Rohlfing AK, Miteva Y, Hannenhalli S, Lamitina T (2010) Genetic and physiological activation of osmosensitive gene expression mimics transcriptional signatures of pathogen infection in C. elegans. PLoS One 5: e9010.

221. Lamitina T, Huang CG, Strange K (2006) Genome-wide RNAi screening identifies protein damage as a regulator of osmoprotective gene expression. Proc Natl Acad Sci U S A 103: 12173-12178.

222. Solomon A, Bandhakavi S, Jabbar S, Shah R, Beitel GJ, et al. (2004) Caenorhabditis elegans OSR-1 regulates behavioral and physiological responses to hyperosmotic environments. Genetics 167: 161-170.

223. Wheeler JM, Thomas JH (2006) Identification of a novel gene family involved in osmotic stress response in Caenorhabditis elegans. Genetics 174: 1327-1336.

224. Rohlfing AK, Miteva Y, Moronetti L, He L, Lamitina T (2011) The Caenorhabditis elegans mucin-like protein OSM-8 negatively regulates osmosensitive physiology via the transmembrane protein PTR-23. PLoS Genet 7: e1001267.

225. Lee SH, Park Y, Yoon SK, Yoon JB (2010) Osmotic stress inhibits proteasome by p38 MAPK-dependent phosphorylation. J Biol Chem 285: 41280-41289.

226. Gentile LB, Piva B, Diaz BL (2011) Hypertonic stress induces VEGF production in human colon cancer cell line Caco-2: inhibitory role of autocrine PGE(2). PLoS One 6: e25193.

227. Fischer OM, Hart S, Gschwind A, Prenzel N, Ullrich A (2004) Oxidative and osmotic stress signaling in tumor cells is mediated by ADAM proteases and heparin-binding epidermal growth factor. Mol Cell Biol 24: 5172-5183.

228. Li JT, Wang LF, Zhao YL, Yang T, Li W, et al. (2014) Nuclear factor of activated T cells 5 maintained by Hotair suppression of miR-568 upregulates S100 calcium binding protein A4 to promote breast cancer metastasis. Breast Cancer Res 16: 454.

229. Kuper C, Beck FX, Neuhofer W (2014) NFAT5-mediated expression of S100A4 contributes to proliferation and migration of renal carcinoma cells. Front Physiol 5: 293.

230. Bortner CD, Scoltock AB, Sifre MI, Cidlowski JA (2012) Osmotic stress resistance imparts acquired anti-apoptotic mechanisms in lymphocytes. J Biol Chem 287: 6284-6295.

231. Braeckman BP (2009) Intermediary metabolism. In: Koen Houthoofd JRV, editor. 16 February 2009 ed. wormbook.

232. McGhee JD (2007) http://wwwwormbookorg/chapters/www_intestine/intestinehtml.

233. Paupard MC, Miller A, Grant B, Hirsh D, Hall DH (2001) Immuno-EM localization of GFP-tagged yolk proteins in C. elegans using microwave fixation. J Histochem Cytochem 49: 949-956.

234. Chotard L, Skorobogata O, Sylvain MA, Shrivastava S, Rocheleau CE (2010) TBC-2 is required for embryonic yolk protein storage and larval survival during L1 diapause in Caenorhabditis elegans. PLoS One 5: e15662.

235. Herndon LA, Schmeissner PJ, Dudaronek JM, Brown PA, Listner KM, et al. (2002) Stochastic and genetic factors influence tissue-specific decline in ageing C. elegans. Nature 419: 808-814.

236. Horikawa M, Sakamoto K (2009) Fatty-acid metabolism is involved in stress-resistance mechanisms of Caenorhabditis elegans. Biochem Biophys Res Commun 390: 1402-1407.

237. Tauffenberger A, Parker JA (2014) Heritable transmission of stress resistance by high dietary glucose in Caenorhabditis elegans. PLoS Genet 10: e1004346.

238. LaMacchia JC, Frazier HN, 3rd, Roth MB (2015) Glycogen Fuels Survival During Hyposmotic-Anoxic Stress in Caenorhabditis elegans. Genetics.

239. LaMacchia JC, Roth MB (2015) Aquaporins 2 and 4 Regulate Glycogen Metabolism and Survival during Hyposmotic-Anoxic Stress in Caenorhabditis Elegans. Am J Physiol Cell Physiol: ajpcell 00131 02015.

240. Edwards C, Canfield J, Copes N, Brito A, Rehan M, et al. (2015) Mechanisms of amino acid-mediated lifespan extension in Caenorhabditis elegans. BMC Genet 16: 8.

241. Butler JA, Mishur RJ, Bhaskaran S, Rea SL (2013) A metabolic signature for long life in the Caenorhabditis elegans Mit mutants. Aging Cell 12: 130-138.

242. Fuchs S, Bundy JG, Davies SK, Viney JM, Swire JS, et al. (2010) A metabolic signature of long life in Caenorhabditis elegans. BMC Biol 8: 14.

243. Behm CA (1997) The role of trehalose in the physiology of nematodes. Int J Parasitol 27: 215-229.

244. Lamitina ST, Strange K (2005) Transcriptional targets of DAF-16 insulin signaling pathway protect C. elegans from extreme hypertonic stress. Am J Physiol Cell Physiol 288: C467-474.

245. Erkut C, Penkov S, Khesbak H, Vorkel D, Verbavatz JM, et al. (2011) Trehalose renders the dauer larva of Caenorhabditis elegans resistant to extreme desiccation. Curr Biol 21: 1331-1336.

246. Muller J, Aeschbacher RA, Wingler A, Boller T, Wiemken A (2001) Trehalose and trehalase in Arabidopsis. Plant Physiol 125: 1086-1093.

247. Honda Y, Tanaka M, Honda S (2010) Trehalose extends longevity in the nematode Caenorhabditis elegans. Aging Cell 9: 558-569.

248. Frazier HN, 3rd, Roth MB (2009) Adaptive sugar provisioning controls survival of C. elegans embryos in adverse environments. Curr Biol 19: 859-863.

249. Jones RG, Thompson CB (2009) Tumor suppressors and cell metabolism: a recipe for cancer growth. Genes Dev 23: 537-548.

250. Warburg O (1956) On the origin of cancer cells. Science 123: 309-314.

251. Favaro E, Bensaad K, Chong MG, Tennant DA, Ferguson DJ, et al. (2012) Glucose utilization via glycogen phosphorylase sustains proliferation and prevents premature senescence in cancer cells. Cell Metab 16: 751-764.

252. Takahashi S, Satomi A, Yano K, Kawase H, Tanimizu T, et al. (1999) Estimation of glycogen levels in human colorectal cancer tissue: relationship with cell cycle and tumor outgrowth. J Gastroenterol 34: 474-480.

253. Zois CE, Favaro E, Harris AL (2014) Glycogen metabolism in cancer. Biochem Pharmacol 92: 3-11.

254. Pelletier J, Bellot G, Gounon P, Lacas-Gervais S, Pouyssegur J, et al. (2012) Glycogen Synthesis is Induced in Hypoxia by the Hypoxia-Inducible Factor and Promotes Cancer Cell Survival. Front Oncol 2: 18.

255. Rousset M, Zweibaum A, Fogh J (1981) Presence of glycogen and growth-related variations in 58 cultured human tumor cell lines of various tissue origins. Cancer Res 41: 1165-1170.

256. Kouchi M, Okimoto K, Matsumoto I, Tanaka K, Yasuba M, et al. (2006) Natural history of the Nihon (Bhd gene mutant) rat, a novel model for human Birt-Hogg-Dube syndrome. Virchows Arch 448: 463-471.

257. Togashi Y, Kobayashi T, Momose S, Ueda M, Okimoto K, et al. (2006) Transgenic rescue from embryonic lethality and renal carcinogenesis in the Nihon rat model by introduction of a wild-type Bhd gene. Oncogene 25: 2885-2889.

258. Wang L, Kobayashi T, Piao X, Shiono M, Takagi Y, et al. (2010) Serine 62 is a phosphorylation site in folliculin, the Birt-Hogg-Dube gene product. FEBS Lett 584: 39-43.

259. Behrends C, Sowa ME, Gygi SP, Harper JW (2010) Network organization of the human autophagy system. Nature 466: 68-76.

260. Carling D, Thornton C, Woods A, Sanders MJ (2012) AMP-activated protein kinase: new regulation, new roles? Biochem J 445: 11-27.

261. Hardie DG (2011) AMPK and autophagy get connected. EMBO J 30: 634-635.

262. Egan DF, Shackelford DB, Mihaylova MM, Gelino S, Kohnz RA, et al. (2011) Phosphorylation of ULK1 (hATG1) by AMP-activated protein kinase connects energy sensing to mitophagy. Science 331: 456-461.

263. Narbonne P, Roy R (2009) Caenorhabditis elegans dauers need LKB1/AMPK to ration lipid reserves and ensure long-term survival. Nature 457: 210-214.

264. Fukuyama M, Sakuma K, Park R, Kasuga H, Nagaya R, et al. (2012) C. elegans AMPKs promote survival and arrest germline development during nutrient stress. Biol Open 1: 929-936.

265. Curtis R, O'Connor G, DiStefano PS (2006) Aging networks in Caenorhabditis elegans: AMP-activated protein kinase (aak-2) links multiple aging and metabolism pathways. Aging Cell 5: 119-126.

266. LaRue BL, Padilla PA (2011) Environmental and genetic preconditioning for long-term anoxia responses requires AMPK in Caenorhabditis elegans. PLoS One 6: e16790.

267. Chen Y, Azad MB, Gibson SB (2009) Superoxide is the major reactive oxygen species regulating autophagy. Cell Death Differ 16: 1040-1052.

268. Robida-Stubbs S, Glover-Cutter K, Lamming DW, Mizunuma M, Narasimhan SD, et al. (2012) TOR signaling and rapamycin influence longevity by regulating SKN-1/Nrf and DAF-16/FoxO. Cell Metab 15: 713-724.

269. Moore MN (2008) Autophagy as a second level protective process in conferring resistance to environmentally-induced oxidative stress. Autophagy 4: 254-256.

270. Kang C, You YJ, Avery L (2007) Dual roles of autophagy in the survival of Caenorhabditis elegans during starvation. Genes Dev 21: 2161-2171.

271. Gutierrez MG, Saka HA, Chinen I, Zoppino FC, Yoshimori T, et al. (2007) Protective role of autophagy against Vibrio cholerae cytolysin, a pore-forming toxin from V. cholerae. Proc Natl Acad Sci U S A 104: 1829-1834.

272. Hosokawa N, Hara Y, Mizushima N (2006) Generation of cell lines with tetracycline-regulated autophagy and a role for autophagy in controlling cell size. FEBS Lett 580: 2623-2629.

273. Shintani T, Klionsky DJ (2004) Cargo proteins facilitate the formation of transport vesicles in the cytoplasm to vacuole targeting pathway. J Biol Chem 279: 29889-29894.

274. Djeddi A, Michelet X, Culetto E, Alberti A, Barois N, et al. (2012) Induction of autophagy in ESCRT mutants is an adaptive response for cell survival in C. elegans. J Cell Sci 125: 685-694.

275. Noguchi N, Yamamoto H, Misawa S (1993) Effects of paraquat on Mg(2+)-ATPase activity in rat liver. Arch Environ Contam Toxicol 24: 483-486.

276. Yu Q, Wang T, Zhou X, Wu J, Chen X, et al. (2011) Wld(S) reduces paraquat-induced cytotoxicity via SIRT1 in non-neuronal cells by attenuating the depletion of NAD. PLoS One 6: e21770.

277. Yang W, Chen L, Ding Y, Zhuang X, Kang UJ (2007) Paraquat induces dopaminergic dysfunction and proteasome impairment in DJ-1-deficient mice. Hum Mol Genet 16: 2900-2910.

278. Padilla PA, Nystul TG, Zager RA, Johnson AC, Roth MB (2002) Dephosphorylation of cell cycle-regulated proteins correlates with anoxia-induced suspended animation in Caenorhabditis elegans. Mol Biol Cell 13: 1473-1483.

279. Altman BJ, Rathmell JC (2012) Metabolic stress in autophagy and cell death pathways. Cold Spring Harb Perspect Biol 4: a008763.

280. Samara C, Tavernarakis N (2008) Autophagy and cell death in Caenorhabditis elegans. Curr Pharm Des 14: 97-115.

281. Takacs-Vellai K, Vellai T, Puoti A, Passannante M, Wicky C, et al. (2005) Inactivation of the autophagy gene bec-1 triggers apoptotic cell death in C. elegans. Curr Biol 15: 1513-1517.

282. Gartner A, Boag PR, Blackwell TK (2008) Germline survival and apoptosis. WormBook: 1-20.

283. Lee I, Hendrix A, Kim J, Yoshimoto J, You YJ (2012) Metabolic rate regulates L1 longevity in C. elegans. PLoS One 7: e44720.

284. Nath N, McCartney RR, Schmidt MC (2003) Yeast Pak1 kinase associates with and activates Snf1. Mol Cell Biol 23: 3909-3917.

285. Woods A, Dickerson K, Heath R, Hong SP, Momcilovic M, et al. (2005) Ca2+/calmodulin-dependent protein kinase kinase-beta acts upstream of AMP-activated protein kinase in mammalian cells. Cell Metab 2: 21-33.

286. Hong SP, Leiper FC, Woods A, Carling D, Carlson M (2003) Activation of yeast Snf1 and mammalian AMP-activated protein kinase by upstream kinases. Proc Natl Acad Sci U S A 100: 8839-8843.

287. Tao L, Xie Q, Ding YH, Li ST, Peng S, et al. (2013) CAMKII and Calcineurin regulate the lifespan of Caenorhabditis elegans through the FOXO transcription factor DAF-16. Elife 2: e00518.

288. Bungard D, Fuerth BJ, Zeng PY, Faubert B, Maas NL, et al. (2010) Signaling Kinase AMPK Activates Stress-Promoted Transcription via Histone H2B Phosphorylation. Science 329: 1201-1205.

289. Wang L, Brautigan DL (2013) alpha-SNAP inhibits AMPK signaling to reduce mitochondrial biogenesis and dephosphorylates Thr172 in AMPKalpha in vitro. Nat Commun 4: 1559.

290. Suzuki T, Bridges D, Nakada D, Skiniotis G, Morrison SJ, et al. (2013) Inhibition of AMPK catabolic action by GSK3. Mol Cell 50: 407-419.

291. Liang J, Mills GB (2013) AMPK: A Contextual Oncogene or Tumor Suppressor? Cancer Res.

292. Faubert B, Boily G, Izreig S, Griss T, Samborska B, et al. (2013) AMPK Is a Negative Regulator of the Warburg Effect and Suppresses Tumor Growth In Vivo. Cell Metab 17: 113-124.

293. Jeon SM, Chandel NS, Hay N (2012) AMPK regulates NADPH homeostasis to promote tumour cell survival during energy stress. Nature 485: 661-665.

294. Mikhaylova O, Stratton Y, Hall D, Kellner E, Ehmer B, et al. (2012) VHL-regulated MiR-204 suppresses tumor growth through inhibition of LC3B-mediated autophagy in renal clear cell carcinoma. Cancer Cell 21: 532-546.

295. Folkman J (2007) Angiogenesis: an organizing principle for drug discovery? Nat Rev Drug Discov 6: 273-286.

296. Liu L, Ulbrich J, Muller J, Wustefeld T, Aeberhard L, et al. (2012) Deregulated MYC expression induces dependence upon AMPK-related kinase 5. Nature 483: 608-612.

297. Leprivier G, Remke M, Rotblat B, Dubuc A, Mateo AR, et al. (2013) The eEF2 Kinase Confers Resistance to Nutrient Deprivation by Blocking Translation Elongation. Cell 153: 1064-1079.

298. Dupuy F, Griss T, Blagih J, Bridon G, Avizonis D, et al. (2013) LKB1 is a central regulator of tumor initiation and pro-growth metabolism in ErbB2-mediated breast cancer. Cancer Metab 1: 18.

299. Tennakoon JB, Shi Y, Han JJ, Tsouko E, White MA, et al. (2013) Androgens regulate prostate cancer cell growth via an AMPK-PGC-1alpha-mediated metabolic switch. Oncogene.

300. Hanahan D, Weinberg RA (2011) Hallmarks of cancer: the next generation. Cell 144: 646-674.

301. Kenyon C, Chang J, Gensch E, Rudner A, Tabtiang R (1993) A C. elegans mutant that lives twice as long as wild type. Nature 366: 461-464.

302. Hoogewijs D, Houthoofd K, Matthijssens F, Vandesompele J, Vanfleteren JR (2008) Selection and validation of a set of reliable reference genes for quantitative sod gene expression analysis in C-elegans. Bmc Molecular Biology 9.

303. MacIver NJ, Blagih J, Saucillo DC, Tonelli L, Griss T, et al. (2011) The Liver Kinase B1 Is a Central Regulator of T Cell Development, Activation, and Metabolism. Journal of Immunology 187: 4187-4198.

304. Hardie DG, Ashford ML (2014) AMPK: regulating energy balance at the cellular and whole body levels. Physiology (Bethesda) 29: 99-107.

305. Possik et al. Manuscript in preparation.

306. Barnes K, Ingram JC, Porras OH, Barros LF, Hudson ER, et al. (2002) Activation of GLUT1 by metabolic and osmotic stress: potential involvement of AMP-activated protein kinase (AMPK). J Cell Sci 115: 2433-2442.

307. Sanz P (2003) Snf1 protein kinase: a key player in the response to cellular stress in yeast. Biochem Soc Trans 31: 178-181.

308. Jorgensen SB, Nielsen JN, Birk JB, Olsen GS, Viollet B, et al. (2004) The alpha2-5'AMP-activated protein kinase is a site 2 glycogen synthase kinase in skeletal muscle and is responsive to glucose loading. Diabetes 53: 3074-3081.

309. Wojtaszewski JF, Jorgensen SB, Hellsten Y, Hardie DG, Richter EA (2002) Glycogen-dependent effects of 5-aminoimidazole-4-carboxamide (AICA)-riboside on AMP-activated protein kinase and glycogen synthase activities in rat skeletal muscle. Diabetes 51: 284-292.

310. Miyamoto L, Toyoda T, Hayashi T, Yonemitsu S, Nakano M, et al. (2007) Effect of acute activation of 5'-AMP-activated protein kinase on glycogen regulation in isolated rat skeletal muscle. J Appl Physiol (1985) 102: 1007-1013.

311. Hunter RW, Treebak JT, Wojtaszewski JF, Sakamoto K (2011) Molecular mechanism by which AMP-activated protein kinase activation promotes glycogen accumulation in muscle. Diabetes 60: 766-774.

312. Aschenbach WG, Hirshman MF, Fujii N, Sakamoto K, Howlett KF, et al. (2002) Effect of AICAR treatment on glycogen metabolism in skeletal muscle. Diabetes 51: 567-573.

313. Luptak I, Shen M, He H, Hirshman MF, Musi N, et al. (2007) Aberrant activation of AMP-activated protein kinase remodels metabolic network in favor of cardiac glycogen storage. J Clin Invest 117: 1432-1439.

314. Arad M, Benson DW, Perez-Atayde AR, McKenna WJ, Sparks EA, et al. (2002) Constitutively active AMP kinase mutations cause glycogen storage disease mimicking hypertrophic cardiomyopathy. J Clin Invest 109: 357-362.

315. Ahmad F, Arad M, Musi N, He H, Wolf C, et al. (2005) Increased alpha2 subunit-associated AMPK activity and PRKAG2 cardiomyopathy. Circulation 112: 3140-3148.

316. Zou L, Shen M, Arad M, He H, Lofgren B, et al. (2005) N488I mutation of the gamma2-subunit results in bidirectional changes in AMP-activated protein kinase activity. Circ Res 97: 323-328.

317. Wang Z, Wilson WA, Fujino MA, Roach PJ (2001) Antagonistic controls of autophagy and glycogen accumulation by Snf1p, the yeast homolog of AMP-activated protein kinase, and the cyclin-dependent kinase Pho85p. Mol Cell Biol 21: 5742-5752.

318. Yu H, Hirshman MF, Fujii N, Pomerleau JM, Peter LE, et al. (2006) Muscle-specific overexpression of wild type and R225Q mutant AMP-activated protein kinase gamma3-subunit differentially regulates glycogen accumulation. Am J Physiol Endocrinol Metab 291: E557-565.

319. Milan D, Jeon JT, Looft C, Amarger V, Robic A, et al. (2000) A mutation in PRKAG3 associated with excess glycogen content in pig skeletal muscle. Science 288: 1248-1251.

320. Bouchard M, Souabni A, Busslinger M (2004) Tissue-specific expression of cre recombinase from the Pax8 locus. Genesis 38: 105-109.

321. Slattery ML, Lundgreen A, Bondurant KL, Wolff RK (2011) Tumor necrosis factor-related genes and colon and rectal cancer. Int J Mol Epidemiol Genet 2: 328-338.

322. Hall DH (1995) Electron microscopy and three-dimensional image reconstruction. Methods in Cell Biology, Vol 48 48: 395-436.

323. Murphy CT, McCarroll SA, Bargmann CI, Fraser A, Kamath RS, et al. (2003) Genes that act downstream of DAF-16 to influence the lifespan of Caenorhabditis elegans. Nature 424: 277-283.

324. Irazoqui JE, Troemel ER, Feinbaum RL, Luhachack LG, Cezairliyan BO, et al. (2010) Distinct pathogenesis and host responses during infection of C. elegans by P. aeruginosa and S. aureus. PLoS Pathog 6: e1000982.

325. Troemel ER, Chu SW, Reinke V, Lee SS, Ausubel FM, et al. (2006) p38 MAPK regulates expression of immune response genes and contributes to longevity in C. elegans. PLoS Genet 2: e183.

326. Budovskaya YV, Wu K, Southworth LK, Jiang M, Tedesco P, et al. (2008) An elt-3/elt-5/elt-6 GATA transcription circuit guides aging in C. elegans. Cell 134: 291-303.

327. Bansal A, Zhu LJ, Yen K, Tissenbaum HA (2015) Uncoupling lifespan and healthspan in Caenorhabditis elegans longevity mutants. Proc Natl Acad Sci U S A 112: E277-286.

328. Lapierre LR, De Magalhaes Filho CD, McQuary PR, Chu CC, Visvikis O, et al. (2013) The TFEB orthologue HLH-30 regulates autophagy and modulates longevity in Caenorhabditis elegans. Nat Commun 4: 2267.

329. Settembre C, De Cegli R, Mansueto G, Saha PK, Vetrini F, et al. (2013) TFEB controls cellular lipid metabolism through a starvation-induced autoregulatory loop. Nat Cell Biol 15: 1016.

330. Visvikis O, Ihuegbu N, Labed SA, Luhachack LG, Alves AM, et al. (2014) Innate host defense requires TFEB-mediated transcription of cytoprotective and antimicrobial genes. Immunity 40: 896-909.

331. Parsell DA, Lindquist S (1993) The function of heat-shock proteins in stress tolerance: degradation and reactivation of damaged proteins. Annu Rev Genet 27: 437-496.

332. Strayer A, Wu Z, Christen Y, Link CD, Luo Y (2003) Expression of the small heat-shock protein Hsp16-2 in Caenorhabditis elegans is suppressed by Ginkgo biloba extract EGb 761. FASEB J 17: 2305-2307.

333. Menzel R, Bogaert T, Achazi R (2001) A systematic gene expression screen of Caenorhabditis elegans cytochrome P450 genes reveals CYP35 as strongly xenobiotic inducible. Arch Biochem Biophys 395: 158-168.

334. Anzenbacher P, Anzenbacherova E (2001) Cytochromes P450 and metabolism of xenobiotics. Cell Mol Life Sci 58: 737-747.

335. Hwang YJ, Lee SP, Kim SY, Choi YH, Kim MJ, et al. (2009) Expression of heat shock protein 60 kDa is upregulated in cervical cancer. Yonsei Med J 50: 399-406.

336. Hessenkemper W, Baniahmad A (2013) Targeting heat shock proteins in prostate cancer. Curr Med Chem 20: 2731-2740.

337. McFadyen MC, Melvin WT, Murray GI (2004) Cytochrome P450 enzymes: novel options for cancer therapeutics. Mol Cancer Ther 3: 363-371.

338. Kroemer G, Jaattela M (2005) Lysosomes and autophagy in cell death control. Nat Rev Cancer 5: 886-897.

339. Salminen A, Kaarniranta K (2012) AMP-activated protein kinase (AMPK) controls the aging process via an integrated signaling network. Ageing Res Rev 11: 230-241.

340. Hurley RL, Anderson KA, Franzone JM, Kemp BE, Means AR, et al. (2005) The Ca2+/calmodulin-dependent protein kinase kinases are AMP-activated protein kinase kinases. J Biol Chem 280: 29060-29066.

341. Momcilovic M, Hong SP, Carlson M (2006) Mammalian TAK1 activates Snf1 protein kinase in yeast and phosphorylates AMP-activated protein kinase in vitro. J Biol Chem 281: 25336-25343.

342. Sun Y, Connors KE, Yang DQ (2007) AICAR induces phosphorylation of AMPK in an ATM-dependent, LKB1-independent manner. Mol Cell Biochem 306: 239-245.

343. Alepuz PM, Cunningham KW, Estruch F (1997) Glucose repression affects ion homeostasis in yeast through the regulation of the stress-activated ENA1 gene. Mol Microbiol 26: 91-98.

344. Han Q, Zhang X, Xue R, Yang H, Zhou Y, et al. (2011) AMPK potentiates hypertonicity-induced apoptosis by suppressing NFkappaB/COX-2 in medullary interstitial cells. J Am Soc Nephrol 22: 1897-1911.

345. Perez-Perez ME, Lemaire SD, Crespo JL (2012) Reactive oxygen species and autophagy in plants and algae. Plant Physiol 160: 156-164.

346. Perez-Perez ME, Crespo JL (2010) Autophagy in the model alga Chlamydomonas reinhardtii. Autophagy 6: 562-563.

347. Xiong Y, Contento AL, Bassham DC (2007) Disruption of autophagy results in constitutive oxidative stress in Arabidopsis. Autophagy 3: 257-258.

348. Scherz-Shouval R, Shvets E, Fass E, Shorer H, Gil L, et al. (2007) Reactive oxygen species are essential for autophagy and specifically regulate the activity of Atg4. EMBO J 26: 1749-1760.

349. Lemasters JJ (2005) Selective mitochondrial autophagy, or mitophagy, as a targeted defense against oxidative stress, mitochondrial dysfunction, and aging. Rejuvenation Res 8: 3-5.

350. Nunes P, Ernandez T, Roth I, Qiao X, Strebel D, et al. (2013) Hypertonic stress promotes autophagy and microtubule-dependent autophagosomal clusters. Autophagy 9: 550-567.

351. Jiang LB, Cao L, Yin XF, Yasen M, Yishake M, et al. (2015) Activation of autophagy via Ca(2+)-dependent AMPK/mTOR pathway in rat notochordal cells is a cellular adaptation under hyperosmotic stress. Cell Cycle 14: 867-879.

352. Han YK, Kim YG, Kim JY, Lee GM (2010) Hyperosmotic stress induces autophagy and apoptosis in recombinant Chinese hamster ovary cell culture. Biotechnol Bioeng 105: 1187-1192.

353. Onodera J, Ohsumi Y (2005) Autophagy is required for maintenance of amino acid levels and protein synthesis under nitrogen starvation. J Biol Chem 280: 31582-31586.

354. Seibold GM, Eikmanns BJ (2007) The glgX gene product of Corynebacterium glutamicum is required for glycogen degradation and for fast adaptation to hyperosmotic stress. Microbiology 153: 2212-2220.

355. Karantza-Wadsworth V, White E (2007) Role of autophagy in breast cancer. Autophagy 3: 610-613.

356. Iida Y, Aoki K, Asakura T, Ueda K, Yanaihara N, et al. (2012) Hypoxia promotes glycogen synthesis and accumulation in human ovarian clear cell carcinoma. Int J Oncol 40: 2122-2130.

357. Mourad WA, Mackay B, Ordonez NG, Ro JY, Swanson DA (1993) Clear cell melanoma of the bladder. Ultrastruct Pathol 17: 463-468.

358. Wang CJ, Grantham JJ, Wetmore JB (2013) The medicinal use of water in renal disease. Kidney Int 84: 45-53.

359. Nagao S, Nishii K, Katsuyama M, Kurahashi H, Marunouchi T, et al. (2006) Increased water intake decreases progression of polycystic kidney disease in the PCK rat. J Am Soc Nephrol 17: 2220-2227.

360. Strippoli GF, Craig JC, Rochtchina E, Flood VM, Wang JJ, et al. (2011) Fluid and nutrient intake and risk of chronic kidney disease. Nephrology (Carlton) 16: 326-334.

361. Gattone VH, 2nd, Maser RL, Tian C, Rosenberg JM, Branden MG (1999) Developmental expression of urine concentration-associated genes and their altered expression in murine infantile-type polycystic kidney disease. Dev Genet 24: 309-318.

362. Gattone VH, 2nd, Wang X, Harris PC, Torres VE (2003) Inhibition of renal cystic disease development and progression by a vasopressin V2 receptor antagonist. Nat Med 9: 1323-1326.

363. Grantham JJ (2008) Therapy for polycystic kidney disease? It's water, stupid! J Am Soc Nephrol 19: 1-7.

364. Beale EG (2008) 5'-AMP-activated protein kinase signaling in Caenorhabditis elegans. Exp Biol Med (Maywood) 233: 12-20.

365. Wan Z, Root-McCaig J, Castellani L, Kemp BE, Steinberg GR, et al. (2014) Evidence for the role of AMPK in regulating PGC-1 alpha expression and mitochondrial proteins in mouse epididymal adipose tissue. Obesity (Silver Spring) 22: 730-738.

366. Gleyzer N, Vercauteren K, Scarpulla RC (2005) Control of mitochondrial transcription specificity factors (TFB1M and TFB2M) by nuclear respiratory factors (NRF-1 and NRF-2) and PGC-1 family coactivators. Mol Cell Biol 25: 1354-1366.

367. Giguere V (2008) Transcriptional control of energy homeostasis by the estrogen-related receptors. Endocr Rev 29: 677-696.

368. Li XN, Song J, Zhang L, LeMaire SA, Hou X, et al. (2009) Activation of the AMPK-FOXO3 pathway reduces fatty acid-induced increase in intracellular reactive oxygen species by upregulating thioredoxin. Diabetes 58: 2246-2257.

369. Settembre C, Fraldi A, Medina DL, Ballabio A (2013) Signals from the lysosome: a control centre for cellular clearance and energy metabolism. Nat Rev Mol Cell Biol 14: 283-296.

370. Medendorp K, van Groningen JJ, Schepens M, Vreede L, Thijssen J, et al. (2007) Molecular mechanisms underlying the MiT translocation subgroup of renal cell carcinomas. Cytogenet Genome Res 118: 157-165.

371. Kuroda N, Mikami S, Pan CC, Cohen RJ, Hes O, et al. (2012) Review of renal carcinoma associated with Xp11.2 translocations/TFE3 gene fusions with focus on pathobiological aspect. Histol Histopathol 27: 133-140.

372. Muller RU, Zank S, Fabretti F, Benzing T (2011) Caenorhabditis elegans, a model organism for kidney research: from cilia to mechanosensation and longevity. Curr Opin Nephrol Hypertens 20: 400-408.

373. Barr MM (2005) Caenorhabditis elegans as a model to study renal development and disease: sexy cilia. J Am Soc Nephrol 16: 305-312.

Appendix I

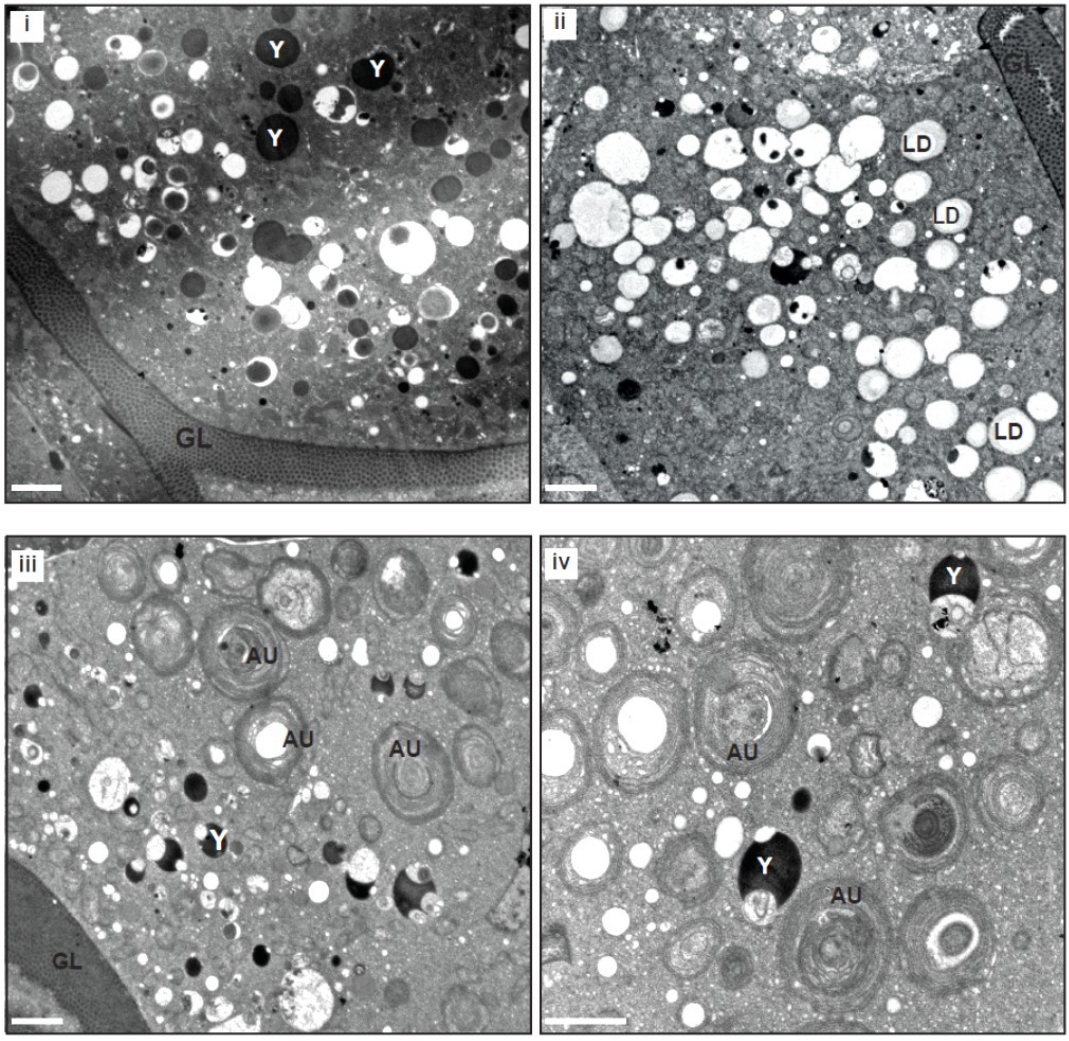

Accumulation of impaired autophagosomes upon exposure of wild-type animals to 400mM NaCl for 16 hours. Electron micrographs are taken in the intestine of untreated animals (i) in comparison to treated animals (ii, iii, iv). GL: gut lumen. LD: lipid droplet. Y: Yolk. AU: autophagosomes. Scale bars indicate 2µm.

Appendix II

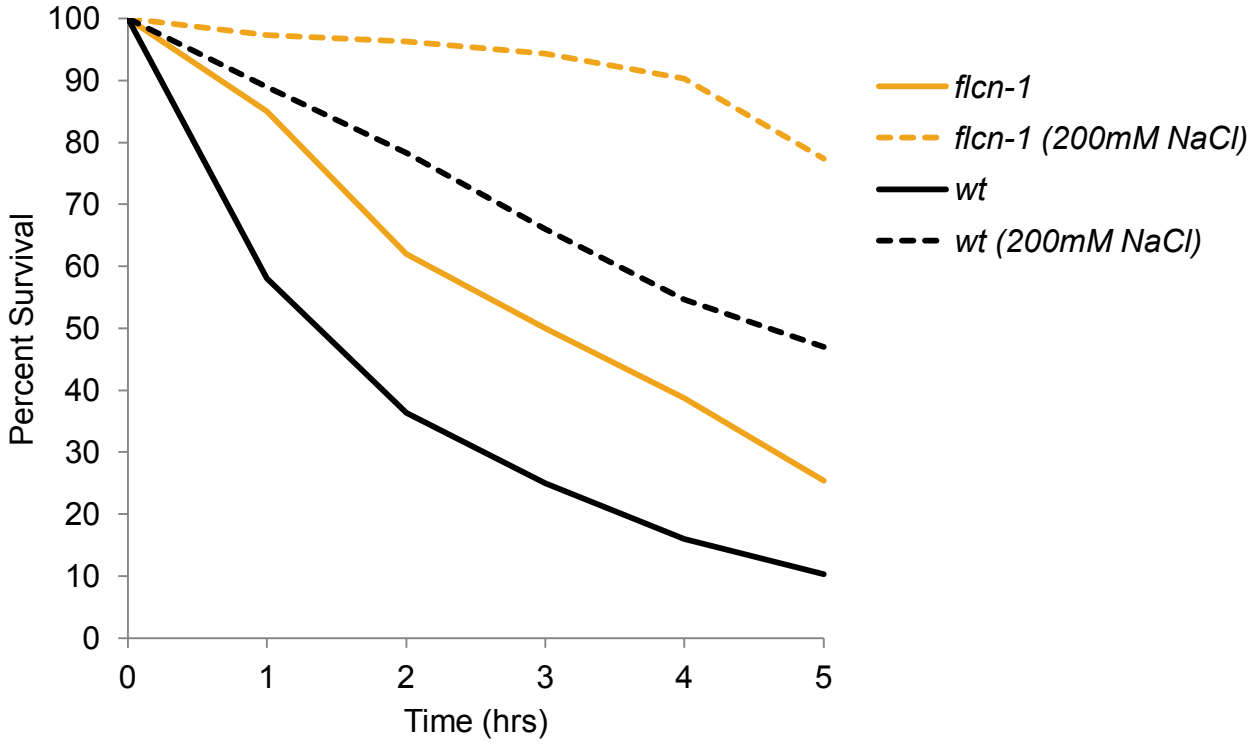

Preconditioning with NaCl increases survival to PQ.

Percent survival of indicated strains to indicated conditions. Worms were preconditioned or not with 200mM NaCl and then exposed to PQ.